ERNEST HENRY SUPERGENE PROJECT

REPORT ON WORK CARRIED OUT BY MIM EXPLORATION

(SEPTEMBER 1993 - APRIL 1994)

VOLUME 1

D. Lewis, K. Jennings, K. Hannan, A. Barber, C. Mawer, P. Rowston

MIM EXPLORATION PTY LTD

TECHNICAL REPORT No. 2228

APRIL, 1994

This, digital version has no maps but otherwise the same content as the original release (except for 'typo' corrections and format improvements); most Tables and all Figures are derived from scans of the old paper version; all edits and formatting by KW Hannan, October, 2015

ERNEST HENRY SUPERGENE PROJECT

REPORT ON WORK CARRIED OUT BY MIM EXPLORATION

(SEPTEMBER 1993 - APRIL 1994)

VOLUME 2
Figures 4.1, 4.2, 6.1, 6.2
Sections and Plans

D. Lewis, K. Jennings, K. Hannan, A. Barber, C. Mawer, P. Rowston

MIM EXPLORATION PTY LTD

TECHNICAL REPORT No. 2228

APRIL, 1994

Volume 2 not available to the editor (KW Hannan, 2015), but should be held in the relevant library or archive of Glencore Xstrata Copper Exploration.

EXECUTIVE SUMMARY

The Ernest Henry deposit was reported by Western Mining Corporation as a mineable resource of 85Mt at 1.44% Cu and 0.7 g/t Au, of which approximately 10% lies within the supergene enriched portion of the orebody (Ernest Henry Prefeasibility Study, WMC, June 1993).

In September 1993, a team of four MIM Exploration geologists, on behalf of Ernest Henry Mining, carried out an extensive drilling programme to investigate the nature of the supergene resource, with particular reference to the delineation of its margins and its likely metallurgical behaviour. With the added requirements of lease sterilisation and metallurgical materials sampling, the original drilling programme was extended from 6730 to 13119m.

The Ernest Henry deposit is a large copper-gold-iron oxide orebody hosted by altered and locally deformed Proterozoic volcanics. It is unconformably overlain by 40-50 metres of Mesozoic to Recent sediments and plunges to the southeast between southeast-dipping shear zones. The upper and northern portion of the deposit was exposed and strongly weathered prior to a marine transgression in the Cretaceous period, resulting in the formation of a supergene resource with markedly different mineralogical and mechanical characteristics to the primary orebody.

The supergene zone extends to a maximum depth of 200m, deepens along faults, and in plan has a maximum length of 650m and width of 550m. Ore minerals of the supergene zone are dominated by chalcocite and native copper with lesser bornite and chalcopyrite. The zone was logged systematically to define four broad gangue sub-zones, as was the distribution of the main sulphide minerals relative to the gangue zones. This work confirms that the supergene zone developed by a series of overprinting oxidation/ reduction events with subsequent complex redistribution of sulphides and gold in the present profile. Although the proportion of total sulphide and native copper grossly increases towards the base of the supergene zone, the relative proportions of individual ore minerals and their absolute abundances vary considerably over short distances. Consequently, ore mineral distributions and abundances appear to bear little relationship to gangue mineralogy.

As observed for sulphide and native copper abundances, copper/gold ratios grossly increase with depth, from less than the primary ore value of 2.0 in the clay zone at the top of the supergene profile, to more than 3 in the silica zone near the base of complete oxidation. This feature reflects the greater susceptibility of copper to mobilisation and enrichment than gold. Bulk copper/arsenic ratios also increase with depth. Bulk copper/cobalt ratios are an exception to this pattern with elevated

cobalt levels associated with pyrite-rich zones near the base of the supergene profile. Systematic XRD analysis of continuous core from two drill holes highlights and quantifies the short-range chemical and mineralogical variability of gangue materials and confirms the unpredictability of sulphide and metal distributions.

Detailed petrographic investigations with an emphasis on ore beneficiation were undertaken by the Minerals Research team at MIM on core from the same drillholes that were analysed by XRD. Petrographic investigations of a general petrologic nature were conducted by Dr. Bill Croxford (ROCKCO) on both supergene and primary zone samples. Although the primary mineralisation was not extensively studied, several of the EHM drill holes penetrated primary ore and several WMC holes were relogged, allowing a number of observations to be made concerning alteration styles and controls on mineralisation.

Further drilling of the Eastern Lens' mineralisation, another objective of the project, indicates that it is progressively down-faulted to the east by late, brittle, steep normal faults of the Badj Kharkl Fault Zone. The western margin of the orebody appears to pinch out toward, and is locally truncated by, the Revwood Fault Zone. The interpretations of geological and structural features in drill core indicate that future mine-scale exploration should focus on the possibility of fault-offset extensions to economic mineralisation on the margins of the currently defined resource.

Several sets of variably oriented fractures were recorded during the geotechnical phase of core logging. Competent joints at about 45ø to drillhole traces dominate, and occur as conjugate sets in some areas. A commonly slickensided, chlorite and locally clay-coated set of sub-vertical and north-trending fractures is associated with most of the observed zones of low rock quality. This fabric corresponds to the brittle faults that offset ore blocks throughout the deposit.

Other objectives of the project included the acquisition of wide-diameter drill core from the supergene zone for metallurgical testing, pit optimisation drilling and sterilisation drilling of the mine lease. Specialist studies of the deposit were also undertaken to characterise its geophysical and geochemical expression at the surface and to facilitate a greater understanding of the genesis of the deposit and the structural controls on ore localisation. The geophysical investigations indicate that the strong electromagnetic anomaly drilled by WMC leading to the discovery of the deposit was sourced by native copper within the upper levels of the supergene zone. This and other knowledge gained from the specialist studies is actively being applied to regional exploration programmes.

TABLE OF CONTENTS

List of Figures

(coloured text indicates a missing figure, held by MIM/Xstrata/Glencore)

List of Tables

page

List of Appendices

1. INTRODUCTION

The Ernest Henry Cu-Au deposit, situated on ML2671 and 35 km northeast of Cloncurry in NW Queensland (Fig.1), was acquired from Western Mining Corporation by Savage Resources (49%) and MIM Holdings (51%) following extensive litigation in 1992-1993. Savage and MIM later formed a company called Ernest Henry Mining Pty. Ltd (EHM), to be operators of the Ernest Henry Project. This report outlines work carried out by EHM in the latter part of 1993.

Ernest Henry is a large south-easterly plunging copper-gold-iron oxide orebody within altered and locally deformed Proterozoic volcanics of probable andesite affinity. It is unconformably overlain by a 40-50m thick sequence of Mesozoic to Recent sediments and appears to be bound by southeast-dipping shear zones (the Hangingwall and Footwall Shear Zones). The current surface comprises a grass-covered black soil plain that slopes gently to the Cloncurry River system to the west. The nearest outcrop is at Mount Fort Constantine, 14 km to the southwest, containing deformed granite and brecciated volcanics possibly similar to those at Ernest Henry.

The Ernest Henry deposit was quoted by WMC as containing a mineable resource of 85Mt at 1.44% Cu and 0.7 g/t Au, of which approximately 10% lies within the supergene enriched portion of the orebody (Ernest Henry Prefeasibility Study, WMC, June 1993).

In September 1993, a team of four MIM Exploration geologists were contracted to EHM to further delineate the supergene portion of Ernest Henry deposit. The programme was specifically intended:

- to determine, for the purpose of later metallurgical investigations, whether the distribution of copper and gold minerals is controlled by gangue minerals of the supergene zone;
- to ascertain controls on the Eastern Lens' mineralisation, which had been penetrated by a WMC hole FTCD-60 on section 9240mN; and
- more fully delineate the margins of the orebody for pit optimisation purposes.

A combined RC and diamond drilling programme of 6685m was planned to meet the above criteria, and was to be completed in the latter months of 1993 prior to the northern wet season. The programme was subsequently extended to 13119m, to meet sterilisation, metallurgical and geotechnical requirements, and was completed on 17th December 1993.

Ancillary activities carried out during this period included petrographical, XRD, structural and geophysical studies, environmental monitoring and sampling, and ongoing organisational, assay quality control and planning tasks.

As the primary focus of the project was to delineate the supergene resource the primary ore body was not examined in detail. Thus, further work is needed to determine the geological controls on primary ore grade and continuity.

This report describes the drilling programmes (resource, metallurgical, sterilisation, geotechnical), supergene zone metal and mineralogical distributions, assay quality control procedures, and structural and geophysical investigations. Results and conclusions resulting from these activities are discussed and recommendations for further work are provided.

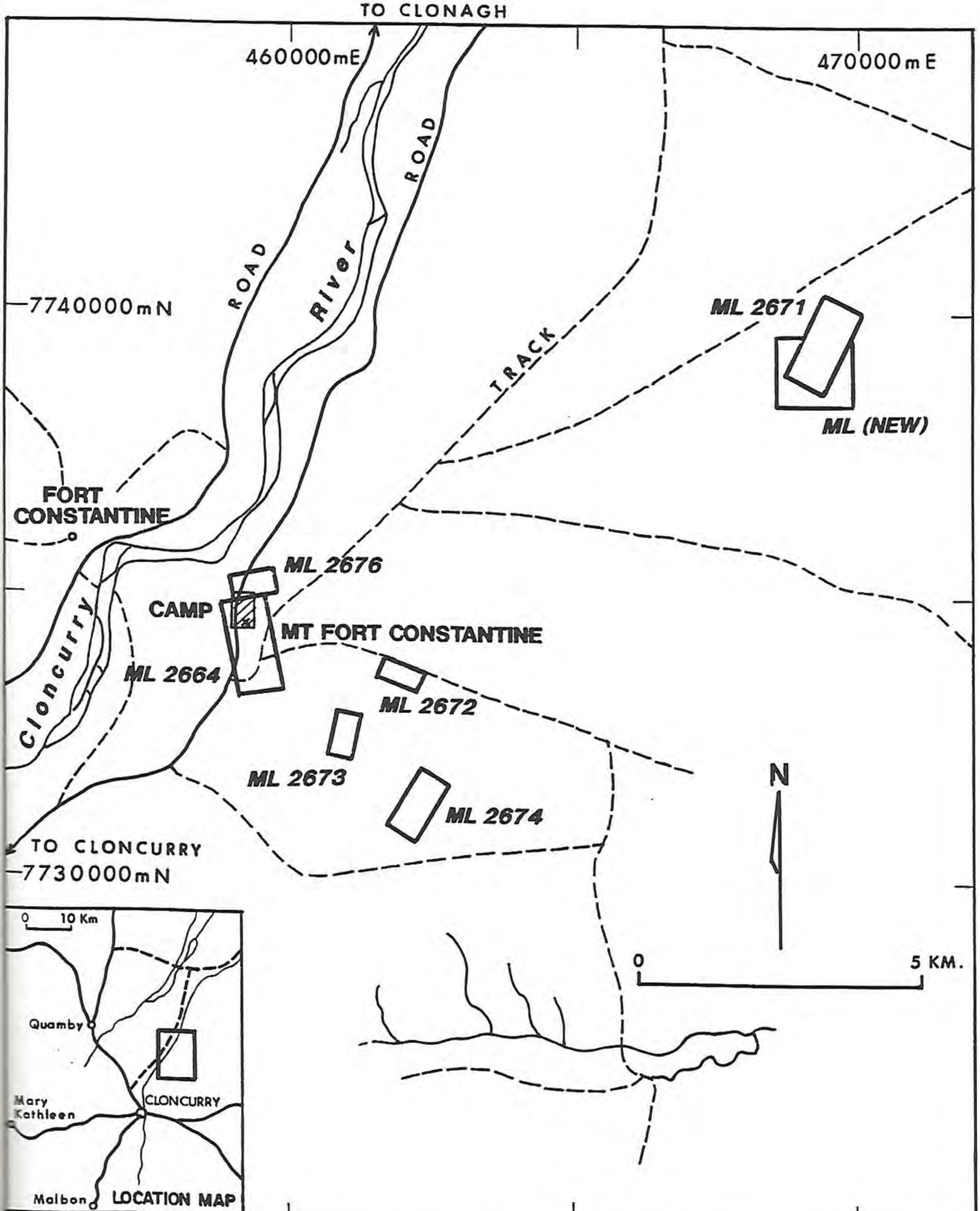

Figure 1

LOCATION MAP
ERNEST HENRY ML 2671 AND OTHERS

Drg.No.43200

2. TENEMENT HISTORY and PREVIOUS INVESTIGATIONS

The Mount Fort Constantine area is situated on extensive black soil plains, where Mesozoic and Tertiary sediments 20 - 100 m thick overly Proterozoic basement rocks. The area is flat and forms part of the floodplain of the nearby Cloncurry River. Vegetation is dominated by Mitchell grass and Queensland blue grass with sparse shrub layers of Acacia sp. and low Whitewood trees.

Historically, very little exploration has been carried out over covered rocks in the eastern part of the Mount Isa Inlier due to the lack of effective exploration techniques. With the advancement of remote geophysical techniques such ground has become increasingly prospective in the search for mineralisation.

The Mount Fort Constantine area was held under tenement and explored by BHP during the mid 1980's. Although there were indications of copper and gold, technical problems, including the difficulty of drilling through the Phanerozoic cover, led them to abandon the area.

In 1989, Hunter Resources targeted the Eastern Succession (i.e., eastern Mount Isa Inlier) following a review of geological models for Cu-Au mineralisation associated with granitic intrusions. In particular the Mount Fort Constantine area was selected on the basis:

1. of the occurrence of granite with compositional affinities to the high rare earth elements and fluorine granitoids of the Stuart Shelf, South Australia\;
2. that it was situated in the roof zone of the hydrothermally altered Naraku Granite;
3. of numerous high intensity magnetic anomalies in the region; and
4. that it was inadequately explored for possible sulphides associated with magnetite.

A joint venture for developing targets within this area was negotiated between Savage Resources, Hunter Resources, and Western Mining Corporation. WMC took a 70% interest and operated the project which became known as the Mt. Fort Constantine Joint Venture. The area of interest included six mining leases held by Savage Resources, including ML2671.

Work during 1990 focussed on the development of a conceptual model, by the integration and analysis of aeromagnetic data and postulated geology. Any mineralisation was postulated to be retrograde, and as such would be associated with local demagnetisation. Consequently, the data was examined for broken magnetic patterns and coincident EM anomalies.

In 1991 WMC Exploration commenced drilling. The second diamond drillhole, FTCD 2, situated several kilometres south of the first and over an EM anomaly, intersected 100m of supergene and primary copper mineralisation.

During 1992, intensive drilling successfully delineated a major Cu-Au resource. Drilling was carried out on an 80 metre spacing. A pre-feasibility study was commissioned and metallurgical, environmental, and geotechnical test work undertaken. The project was ear-marked for fast-track development of the resource and a number of mining operation plans considered. Production was scheduled for early 1996.

In October 1992, proceedings were initiated against WMC by Savage for trespass on mining lease ML2671 prior to an option agreement being executed. Protracted legal debate culminated on July 26 1993, with a settlement between WMC and Savage Resources that included the surrender by WMC of any option over ML2671.

During the exploration and subsequent court proceedings, MIM Holdings had negotiated to purchase Hunter Resources who held 30% of the original Mount Fort Constantine Joint Venture. Following the court case, MIM Holdings acquired 51% interest of Savage Resources, and took over as operator of the lease exploration. Western Mining Corporation remains operators of the Mt. Fort Constantine Joint Venture.

A separate company, Ernest Henry Mining Proprietary Limited, was established to conduct feasibility studies and development of the Cu-Au resource. In September 1993 an intensive drilling campaign was carried out to close up the drill spacing of the resource, and more importantly to determine the nature and distribution of ore minerals within the supergene zone. This report forms the summary of that program.

3. PROGRAMME MANAGEMENT

The MIM Exploration team, as project managers of the first phase of work carried out at Ernest Henry, was required to ensure that certain statutory and logistical matters were attended to, prior to or shortly after the commencement of drilling. This section presents an outline of the operational and logistical arrangements which were carried out by the team.

3.1 LOGISTICS

The following logistical matters were attended to as part of the programme management.

- **Budget**

A budget proposal was submitted for the establishment of suitable personal and office accommodation, core logging, cutting and storage facilities, drilling costs, vehicle hire, labour costs and sundry items required for the day to day running of the project. The total budget proposal as approved was $1.2m for 6685m of drilling.

A series of Capital Work Orders were prepared for major cost items, including computer hardware and software (Table 3.1) and minor equipment purchases were made (Table 3.2). Field assistants were recruited locally.

- **Land Tenure**

The landowner (Stanbroke Pastoral Co.) of Fort Constantine Station was notified of our intention to build a camp on ML2664, held by Savage Resources, proximal to Mount Fort Constantine. Permission was sought to erect a fence and to drill a water bore for the camp, which was granted by the then manager of the property, Mr. John Betts. The issue of compensation was dealt with later by Stanbroke Pastoral Co. and EHM management. The Department of Primary Industries (Longreach) was notified of the drilling of a water bore beside the Cloncurry River to supply the camp.

A building permit (number 1186) to erect the camp at Mount Fort Constantine was obtained from Cloncurry Shire Council and was approved by Mr. Brian Stirrup, Building Inspector, on completion of satisfactory plumbing and drainage facilities on 13.12.93.

A possibility arose that a Notice of Permit to Occupy may have been required by the Department of Lands at Cloncurry in order to fence in the camp at Mount Fort Constantine, due to our proximity to the Zingari Road stock route. The site was inspected by Mr. Mark Cranitch of Dept. Lands, whereupon it was decided that the Permit was not required.

- **Plan of Operations**

A Plan of Operations for ML2671 was submitted to the Mining Registrar, Mr. Peter Little, at the Department of Minerals & Energy in Mount Isa. Dr. Deirdre Lewis was nominated as the Registered Manager until December 31, 1993. A subsequent Plan of Operations for the lease was also prepared for the quarter 1.1.94 - 31.3.94.

- **Telecommunications**

Telecom was requested to supply two lines (telephone and fax) to the camp at Mount Fort Constantine. This proved to be a lengthy business and the lines were finally established in early March 1994.

- **Power**

A power supply for the camp was required and NORQEB in Mount Isa were approached (Mr. Jim Lonergan - Regional Manager, NWQ). As technical problems arose concerning supply via the Fort Constantine line, this has not been resolved to date. A contingency plan was made to provide power via a purchased 50kva generator.

TABLE 3.1 ERNEST HENRY: MAJOR EQUIPMENT PURCHASE

PURCHASE ITEM		Cost
Computers	Hardware	15000
	Software	17100
	Set-up	3000
Mag.Sus.Meter		1800
Radios		5616
Generators	50kva	11000
	5kva	4118
Core Saw		7800
Fork Lift		12000
Camera		1000
Water Tank	9000 litre	1500
Septic Tank		1200
SubmersiblePump		2665
Onga Pump		2000
Poly Pipe	800m camp	1500
	1500m drill	2800
50mmPVC	1400m	4000
Paving	incl. labour	1900
Core shed		1200
Pavex	Shed floor	1000
Earthmoving	G&D Plant	11680
	for Fort Con	2500
	Geotech pits	4980
Office	Light-table	840
	Furniture	4000
	Stationary	1000
Kitchen	equipment	500
BBQ		125
Safety	Fire Extinguishers	1200
	First Aid Kits	180
Electrician	incl cable etc	8400
Plumber	incl. fittings	1000
TOTALS		**134604**

TABLE 3.2 ERNEST HENRY: MINOR EQUIPMENT PURCHASES

2 x Scribes $24	4 x Desks	Washing Machine
Logging Sheets (Geol;Geotech)	Stationary Cabinet	Camp Table
HCl acid	6 x chairs	4x camp chairs
Acid Bottles	Bookcase	4x high Stools $160
6 Tape Measures	Filing Cabinet	Kitchen gear $236
Slide Film x 40 ($480)	Vertiplan	BBQ plate $346
Sample Numbers (EA10001- EA20000)	Photocopier $120/mth	
Core Orientation Device $300	Light Table $860	First Aid kit
25 boxes Marking pens $530	1 x Noticeboard *MIMEX	Ear Plugs
Douglas Square	3 x Whiteboards $420	Ear Muffs
	Floppy Disks	Safety Gloves
4 x Sump Fences	6 x window blinds $840	Hard hats
10 x Sump liners		Hardware $2000
100m 1/2" hoses	Fuel Pump $200	
2km 40mm Rural Poly	Pallet jack (loan: UTO)	**Metallurgy**
Fittings	100 treated pallets $7500	Freezers Hire $2250
Heavy duty Stapler		Bubble Wrap $102
Funnel	2 x 6m Ratchet Straps	200 PQ coretrays$4000
	Core strapping	200 PQ lids $1400
75 Chip Trays	Strapping dispenser	
700 plastic bags	20 Buckets/ brushes	
1000 calico 12 x 18" $300	3 x wheelbarrows	
2000 calico 10 x 14' $250	2 x Core trolleys $966	
500 Yellow poly bags $500	30 x core horses	
Splitter @ $460	80 x 50mm PVC $1160	
2000 HQ/NQ core trays $35000	100 x 40mm PVC $1000	
2000 Core tray lids $14000	Shade Cloth 12 x 6m	
50 PVC 125mm/150mm caps	Marking Paint	
Core Blocks $160	2 x boxes Pink Flagging	
	PVC wet sampling	

- **Drilling contract**

A drilling contract was drawn up between MIM Exploration and Leanda Drilling Pty. Ltd. of Charters Towers to complete 6700m of combined RC and diamond drilling by the end of 1993. Prices were agreed for HQ/NQ/PQ core and for percussion drilling, casing and rotary mud drilling through the Phanerozoic cover. Leanda provided the submersible pump for the drilling requirements, while EHM provided that required for domestic consumption at the camp.

- **Safety Training**

Under the current Mines Regulation Act, MIMEX is required to provide safety training and equipment to all personnel and to ensure safe work areas and practises. Inductions for new starters was provided on 27.9.93 and MIMEX Safety Booklets were distributed to all employees (D. Lewis). Fire extinguishers were purchased and placed in suitable areas. Leanda Drilling personnel were inducted in safety issues by their company prior to arrival on-site. Hard-hats and boots were compulsorily worn at work at all times.

- **Environment**

MIMEX Environmental Policy booklets were distributed in the MIMEX and Leanda Drilling camps and personnel were constantly reminded of the necessity of sound environmental practise. Biodegradable drilling muds were used at all times and following advice from the Environmental Science Unit at MIM in Mount Isa, sumps did not require draining.

A weather station was purchased from Environdata Pty. Ltd. and established on the northeastern corner of ML2671 in November 1993. Monitoring is continuing through the wet season.

- **Earthworks**

Earthmoving was arranged to be undertaken by G&D Plant Hire of Cloncurry for all sumps, tracks, grading of ML2671, MLA, Red & Green boundaries, followed by environmental rehabilitation at the end of the project.

- **Surveying**

Aerial photography was undertaken following the grading of the lease edges and marking of their respective corners: ML2671, MLA, Red & Green areas.

3.2 DRILLING PARAMETERS

Drilling at Ernest Henry in the period totalled 13119m, extended from the original proposal of 6730m. The drilling was undertaken by Leanda Drilling Pty. Ltd. of Charters Towers and was completed efficiently and safely.

For most of the programme, three rigs were used: two UDR Warman 1000's and a UDR Warman 650. Occasionally, an Ingersoll Rand T4 was employed to drill precollars through the Phanerozoic cover to basement, which were then core drilled by one or other of the Warmans.

Initially the standard procedure was to hammer through the Phanerozoic sediments to Proterozoic basement using a 53/4" hammer and casing off at the base of an unconsolidated gravel horizon at about 32m with 150mm PVC. The holes were then HQ core drilled to below the base of partial oxidation at the base of the supergene zone, and into fresh rock.

However, due to caving and excessive water pressures in the unconsolidated running sands and gravels at 26-32m, it was found that drilling was more effective by blading (81/2" or 73/4") to above the gravels, injecting mud to support the hole from collapse through the gravels and then casing off with 125mm PVC. Blading then continued through the underlying Mesozoic black shales to basement at a typical depth of 40-45m. HQ drilling continued as per normal through the oxidised Proterozoic profile. Holes were occasionally were deepened to penetrate primary ore zones; these were cased off at the base of oxidation and reduced to NQ diameter to the required depth.

Four PQ diameter holes were drilled for metallurgical test work. This involved triple tubing through the Phanerozoic cover to the Cretaceous gravels, injecting mud to maintain the hole through the gravels, and then triple tubing to basement thereby recovering most of the sequence. The Proterozoic basement was drilled by standard PQ core equipment (see section 4.3 for detail).

3.3 CORE MANAGEMENT

3.3.1 Core Handling

- The core was removed from the drill site twice daily to the logging shed. All holes were logged geologically and geotechnically by the on-site geologists. Routine tests with nitric acid were carried out to determine the presence of fine grained chalcocite.

- The geological splits were established and marked, and assay splits were established within each geological split at ó 2m intervals. The latter was reduced later to 1m maximum splits for all supergene intervals to reduce reputed variographical problems with statistical correlations. Each hole was also logged geotechnically.

- Selected samples were submitted for petrographical description.

- Downhole magnetic susceptibilities for each hole were recorded and the core photographed prior to removal to the core shed for cutting and sampling.

- The sample splits were then entered to Micromine, where each sample was accorded a specific assay number from the Ernest Henry series EA10000 - 20001 and passed to the core shed.

- The core was then cut, bagged and despatched to ALS laboratories for routine analysis, the details of which are discussed in Chapter 8.

- The geological information pertaining to rock-type, alteration, gangue zones, base of oxidation and structures, was entered to Micromine to produce geological cross-sections from which interpretations and further drilling requirements could be generated (Section 7.2).

3.3.2 Core Logging

- ***Logging schemes***
  Geological and geotechnical parameters were established which reflect local geological and structural characteristics at Ernest Henry. The geological scheme was partly modified from WMC's to ensure continuity, but simplified to ensure logging of the more important features. A representative from Coffeys International visited the site in October 1993 to instruct the team on geotechnical data collection.

- ***Western Mining Corporation***
  Western Mining Corporation employs a cumbersome logging scheme in order to maximise "data capture". The scheme uses a series of alphabetics and abbreviations to describe a wide range of rock types, textures, structures, and any mineralisation. In practical terms the geologist uses the codes somewhat haphazardly and the result appears confusing on the log form. We believe that the complexity of the logging scheme allows for greater subjectivity and therefore inconsistency in the logging. However, the fundamental rock types are correct and these have formed the basis for a simplified logging scheme designed by the Ernest Henry team (Table 3.3). All WMC data was later converted into Ernest Henry team logging using a find and replace' function on Micromine. We concede that much of the data is compromised on such a conversion, but it allows the simplest representation of the basic rock types.

TABLE 3.3

ERNEST HENRY GEOLOGICAL LOGGING CODES

ROCK TYPE	DESCRIPTION	LOGGING SYMBOL
S	Undifferentiated Sediments	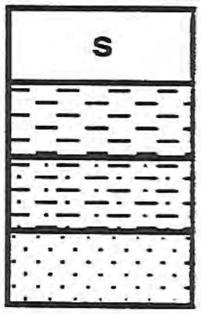
Sfg	Fine Grained Sediment	
Sfmg	Medium Grained Sediment	
Scg	Coarse Grained Sediment	
FELSIC VOLCANICS		
FV	Felsic Volcanics	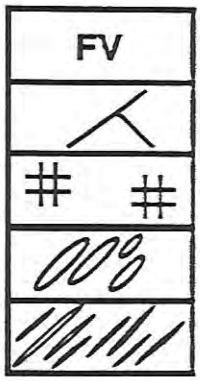
FV_1	Fractured Felsic Volcanics	
FV_2	Mosaic Felsic Volcanics	
FV_3	Lithon Felsic Volcanics	
FV_4	Banded Felsic Volcanics	
FVwd	Felsic Volcanics - weakly digested	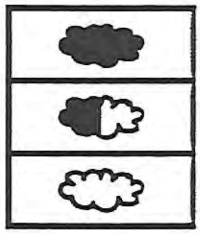
FVmd	Felsic Volcanics - moderately digested	
FVsd	Felsic Volcanics - strongly digested	
suffix		
a	amgydaloidal	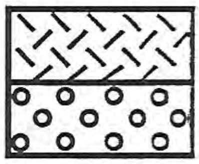
p	porphyritic	
DR	"Dark Rock" - No obvious clasts dominated by magnetite, biotite, chlorite	
SR	"Spotted Rock" - Carbonate or albite altered rock with spotted appearance	
GF	Granofels	
MMB	Marble Matrix Breccias - Massive carbonate rock. Generally reserved for the footwall of mineralised zone.	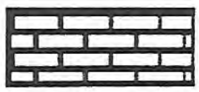
CLAY	Highly weathered/altered rock - unclear origin	

Drawn: H.M.R. Drg.No.42110
File name: ERNGLOG1.CDR Date: 22 4 94

STRUCTURE	
HWS	Hangingwall Shear
FWS	Footwall Shear
MSZ	Marshall Shear Zone
Vn	Vein
Ft	Fault
Jt	Joint
ALTERATION	
cb	carbonate
do	dolomite
ca	calcite
sd	siderite
mt	magnetite
hm	hematite
ch	chlorite
am	amphibole
gt	garnet
kf	potassium feldspar
ab	sodium feldspar
mu	muscovite
cl	clay
qz	quartz
rd	red
brd	blood red
pk	pink
MINERALOGY	
cc	chalcocite
cu	native copper
cp	chalcopyrite
bn	bornite
py	pyrite
mo	molybdenite

Drawn: H.M.R. Drg.No. 42111
File name: ERNGLOG2.CDR Date: 22.4.94

TEXTURES	
cs	clast supported breccia
ms	matrix supported breccia
fk	brittle fracture
fo	foliation
wfo	weak foliation
mfo	moderate foliation
sfo	strong foliation
sc	schistose
fg	fine grained
cg	coarse grained
le	leached
SUPERGENE GANGUE ZONES	
CLAY	
CHLORITE	
HEMATITE	red wash colour
LIMONITE	orange-brown wash colour
silica	
MINERALOGY	Mineral abbreviations separated by hyphens (in order of decreasing abundance)
a	Dominant mineral
b	Second most dominant
c	etc
d	etc
SULPHIDE ASSEMBLAGE	2 digit code, first corresponds to the dominant sulphide
1	native copper
2	chalcocite
3	pyrite
4	chalcopyrite

COPPER GRADE %	
Visual estimate of weight % copper	

Drawn: H.M.R. Drg.No. 42112
File name: ERNGLOG3.CDR Date: 22.4.94

- ***Ernest Henry Mining***

  An in-house logging scheme was devised to determine the most efficient and concise method of summarising the volume of information entering the database. Features recorded include the basic rock type and then qualifiers with respect to the degree of alteration, mineralogy, colour, structural information, and the presence and nature of any copper minerals present (refer Table 3.3).

- ***Metallurgical Logging***

  An attempt was made to derive a predictive method for logging based on meso-textures observed within the core and micro-textures observed within selected thin sections (Marcault, 1994). A strong correlation was established between meso-textures and ore grade. This was to be expected given that increasing matrix content of brecciated material correlates with higher grades of mineralisation. The meso=texture approach largely ignores features that may assist with determining the genesis of the deposit, and as such was not favoured by the Ernest Henry Project geologists. However, the method may yet prove useful for metallurgical prediction.

- ***Geotechnical Logging***

  Following a briefing session by Mr Alex Duran of Coffeys International, all EHM holes were routinely geotechnically logged. A logging sheet was designed by the team to record salient structural features such as foliations, fault/shear zones and orientations, together with Rock Quality Designate (RQD) and joint frequencies/ orientations. The oriented structural dataset was entered to MicroMine and can be retrieved from the database as required for mine design and planning. See Chapter 5.1 for more detail on geotechnical logging.

3.4 ASSAYS AND MINERALOGICAL INVESTIGATIONS

- ***Analytical Schemes***

Following comparative analytical test work on two Western Mining Corporation drillholes, FTCD76 and FTCD49, by AMDEL and ALS Laboratories, an analytical scheme for routine assaying of the Ernest Henry core was devised. The scheme took account of the presence of coarse native copper, leading to routine screening of all native copper-bearing samples for the duration of the project. Quality control procedures were also followed for the duration of the programme (section 8.1).

- ***Petrography***

It was arranged by Mr Ian Willis that the Minerals Research Team at Isa Mine would conduct petrographical studies of samples submitted from selected core, with particular reference to metallurgical characteristics of the supergene ore. It was also arranged that Ms. Laurence Marcault would visit Cloncurry and later Ernest Henry to test a rock texture classification scheme developed for possible metallurgical application at Hilton Mine. Routine petrographical examination was carried out by Dr. Bill Croxford in Brisbane.

Quantitative XRD analyses to help characterise supergene zone materials were carried out by AMDEL laboratories (refer section 7.3.4) and single mineral XRD analysis by the Minerals Research team in Mount Isa.

3.5 DATA MANAGEMENT

WMC data became available to Ernest Henry Mining according to the Terms of Settlement of the litigation. These contain important information on a number of facets of mine development, including metallurgical test work, engineering reports, and petrographic assessment of sulphides. To facilitate easy access to this data it was catalogued by an "SV" number, assigned by Savage Resources, then organised into subject material. A library of material sourced from this data is available at the offices of MIMEX and EHM. A full listing of this data is presented in Table 3.4.

Digital data was in the form of a Paradox database, and this was converted for use in a Microsoft Access database. From here, the data was examined by Ken Harvey (MIM Exploration Pty. Ltd. Manager - Information Services) and the integrity confirmed before transferring it into Micromine. All routine manipulations of the data and production of geological and assay plots were carried out using Micromine. A listing of computer files is available in Appendix I.

On receiving the assay data, Mineral Sampling Consultants were commissioned to create a statistical database. This allows manipulation of data to determine correlations and to generate graphical representations of the latter. This database operates through Microsoft Excel and is now held by EHM.

Thus the following databases are currently established:

- Hard copy library material relating to investigations on the Ernest Henry Project.
- Microsoft Access for WMC lithological, structural, and metallurgical data
- Micromine for manipulated assay data (both WMC and EHM) and plot production.
- Microsoft Excel for all geochemical data statistical manipulations

Table 3.4 Library Listings for Ernest Henry Project Investigatons (WMC)

Prefeasibility, Budgets, and Technical Reports

SV 9 - Ernest Henry Prospect, Pre-feasibility Budget Design Estimates; Waste Dumps, Tailings Dams, Water Supply Dams.

SV 32 - Period Reports, Feasibility Studies, Mining Schedules.

SV 34 - Pre-Feasibility Draft.

Geology

SV 27 - The Geology of the Ernest Henry Copper-Gold Deposit, Cloncurry, Queensland.

SV 28 - Composition, Texture, and Origin of Ferruginous Pisolites from Ernest Henry.

SV 137 - Results of a Fluid Inclusion Reconnaissance of Samples from Ernest Henry.

Geophysics

SV 70 - Geophysics at FC5 (magnetics).

SV 73 - Geophysics at FC5 (IP and TEM).

SV 80 - Down-hole Geophysics at Mt Fort Constantine.

SV 108 - Geophysics on Ernest Henry for the first half of 1992.

SV 111 - Determination of Magnetite Content from Downhole Magnetic Susceptibility Logging.

Geochemistry

SV 43 - Geochemical General Memoranda (20 assorted memos.).

SV 90 - Assays from First and Second Lot of Composites.

SV 120 - Uranium in Concentrate from Ernest Henry.

Surveying

SV 10 - Fort Constantine Survey Control.

Petrography

SV 20 - Further Studies of Samples from the Ernest Henry Prospect.

SV 21 - Mineralogic and Mineragraphic Studies of the Ernest Henry Concentrate and Tails.

SV 22 - Mineralogy, Mineragraphy, and Petrography of Primary Mineralisation from FTCD 11 at Ernest Henry.

SV 24 - Mineralogic and Mineragraphic Studies of Metallurgical Test Samples from Ernest Henry.

SV 25 - Studies of the Supergene Profile at Ernest Henry.

SV 26 - Mineragraphic and Petrographic Descriptions of Supergene and Primary Mineralisation in Drill Hole FTCD 36 at Ernest Henry.

SV 82 - Further Microscopic Assessment of Mt Fort Constantine flotation concentrate.

SV 83 - Further Microscopic Assessment of Mt Fort Constantine Flotation Concentrate.

SV 84 - Microscopic Assessment of Mt. Fort Constantine Flotation Concentrates.

SV 89 - Petrography, Mineragraphy, and Mineralogy of Samples from Ernest Henry Prospect, Cloncurry.

SV 100 - Further Studies of Samples from Ernest Henry Prospect.

SV 104 - Mineralogic and Mineragraphic Studies of Ernest Henry Concentrates and Tails.

SV 119 - Copper in Tail from Ernest Henry.

SV 126 - Mineralogy, Mineragraphy, and Petrology of Primary Mineralisation From FTCD 11 at Ernest Henry.

SV 127 - Mineragraphic and Mineralogical Data on Metallurgical Test Samples from Ernest Henry.

SV 128 - Mineralogic and Mineragraphic Data on Metallurgical Test Samples from Ernest Henry.

SV 134 - Studies of the Supergene Profile at Ernest Henry.

SV 140 - Mineragraphic and Petrographic Descriptions of Supergene and Primary Mineralisation in Drill FTCD 36 at Ernest Henry.

Geotechnical/Engineering

SV 1 - Preliminary Wast Characterisation Studies.

SV 7 - Geotechnical and Hydrological Appraisal of Ernest Henry.
SV 13 - Calculations and Estimates of Tailings Dams; Internal Draft.
SV 17 - Preliminary Dewatering and Water Supply Schedule for the Ernest Henry Copper Project.
SV 50 - Geotechnical General (assorted memos. and notes).

Metallurgical Testwork

SV 4 - Metallurgical Testwork Carried Out at Ernest Henry.
SV 5 - Assessment of Grinding Characteristics of a North Queensland Copper Ore.
SV 11 - Ernest Henry Metallurgical Testwork; Progress Report.
SV 12 - A Testwork Program Supporting the Flowsheet Development of the Ernest Henry Cu/Au Deposit.
SV 14 - Ernest Henry Cu/Au Deposit, Metallurgical Testwork - Sept. 1992.
SV 15 - Ernest Henry Cu/Au Deposit, Review and Planning of Metallurgical Testwork.
SV 16 - Ernest Henry Cu/Au Deposit - Metallurgical Testwork- FTCD 11, Oct. 1992.
SV 29 - Metallurgical Data/Testing - costs, design, reports/meetings, samples, concentrates.
SV 30 - Metallurgical Data/Testing - thickeners, Amdel tests, WMC tests, cobalt.
SV 31 - Metallurgical Data/Testing - research, general administration, budgets.
SV 76,76A- Flotation Tests, Primary Copper Mineralisation, Cloncurry Area.
SV 78 - Primary Copper Mineralisation Flotation Testwork (MCF 100).
SV 87 - Stage 2 Metallurgical Tests, FC 5 Primary Mineralisation.
SV 88 - Analyses of Metallurgical Samples.
SV 95 - Assays of Composite Sample Test.

Drilling

SV 37 - Diamond Drill Hole Request Sheets.
SV 38 - Sample Data Sheets.
SV 48 - Significant Intersection Listing (FTCD 2 - 77).

Environmental

SV 8 - Flora and Fauna Assessment - Mt. Fort Constantine Area.

Resource Calculations

SV 18 - Ernest Henry Indicated Resource Calculations.
SV 19 - Ernest herny Cu, Au, TCM Comparisons.
SV 33 - Geology and Ore Reseves Data.

Administrative/Miscellaneous

SV 41 - Monthly Reports: Cloncurry Copper Project - Ernest Henry Evaluation (PeriodReports) July 1992 to May 1993.

4. DRILLING PROGRAMME

In the period September to December 1993, a total of 13119m of Reverse Circulation (RC) and diamond drilling was carried out to investigate the nature of the supergene resource of the Ernest Henry orebody. The drilling parameters are described in Section 3.2. Full details of hole co-ordinates and depths are shown in Table 4.1, and drill hole collar locations presented in Figures 4.1 and 4.2.

4.1 RESOURCE DRILLING

Resource drilling of the supergene profile, together with investigations of the Eastern Lens, comprised a total 9175m, sterilisation drilling comprised 2719m for 11 holes on ML2671, metallurgical drilling comprised 770m for four PQ holes, and geotechnical terrain drilling comprised 440m for nine holes.

Drilling of the supergene zone was conducted on true east-west sections, using the 40 x 40m grid established by WMC on AMG co-ordinates. Each of the collar pegs were previously surveyed by WMC, but due to differential subsidence in the montmorillonite-rich black soils, many of the pegs moved. Where this occurred, the pegs were rehabilitated as best as possible.

Alternate 40m sections were drilled to easterly and westerly azimuths respectively, such that Section 7739240m N was drilled to easterly decline, while 7739320m N was drilled to westerly decline and so on. The magnetite content in the orebody rendered the compass ineffective, so rigs were lined up by gridline sighting. Surveys were taken downhole at 30m intervals using an Eastman camera but where the magnetite content increased azimuth details were unreliable. Core orientations using a spear and chinagraph pencil were also taken at approximately 30m intervals; those which were unreliable were disregarded and not utilised for orientations.

Four key geological sections are presented in this report which also include the primary mineralised zone. These sections reflect the re-logging of some WMC holes together with interpretations of recorded geology (Figs.7.1-7.4). Plan sections showing copper grade and geology are presented also at 50m RL intervals (Figs.7.5-7.10). The supergene gangue zones for each of the EHM sections drilled on, and north of, 7739180mN were recorded and are presented as a series of plots (Figs.7.1-7.14 of this report, plus eight infill sections).

The best results of the EHM drilling programme are presented in Table 4.2 on a hole-by-hole basis (weighted average grades).

4.2 STERILISATION DRILLING

A total of eleven holes for 2719m were drilled on the northern end of ML 2671 to test ground planned for future mine infrastructure (Figure 4.2). The holes were drilled on 400m x 400m grid to the limits of the M.L., while two holes were targeted on discrete peaks of a NE-trending magnetic anomaly. The holes were drilled as far as possible by Reverse Circulation (R.C.), usually 100 - 150m, and then continued to about 250m by NQ2 diamond drilling.

RC chip samples were collected over 2m intervals from the cyclone and stored in polyethylene bags. Large amounts of water were encountered throughout the programme, leading to collapse within Phanerozoic cover of the early holes. Consequently, as with the resource drilling, all of the R.C. collars were cased to basement to prevent the hole from blowing-out. Hammering continued to variable depths dependant upon water flow which usually became too great to lift the sample at ÷120m. The hole was then cased off and NQ diamond drilling ensued to ÷250m. The water levels and flow rates were recorded in most of the sterilisation holes (see Tables 5.2 and 5.3).

TABLE 4.1 – ERNEST HENRY DRILLING PROGRESS

			PROPOSED			PRE			PRECOLLAR			CORING		
HOLE NAME	NORTH	EAST	DIP	BRG	DEPTH	COLL	CORE	EOH	RIG	START	FINISH	START	FINISH	STATUS
FTCD60	9240	9360	70	E	571	0	135	606	1000			28-Sep	1-Oct	complete
EH100	9080	9160	65	E	200	48.7	42.4	91.1	650	28-Sep	28-Sep	29-Sep	30-Sep	complete
EH100A	9080	9159	65	E	200	56.3	153.2	201.2	650	1-Oct	2-Oct	2-Oct	3-Oct	complete
EH101	9160	9160	60	W	140	52.2	85.8	138	650	1-Oct	3-Oct	4-Oct	5-Oct	complete
EH102	9160	9320	60	W	220	48.8	170.2	219	1000	2-Oct	3-Oct	3-Oct	5-Oct	complete
EH103	9160	9480	60	W	200	50.7	141.5	192.2	650	3-Oct	5-Oct	5-Oct	8-Oct	complete
EH104	9240	9160	70	E	160	47.5	120.8	168.3	650	6-Oct	8-Oct	8-Oct	10-Oct	complete
EH105	9240	9440	70	E	550	47.5	523.7	571.2	1000	6-Oct	6-Oct	6-Oct	12-Oct	complete
EH106A	9240	9240	70	E	650	47.6	600.9	648.5	1000	6-Oct	7-Oct	21-Oct	30-Oct	complete
EH107	9240	9320	70	E	100	47.6	62.4	110	650	8-Oct	8-Oct	10-Oct	11-Oct	complete
EH108	9240	9080	70	E	160	47.5	139.7	187.2	650	9-Oct	9-Oct	1-Nov	2-Nov	complete
EH109	9200	9120	60	E	180	44	183.2	224.7	1000	9-Oct	10-Oct	13-Oct	16-Oct	complete
EH110	9200	9280	60	E	140	47.6	103.2	144.2	650	10-Oct	12-Oct	14-Oct	16-Oct	complete
EH111	9280	9080	60	W	120	41.9	90.4	132.3	1000	12-Oct	12-Oct	13-Oct	18-Oct	complete
EH112	9280	9160	60	W	120	35.7	87	122	650	12-Oct	13-Oct	13-Oct	14-Oct	complete
EH113	9280	9240	60	W	160	41.9	168.4	210.3	650	16-Oct	16-Oct	16-Oct	18-Oct	complete
EH114	9280	9320	60	W	120	41.7	108.4	150.1	650	19-Oct	19-Oct	19-Oct	20-Oct	complete
EH115	9200	9200	60	E	180	40.8	144.9	185.7	1000	19-Oct	19-Oct	19-Oct	20-Oct	complete
EH116	9120	9160	80	W	180	41.7	129.8	171.5	1000	21-Oct	21-Oct	23-Oct	24-Oct	complete
EH117	9120	9160	70	E	200	36.4	171	207	1000	25-Oct	26-Oct	26-Oct	28-Oct	complete
EH118	9120	9240	70	E	200	38.7	120.4	159.1	650	21-Oct	21-Oct	21-Oct	23-Oct	complete
EH119	9120	9320	70	E	140	41.7	116.8	158.5	650	23-Oct	23-Oct	24-Oct	25-Oct	complete
EH120	9320	9400	60	W	220	42	168.2	210.2	650	25-Oct	25-Oct	26-Oct	28-Oct	complete
EH121	9320	9320	60	W	120	41	232	273	650	28-Oct	28-Oct	5-Nov	12-Nov	complete
EH122	9360	9240	70	E	200	34.8	127.2	162	1000	28-Oct	28-Oct	28-Oct	30-Oct	complete
EH123	9400	8920	70	E	160	33.4	145.6	179	1000	30-Oct	30-Oct	30-Oct	1-Nov	complete
EH124	9400	9160	70	E	100	34.4	187.6	222	1000	30-Oct	31-Oct	1-Nov	4-Nov	complete
EH125	9400	8920	70	E	120	37.6	88.7	126.3	650	30-Oct	31-Oct	31-Oct	1-Nov	complete
EH126	9480	9080	60	W	100	34	64.8	98.8	1000	30-Oct	31-Oct	31-Oct	31-Oct	complete
EH127	9400	9080	70	E	100	35.7	171.6	207.3	1000	31-Oct	1-Nov	2-Nov	3-Nov	complete
EH128	9480	9160	60	W	100	31.3	101.2	132.5	1000	1-Nov	1-Nov	1-Nov	1-Nov	complete
EH129	9400	9000	70	E	100	34.9	103.1	138	1000	1-Nov	1-Nov	4-Nov	6-Nov	complete
EH130	9000	9680	60	W	600	49.9	550.1	600	1000	1-Nov	1-Nov	2-Nov	12-Nov	complete
EH131	9480	9240	60	W	100	31	77	108	1000	6-Nov	6-Nov	6-Nov	8-Nov	complete
EH132	9360	9820	70	E	130	36	96	132	1000	8-Nov	8-Nov	8-Nov	10-Nov	complete
EH133	9360	9200	70	E	200	35.3	164.7	200	650	9-Nov	9-Nov	9-Nov	11-Nov	complete
EH134	9440	8960	70	E	100	37	74	111	1000	10-Nov	10-Nov	10-Nov	11-Nov	complete

Drilling Totals for 1993.

TABLE 3.1 - ERNEST HENRY DRILLING PROGRESS
(Cont'd)

			PROPOSED			PRE			PRECOLLAR			CORING		
HOLE NAME	NORTH	EAST	DIP	BRG	DEPTH	COLL	CORE	EOH	RIG	START	FINISH	START	FINISH	STATUS
EH135	9440	9200	70	E	130	30.6	124.4	155	1000	11-Nov	11-Nov	11-Nov	12-Nov	complete
EH136	9360	9320	70	E	200	36.7	167.1	203.8	650	11-Nov	12-Nov	12-Nov	17-Nov	complete
EH137	9080	9150	85	W	420	41.8	378.2	420	1000	12-Nov	12-Nov	13-Nov	18-Nov	complete
EH138	40210	9555	90		100	79	0	79	1000	13-Nov	15-Nov	-	-	Water Bore
EH139	9440	9240	70	E	120	30	84.2	114.2	650	16-Nov	16-Nov	16-Nov	17-Nov	complete
EH140	9520	9160	60	E	100	27.3	81.9	109.2	650	17-Nov	17-Nov	17-Nov	19-Nov	complete
EH141	9320	9600	70	W	450	41.6	405.8	447.4	1000	18-Nov	18-Nov	18-Nov	24-Nov	complete
EH142	9520	9200	60	E	100	27.3	75	102.3	650	19-Nov	19-Nov	19-Nov	21-Nov	complete
EH143	9520	9120	60	E	100	5	97.3	102.3	1000	21-Nov	22-Nov	21-Nov	22-Nov	complete
MET 1	9360	9160	90		180	0	183.7	183.7	1000			17-Nov	22-Nov	complete
MET2	9200	9240	90		220	0	239.3	239.3	1000			22-Nov	26-Nov	complete
MET3	9400	9120	90		150	0	138.3	138.3	1000			26-Nov	29-Nov	complete
MET4	9320	9240	90		220	0	204.7	204.7	1000			30-Nov	2-Dec	complete
EH144	40348	9400	90		250	150	100.4	250.4	650	24-Nov	24-Nov	25-Nov	26-Nov	complete
EH145	40170	9750	90		250	106.3	137.1	243.4	1000	25-Nov	25-Nov	27-Nov	29-Nov	complete
EH146	40000	70085	90		250	104.6	141.4	246	1000	26-Nov	26-Nov	30-Nov	2-Dec	complete
EH147	9640	9920	90		250	66	174.4	240.4	650			3-Dec	5/12/93	complete
EH148	9280	9750	90		250	100	149.3	249.3	1000	28-Nov	29-Nov	30-Nov	11-Dec	complete
EH149	9800	9580	90		250	132	115.4	247.4	1000	1-Dec	2-Dec	4-Dec	5/12/93	complete
EH150	40000	9230	90		250	138	111.4	249.4	1000	3-Dec	4-Dec	4-Dec	7-Dec	complete
EH151	9640	9050	90		250	135.5	113.9	249.4	1000	4-Dec	4-Dec	5-Dec	7-Dec	complete
EH152	9670	9390	90		250	106	133.4	239.4	650	4-Dec	5-Dec	6-Dec	7/12/93	complete
EH153	9455	9395	90		250	118	133.5	251.5	1000	5-Dec	6-Dec	7-Dec	12-Dec	complete
EH154	9670	9800	90		250	102	150.4	252.4	1000	5/12/93	6-Dec	6-Dec	8/12/93	complete
EH155	9600	70575	90			60		60	1000	8-Dec	8-Dec			complete
EH156	41100	69900	90			39		39	1000	8-Dec	8-Dec			complete
EH157	42000	69000	90			39		39	1000	8-Dec	9-Dec			complete
EH158	39300	67300	90			60		60	1000	9-Dec	9-Dec			complete
EH159	42000	67500	90			48		48	1000	9-Dec	9-Dec			complete
EH160	40700	67800	90			48		48	1000	9-Dec	9-Dec			complete
EH161	38100	66900	90			58		58	1000	9-Dec	10-Dec			complete
EH162	37325	68250	90			46		46	1000	10-Dec	10-Dec			complete
EH163	37450	69900	90			57		57	1000	10-Dec	10-Dec			complete
TOTAL						3528	9591	13119						

Drilling Totals for 1993.

TABLE 4.2 SUMMARY OF BEST RESULTS : ERNEST HENRY SUPERGENE DRILLING PROGRAMME

EH100A	62.7m @ 1.2g/t Au 126.5 - 189.2m
	13.3m @ 1.8% Cu 118.7 - 132.0m
	35.6m @ 3.9% Cu 160.4 - 196.0m
EH102	78.0m@ 2.8% Cu 99.0 - 177.0m including
	16.0m @ 5.9% Cu 134.5 - 150.5m
	77.8m @ 0.79g/t Au 86.8 - 164.6m
EH102ext	43.1m @ 1.9% Cu, 1.45g/t Au 232.9 - 276.0m
EH103	5.3m @ 1.46% Cu 155.7 - 161.0m
EH104	24.7m @ 1.88% Cu, 0.74g/t Au 137.0 - 161.7m
EH105	No significant mineralisation
EH106a	19.8m @ 1.9% Cu, 0.6g/t Au 82.1-101.9m
	9.5m @ 1.7% Cu, 0.6g/t Au 213.7-223.2m
EH107	7.9m @ 1.87% Cu 71.7 - 79.6m
	26.9m @ 1.06g/t Au 49.1 - 76.0m
EH108	3.1m @ 1.85% Cu 63.6 - 66.7m
	4.4m @ 1.09g/t Au 52.0 - 56.4m
EH108ext	18.9m @ 1.6% Cu, 0.8g/t Au 148.3-167.2m
	6.2m @ 1.4% Cu, 0.7g/t Au 181.0-187.2m
EH109	16.3m @ 8.3% Cu 57.1 - 73.4m
	15.5m @ 3.64% Cu 99.1 - 114.6m
	33.9m @ 1.84% Cu 173.2 - 207.1m
	54.6m @ 1.39g/t Au 50.6 - 105.2m
EH110	24.0m @ 2.57% Cu 84.0 - 108.0m
	9.7m @ 1.25g/t Au 89.0 - 98.7m
EH111	19.7m @ 0.22g/t Au 93.6 - 116.0m
EH112	11.9m @ 0.46g/t Au 43.1 - 55.0m
	8.0m @ 3.1% Cu 47.0 - 55.0m
EH113	13.3m @ 0.76g/t Au 44.7 - 58.0m
	4.3m @ 1.25% Cu 44.7 - 49.0m
	13.0m @ 1.27% Cu 71.0 - 84.0m
	6.0m @ 1.69% Cu 112.0 - 118.0m
	19.6m @ 1.71% Cu 158.0 - 177.6m
	21.3m @ 0.89g/t Au 156.3 - 177.7m
EH114	26.2m @ 0.58g/t Au 123.9 - 150.1m includes 8.9m @ 1.6% Cu 0.87g Au 136.4 - 145.3m
EH115	39.0m @ 0.88g/t Au 40.8 - 79.8m includes 15.9m @ 1.48g/t Au 47.9 - 63.8m; 6.1m @ 3.15% Cu 52.0 - 58.1m
	71.8m @ 2.33% Cu 87.2 - 159.0m
	61.5m @ 0.85g/t Au 97.5 - 159.0m
EH116	18.7m @ 0.91g/t Au 110.2 - 105.1m
EH117	15.7m @ 1.43% Cu 89.4 - 105.1m
	30.6m @ 2.15g/t Au 92.4 - 123.0m
	24.2m @ 1.86g/t Au 128.3 - 152.6m
	13.2m @ 3.77% Cu 150.6 - 163.8m
EH118	18.8m @ 1.72% Cu, 0.71g/t Au 105.2-124m
	29.5m @ 2.26% Cu, 0.84g/t Au 129.6-159.1m
EH119	71.5m @ 1.62% Cu, 0.79g/t Au 87.0-158.5m
EH120	2.05m @ 14.36% Cu, 1.16g/t Au 191.7-193.75m
EH121ext	19m @ 1.75% Cu, 1.1g/t Au 186.0-205.0m including 3m @ 4.6% Cu, 4.4g/t Au 199.0-202.0m
EH124	6.0m @ 1.07% Cu, 1.11g/t Au 41.0- 47.0m
	5.3m @ 1.72% Cu, 0.98g/t Au 51.0- 56.3m
	34m @ 1.31% Cu, 0.72g/t Au 113.0-147.0m
EH125	14.5m @ 1.31% Cu, 0.43g/t Au 52.5-67.0m
	7.1m @ 1.09% Cu, 0.32g/t Au 74.5- 81.6m
EH126	No significant results
EH127	37m @ 3.77% Cu, 1.23g/t Au 39.0- 76.0m
	36m @ 2.06% Cu, 1.04g/t Au 86.0-122.0m
	5m @ 1.12% Cu, 0.48g/t Au 144.0 - 149.0m
EH128	9m @ 1.23% Cu, 1.08g/t Au 35.0 - 44.0m (incl. 3m @ 3.13% Cu)
	8m @ 3.29% Cu, 0.98 g/t Au 49.0- 57.0m
	8m @ 1.8% Cu, 0.31 g/t Au 87.0 - 95.0m
EH129	45.3m @ 1.90% Cu, 0.76g/t Au 34.9 - 80.2m
	11.4m @ 1.55% Cu, 0.71 g/t Au 85.1 - 96.5m
	18.8m @ 2.08% Cu, 0.27g/t Au 105.6 - 124.4m
EH132	7 m @ 1.2% Cu, 0.59g/t Au 102.0-109.0m
EH133	45m @ 1.4 % Cu, 0.47g/t Au 91.0-136.0m
EH134	7.5m @ 1.3% Cu, 0.8g/t Au 44.8-52.3m
EH135	5m @ 1.6% Cu, 0.68g/t Au 82.0-87.0m
	9m @ 1.2% Cu, 0.39g/t Au 109.0-118.0m
EH137	35m @ 1.65% Cu, <0.5g/t Au 111.0-146.0m
EH141	36m @ 1.5% Cu, 0.76g/t Au316.0-352.0m
EH138	Water Bore

EH130, 136}
EH139, 140}No significant results
EH142, 143}

Sterilisation Drilling*

EH145} No significant results
EH153, 154}

The above are calculated by weighted average grade.

** Only four sterilisation were selected for assay; no visible significant mineralisation in the others.*

4.3 METALLURGICAL DRILLING

Western Mining carried out extensive metallurgical test work on primary ore while largely ignoring the supergene resource. For details of the metallurgical work carried out by WMC the reader is referred to the reports listed in Table 3.4 of this report. An aim of this program was to characterise the geology and metallurgical behaviour of the supergene zone. In order to achieve this, four PQ size holes were drilled over the Ernest Henry deposit. The holes lay in a roughly long-sectional axis at 150ø magnetic. The core recovered was logged immediately then transferred to a freezer container for storage to prevent oxidation. Both supergene and primary ore zone material was sampled and despatched to various metallurgical laboratories. Table 4.3 gives details of the nature of the samples, and Table 4.4 presents sample numbers and laboratory facilities where they were processed.

Table 4.3
ERNEST HENRY METALLURGICAL SAMPLING DRILLHOLE LOCATIONS

Hole	N	E	Decl.	TD	Comment
EHMet 1	9360	9160	Vert	183.7m	Well dev'd S'gene Cu-Cc zones underlain by uniform geology/grade in primary ore profile.
EHMet 2	9200	9240	Vert	239.3m	Cc dominant S'gene zone, with consistent Cp grade in primary ore profile.
EHMet 3	9400	9120	Vert	38.3m	Condensed S'gene profile with underlying uniform Cp-Py primary mineralisation. Likely to be Au enriched in upper levels.
EHMet 4	9320	9240	Vert	204.7m	Complex S'gene relationships; carbonate textures in primary zone weakly developed.
TOTAL				766 m	

TABLE 4.4 ERNEST HENRY METALLURGICAL SAMPLING: December 1993

HOLE	CANADA	Sample/MunroZone.	JK Tech	Sample/MunroZone.	L. Griffin: MIM	Ore Type
EHMET3	34-38m Cc-Cu-(Au)	EA19979/ Met.1	46-52m Py-Tr. Cc	EA19992/ Met. 3		1, 7, 3
9400N	38-46m Py (Tr.Cp-Cc)	EA19980/ Met.1				Supergene
9120E	52-64m Cu-Cc(Tr.Py-Cp)	EA19981/ Met. 7				
	87-99m Cp-Py	EA19982/ Met. 10	99-105m Cp-Py	EA19993/ Met. 12		10, 18, 12
	126-138m Py-Cp	EA19983/ Met. 18				Primary
EHMET1	58-70m Cu-Cc (Tr.Cp)	EA19984/ Met. 4	76-80m Cu-Cc	EA19994/ Met. 8		4, 8
9360N			80-82m Cc-Py (Cp)	EA19995/ Met. 8		Supergene
9160E						
	120-132m Cp-Py	EA19985/ Met. 13	Nil requested		133-145m Cp-Py	13, 16
					EA20000/ Met.16	Primary
EHMET4	93-105m Cu	EA19986/ Met. 5	73-79m Cu-Tr. Cc	EA19996/ Met.6		5, 6
9320N						Supergene
9240E						
	169-181m Py-Cp	EA19987/ Met. 17	157.5-163.5m Py-Cp	EA19997/ Met. 14		17, 14, 19
			181.0-187m Py-Cp	EA19998/ Met. 19		Primary
EHMET2	85-97m Cc-Py	EA19988/ Met. 2	Nil requested			2, 9
9200N	156-168m Py-Cp	EA19989/ Met. 9				Supergene
9240E						
	178-190m Py-Cp	EA19990/ Met. 11	200-206m Py-Cp	EA19999/ Met. 15		11, 20, 15
	227-239m Cp-Py	EA19991/ Met. 20				Primary

5. GEOTECHNICAL INVESTIGATIONS

Geotechnical materials and hydrogeological investigations for the Ernest Henry Project were contracted to PPK Engineering Consultants of Brisbane and a number of sampling programmes were carried out on their instructions by the MIMEX team (Sections 5.2-5.4 and Chapter 6).

5.1 GEOTECHNICAL LOGGING (see also 3.3.2)

All of the Ernest Henry Mining drill-holes (prefix EH---) were geotechnically logged routinely. A structural orientation device was constructed to allow orientation of core in real space, taking account of azimuth and angle of drilling. Orientation measurements were taken every 30m or so in core by the drilling crews, using a spear and chinagraph pencil. The method had mixed success, but generally provided reliable measurements.

The dominant fabric in the deposit (Fo' on geotechnical logs) generally dips to the southeast at ~30ø in the northwest, gradually steepening to the southeast to ~45-50ø (see Mawer, 1994 and section 7.4.2 for details). The dominant shear zones are effectively parallel to the main foliation, and also steepen to the southeast within the orebody.

As mentioned in the geological descriptions of Chapter 7, a number of late brittle faults marked by rubble zones were recorded in core. However, few measurements were possible due to the intense fracturing.

Overall rock quality within the orebody is excellent, even within the supergene profile, and generally falls in the 85-95% RQD range. Even in zones of intense jointing and/or faulting the RQD rarely drops below 20%.

The joint pattern is highly regular in the orebody. Five class intervals (Joint 0- Joint 4) of oriented joints were established relative to core axis as shown in Table 5.1 below:

Table 5.1 Joint Orientations: Ernest Henry Core

Joint Class	Angle To Core Axis	Comment
J0	25-30 º	
J1	75-90 º	
J2	45-50 º	most frequent; commonly conjugate set at 90ø
J3	15-20 º	
J4	0-10 º	frequently sheared; strongly slickensided

5.2 TERRAIN DRILLING

As part of overall planning of the Ernest Henry development, a shallow percussion drilling programme of nine holes (440m) was carried out in December in the environs of ML 2671 to determine the depths to the Cretaceous aquifer and Proterozoic basement. These data were required to determine the piezometric level and flow direction of the aquifer, and thus provide information needed for planning the open pit. The drill hole locations are shown on Figure 4.2.

The terrain holes were generally drilled by blading down to basement using a UDR Warman 650 rig. Substantial water was encountered in most of the holes and the flow rates were measured approximately and recorded on-site. Samples were taken at 2m intervals and chip sample profiles of all the terrain holes have been retained.

The terrain holes did not always reach basement as the blade bit was incapable of penetrating the relatively fresh rocks under the unconformity. We know from the percussion work carried out in the sterilisation programme that basement away from the orebody comprises relatively unweathered volcanics and schists.

The depths to the water table are variable, depending on the depths of various sand horizons (Table 5.2); there also appear to be other sources of water at depth in the basement (see Table 5.3). In particular, percussion drilling of sterilisation holes on the northern end of ML2671 encountered high water pressures in Proterozoic basement (DDH EH148, 150 and 152).

As the terrain sampling was conducted off the lease at Ernest Henry, all surplus samples are the property of Western Mining Corporation as holders and managers of EPM 8648. This ground is subject to joint venture with MIM (Mount Fort Constantine JV). Consequently, all bagged samples were returned to the WMC camp at Mount Fort Constantine at the end of the programme. A summary of the programme was sent to Steve Hancock, WMC Senior Supervising Geologist in Townsville.

5.3 MATERIALS SAMPLING

PPK conducted materials sampling through the Phanerozoic cover by a series of trenches and pits, both on and in the environs of ML 2671. These activities were all subject to permission from both the holders of the adjacent EPM, Western Mining Corporation, and the landholders, Stanbroke Pastoral Co.

The results of this work are beyond the scope of this study and the reader is referred to PPK reports for further details.

The Phanerozoic PQ core from two of the metallurgical drill holes (EHmet1 and EHmet3) were examined and logged by PPK. Samples of Mesozoic black shale were taken for strength tests from the remaining metallurgical holes.

5.4 TUBE SAMPLING

Undisturbed tube samples of Phanerozoic cover were required by PPK for shear strength tests, with a view to using some of the material later for construction purposes. However, the rig which was scheduled by PPK to carry out the work (Gemco B2 auger drill rig) was unsuitable without a compressor, while the aluminium tubes were too weak for use with a conventional rotary rig. This work was therefore not completed. Further enquires should be directed to Dr. Sue Henderson at PPK.

TABLE 5.2 ERNEST HENRY TERRAIN DRILLING: WATER DEPTHS								
HOLE	N	E	Depth	Yellow Sand Depth (m)	Black Shale Depth (m)	Basal Sand Depth (m)	Water Depth/Host	Standing Water Level
EH 155	39600	70575	60	18-26m	26-52m	52-60m	22-24m damp; yw sand	No record
							42-44m wet; 1m wh. sand 42m	
EH156	41100	69900	39	20-24m	24-28m	30-36m	28-30 damp; black musc. shale	No record
EH 157	42000	69000	39	18-22m	22-26m	26-34m	12-14m damp;sandy silt	No record
							18-22m damp; sandy conglom	
EH158	39300	67300	60	26-34m	26-32m	42-54m	30-32m wet; gy clay rich silt	21.6m
						54-60m (Si)	54-56m wet; gy sandy silt	
EH159	42000	67500	48	22-26m	26-32m	32-48m	22-26m damp; yw sand	18.2m
							32-34m; gy silty sand	
							36m wet; gy silty sand	
EH160	40700	67800	48	26-36m	36-42m	42-48m	18-20m damp; yw silty sand	18.2m
							26-36m damp; yw sand	
							42-44m damp; gy silty sand	
							46-48m damp; gy silty sand	
EH161	38100	66900	58	26-34m	34-44m	44-54m	24-26m damp; br-yw sand	Hole collapse
							42-44m wet; med gy shale	
							44-54m; damp gy sandy shale	
							55m (6000l/hr); gy sand	
EH162	37325	68250	46	26-35m	35-42m		24-32m damp; yw gritty sands	12m
							32-34m wet; yw sand	
							42-44m wet; gy silt	
EH163	37450	69900	57	30-37m	37-48m	48-56m	30m 500l/hr; yw sand	23.25
							50m 6000l/hr; gy sand	

TABLE 5.3 ERNEST HENRY STERILISATION DRILLING: WATER DEPTHS							
HOLE	N	E	Depth to basement	Total depth	Water/Flow		
EH144	40348	69400	26m	250.4	16-26m damp		
EH145	40170	69750	36m	243.4		Gy sand 32-36m	
EH146	40000	70085	44m?	247.5	42m	Gy sand 36-44m	
EH147	39640	69920	48m	240.4	48m	Water in basal conglom. @ 48m	
EH148	39280	69750	50m	249.3	48-50m 6000l/hr		
EH149	39800	69580	38m	247.4	38m (lots!)	Flow not rec.	
					42m	as above	
					80m 1800l/hr		
					132m 3790l/hr		
EH150	40000	69230	n/s	249.4	42-48m 3000l/hr		
EH151	39640	69050	44m	249.4	135m 2880l/hr		
EH152	39670	69390	32m?	249.4	36-38m	Flow not rec.	
					78-80m	as above	
EH153	39455	69395	30m?	251.5	50m 4000l/hr		
EH154	39670	69800	36m	252.4	53m	Flow not rec.	
					72m 2400l/hr		
					90m 8000l/hr		

6. ENVIRONMENTAL MONITORING

Equipment and procedures were established for the environmental assessment and management of the future mine site, including:

a) collection of samples for the characterisation of leachates from waste and ore dumps; and
b) determination of standing water levels, and on-going investigations into the recharge and fluid flow of the water table.

6.1 WASTE ROCK CONTAMINATION

Core from several holes was selected as representative of Phanerozoic cover, Proterozoic waste rock, and Proterozoic ore material. These were then submitted to Energy Resources, Australia Limited (ERA) for evaluation of likely leachate character and competency of geochemical character.

- ***Phanerozoic (cover)***

Two of the metallurgical holes, EHMET 1 and EHMET 3 sampled Phanerozoic sediments and rocks using triple tube PQ barrels. The holes intersected a sequence of black soils underlain by weakly consolidated orange sandstone, an un-cemented pebble conglomerate, and finally black shales interbedded with green sandy lenses. The material was wrapped in plastic film on recovery and transported to a freezer container where it was kept at an ambient temperature of -5º C.

In addition to the whole core samples, percussion chip samples of Phanerozoic material were collected where possible centred along the 9240 N and 9240 E lines (Fig.6.1). Approximately 100 g of material for each metre interval was sampled and placed in plastic containers and stored at room temperature (÷ 25º C).

- ***Proterozoic***

Quarter-core material was sampled from ore, transitional, and waste zones in both the supergene and primary resource blocks. Samples were collected from three holes across the area of mineralisation to determine any spatial variation in the three rock classes. Hole locations are available in Fig.6.2 and sample intervals listed in Table 6.2.

No results are available from ERA on behaviour of the waste rock material.

6.2 WATER TABLE MONITORING

Preliminary assessment of the water table was carried out during the resource drilling programme. One bore hole, EH 138, was tested for a range of physical properties (Table 6.2), and monitored for draw-down during pumping over a three day period. The results of draw-down are presented as Figure 6.3.

Table 6.1 Physical properties of Water: Ernest Henry EH138 (Dec. 1993)

Conductivity	930ms cm^{-1}
pH	7.9
Eh	166
Temperature	29.1º C
Piezometric Level	22.5m
Flow Rate	1.3 l/sec

TABLE 6.2

Listing of Samples for Environmental Characteristics

Hole Name	Interval	Description
EH 117	107.0-109.0	supergene ore
	60.4-62.4	supergene waste
	191.7-194.7	primary waste
EH 127	46.4-47.0	supergene ore
	37.5-38.2	supergene waste
	88.0-89.0	transition material
	91.95-93.0	primary ore
	130.3-131.0	primary ore
EH 136	45.0-46.0	supergene ore
	57.0-58.0	supergene waste
	142.0-143.0	transition material
	161.0-162.0	primary ore
	179.0-180.0	primary waste
EH 142	71.0-72.0	primary waste

FIGURE 6.3 Drawdown of Water Table during Pumping of DDH EH138

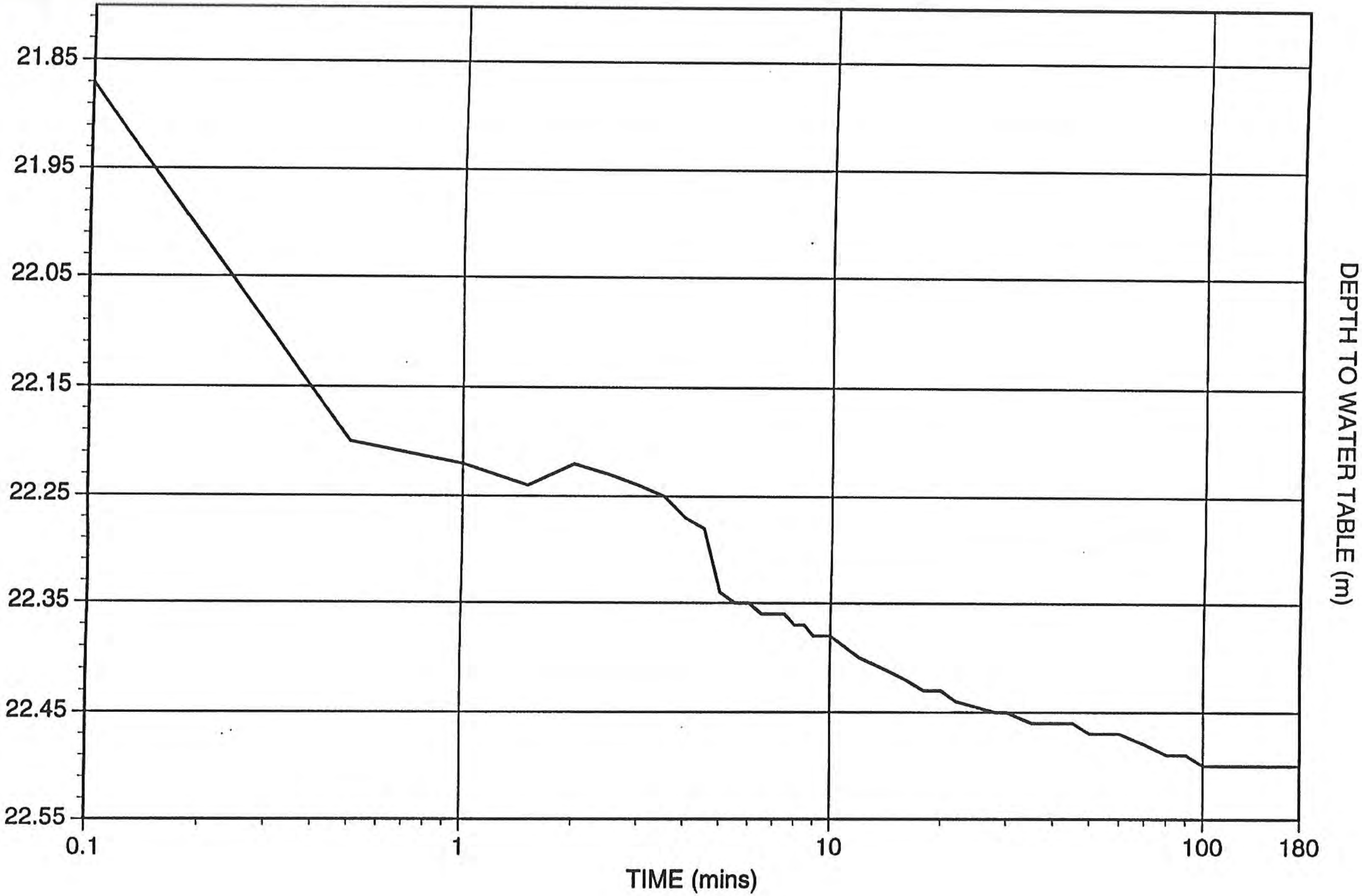

In order to establish flow regimes and recharge patterns, a water monitoring unit was placed within a number of cased holes. These were calibrated for the piezometric level at the time of emplacement, and have been monitoring fluctuations since then. Results from this programme are not yet available.

6.3 WEATHER STATION

Monitoring of the environmental conditions in the vicinity of the mine is currently being undertaken to provide data that may determine scheduling and development of various stages of the mining project. An automatic weather station was supplied by Environdata. The station monitors:

- relative humidity
- solar radiation
- air temperature
- rainfall
- wind direction
- wind speed

Measurements of these variables are made digitally every 15 minutes and the data is then downloaded onto a computer.

6.4 REHABILITATION

In accordance with MIM Exploration environmental policies all sites were kept in a clean and tidy condition. On completion of each drill hole the site was cleared of all refuse, the sump filled, and the pad graded. Prior to withdrawal from the site at the onset of the northern wet season, all pads and access roads were ripped to promote growth within the compacted soil. The site was visited by MIM Exploration Pty. Ltd. geologists on 22 February 1994 and considered to be in a satisfactory condition.

7. GEOLOGY OF THE ERNEST HENRY DEPOSIT

The drilling programme at Ernest Henry, carried out by MIM Exploration on behalf of Ernest Henry Mining, was designed largely to investigate the nature of the supergene profile. In this chapter, a number of observations are recorded concerning mineralogical and geological relationships within both the supergene and primary orebodies. The implications of these observations for exploration are considered in Chapter 11.

7.1 PROTEROZOIC REGIONAL GEOLOGY

The following is taken largely from AGSO Bulletin 243 (Stewart and Blake, 1992), and references contained therein. It concentrates on rocks generally younger than Cover Sequence 1 within the Eastern Succession.

7.1.1 Stratigraphy

The Ernest Henry deposit lies east of the Cloncurry fault zone (or the Cloncurry `Overthrust' of Blake and Stewart, 1992), in a zone of poorly-understood rocks of the Eastern Succession. The stratigraphic position of the volcanics which host the Ernest Henry deposit is unknown, though several authors have speculated that they are equivalent to the felsic metavolcanics which crop out at Mount Fort Constantine, 14km to the southwest of Ernest Henry (e.g. Hronsky, 1993). The Mount Fort Constantine metavolcanics were dated by R.W. Page of AGSO at about 1730ñ10 Ma (R.W. Page, personal communication, 1993). If this is the case, then the Ernest Henry host rocks lie towards the top of the AGSO's Cover Sequence 2 (Blake and Stewart, 1992). It has also been postulated that the Ernest Henry deposit is situated in the roof zone of the younger Naraku Granite, and that the mineralisation is related to, the emplacement of the Williams and Naraku batholiths and associated plutons at around 1500 Ma.

7.1.2 Structure

Most deformation throughout the geological history of the Eastern Succession has been extensional in character, with an intermediate compressional event and a subsequent phase (or phases) of largely transcurrent faulting (Blake, 1987; Blake et al., 1990; Blake and Stewart, 1992; Holcombe et al., 1991; Mawer, 1992b; Oliver, 1992b; Oliver et al., 1991; Pearson et al., 1992). Two phases of rifting and thermal subsidence are postulated between 1790 and 1760 Ma (Cover Sequence 2), with a further significant period of extension being documented post-Cover Sequence 2 and generally spatially associated with granites of Wonga Batholith age (1760-1700 Ma). Further extension is postulated between 1700-1660 Ma, with deposition of Cover Sequence 3-equivalent rocks.

The Isan Orogeny overprints all earlier deformation effects and is interpreted to have occurred between 1620-1520 Ma. This is generally thought to consist of 2 main compressive phases, the earlier directed north-south and the later directed east-west, though evidence for the earlier phase is scanty. The east-west-directed compression developed large-scale, pervasive, north-south-trending, doubly-plunging, upright to reclined folds typical of the Eastern Succession. This compressional event is dated at about 1550 Ma (Page and Bell, 1986).

Emplacement of the Williams and Naraku batholiths and associated plutons at around 1500 Ma implies a further period of crustal extension, though the amount of extension was not necessarily great (e.g., Clemens and Mawer, 1992), and the extension may have been restricted in areal extent to the roof zones of the plutons and their immediate margins.

Subsequent transcurrent faulting has disrupted Isan Orogeny folds and Williams/Naraku-aged plutons. Some of these faults are crustal-scale features (e.g., Quilalar Fault Zone, Pilgrim Fault Zone, etc.), and although undoubtedly Proterozoic in origin, most of these faults have been reactivated several times. Many or most show some Phanerozoic movement, as the regional basal Cambrian unconformity is displaced across them (e.g., Pilgrim Fault Zone).

7.1.3. Igneous Rocks

The Mount Isa Inlier in general and the Eastern Succession in particular, has a long history of igneous intrusion and extrusion. Widespread igneous activity took place during deposition of Cover Sequence 2, with bimodal volcanism occurring at about 1790-1780 Ma (Magna Lynn Metabasalt and overlying felsic metavolcanics of the Argylla Formation). Following this, significant felsic plutonism, minor mafic plutonism, and some felsic and mafic extrusion occurred between about 1760-1720 Ma. During that time, the Wonga Granite, Burstall Granite, Lunch Creek Gabbro, further felsic volcanics of the Argylla Formation, Marraba Volcanics, Toole Creek Volcanics, and numerous small felsic and mafic sills and dykes were intruded or extruded. Age constraints on many of these igneous rocks are poor. The Mount Fort Constantine metavolcanics, with an approximate age of 1730ñ10 Ma (R.W. Page, personal communication, 1993), were extruded during this time.

Minor bimodal volcanics dated at around 1625 Ma are found in the Tommy Creek Block. Several large foliated granitoid plutons (one mapped as Naraku Granite, and the Marramungee Granite and related granites of the Williams Batholith) are interpreted by Blake and others (e.g., Blake and Stewart, 1992) to have been emplaced between about 1680-1620 Ma, though in general Williams- and Naraku-equivalent granitoids are thought to be over 100 m.y. younger than these. This is a considerable problem which needs resolution.

The period between 1540 and 1450 Ma is again interpreted to be a time of significant granitoid intrusion in the Eastern Succession. The main granites of the Williams and Naraku batholiths cut Isan Orogeny structures, and are relatively undeformed and unmetamorphosed. Isotopic dating shows several of these granites to have crystallised around 1500 Ma (see Table 7.1). There are also minor mafic intrusions associated with these felsic intrusions and they are interpreted to be the same age.

Unmetamorphosed dolerite dykes cut all earlier structures and rock types in the eastern Succession, and are interpreted as representatives of the youngest igneous rocks of the Mount Isa Block. These dykes are interpreted to have crystallised at around 1100 Ma.

7.1.4 Radiometric Dating

Reliable radiometric dating of minerals from the Ernest Henry deposit is critical to achieving an understanding of when and how the mineralisation relates to the thermal and metamorphic evolution of the eastern Mount Isa Inlier. In other words, such information helps to refine the genetic models which guide our exploration effort.

Most previous dating in the Eastern Succession has been by either Rb-Sr whole rock or conventional (i.e., digestion) U-Pb zircon methods, with considerable implications for understanding stratigraphic and igneous relationships. Rb-Sr whole rock dates in metamorphosed sequences generally record metamorphic events associated with hydrothermal fluid flow, as the Rb-Sr system is easily reset. This resetting can occur at relatively low temperatures. Conventional U-Pb zircon dates, as they are determined using a population of zircons rather than individual zircon crystals, commonly represent a mixture of ages (inheritance ages, crystallisation ages, and metamorphic ages). Ion microprobe U-Pb zircon dates, combined with careful petrography, stand the best chance of yielding interpretable crystallisation or metamorphic dates, as single zircons (or even single zones within individual zircons) are dated.

There have been few recent radiometric age determinations made in the Eastern Succession. Table 7.1 is a compilation of the most reliable of these dates, but includes several less precise dates for important felsic intrusions where no higher-precision dating has yet been done (data from Hill et al., 1992; Page, 1993; Pearson et al., 1992; Wyborn et al., 1988).

Table 7.1: U-Pb Radiometric Dates, Eastern Succession

Age (Ma)	System	Lithology	Reference
1508±70	U-Pb zircon (conventional) (conventional)	Naraku Granite, main south-eastern pluton	Wyborn et al., 1988
1509±22	U-Pb zircon (conventional)	Yellow Waterhole Granite, southern Williams Batholith	Wyborn et al., 1988
1560+110 -60	U-Pb zircon (conventional)	Wimberu Granite, north-western Williams Batholith	Wyborn et al., 1988
1625±4	U-Pb zircon (ion probe)	felsic volcanic rock,Tommy Creek sequence	Hill et al., 1992
1629±8	U-Pb zircon (ion probe)	mylonitic porphyritic rhyolite, Tommy Creek sequence	Hill et al., 1992
1677±9	U-Pb zircon (ion probe)	Gandry Dam Gneiss, volcaniclastic or detrital component	Page, 1993
1729±5	U-Pb zircon (ion probe)	gneissic microgranite phase, Wonga Granite	Pearson et al., 1992
1730±10 Preliminary	U-Pb zircon (ion probe)	Mount Fort Constantine, metavolcanics	R.W. Page, 1993 (pers. comm.)
1734±6	U-Pb zircon (ion probe)	Gandry Dam Gneiss, provenance terrain component	Page, 1993
1758±8	U-Pb zircon (ion probe)	Wonga Granite, medium-grained microgranite	Pearson et al., 1992

Another dating method, the 40Ar/39Ar technique, can give much precise information about the cooling history of rocks, and it is especially appropriate for rocks containing white micas, dark micas, other phyllosilicates, amphiboles, and some feldspars which have been affected by igneous intrusion.

Dr Caroline Perkins from the Australian National University visited Ernest Henry and collected a series of samples from appropriate rock types for 40Ar/39Ar dating. The sample intervals and types are summarised on Table 7.2 below. In this way we may obtain significant information about the precise timing of introduction of various fluid phases. There are no previously published 40Ar/39Ar dates for the Eastern Succession, though several other studies are underway.

Table 7.3: Samples taken for $^{40}Ar/^{39}Ar$ dating - ANU, November, 1993

Mineral	Drill Hole	down-hole location
biotite	FTCD 28 FTCD 46 FTCD 23	276.0 - 277.4 m 299.7 - 300.7 m 385.9 - 386.9 m
muscovite	EHMet 2 EH 127 FTCD 46	201.7; 201.84 m 81.6 - 82.0 m 275.1 - 275.8 m
amphibole	EH127 EH127 FTCD 23 FTCD 23	91.6 - 91.9 m 124.2 - 124.6 m 529.8 - 530.4 m 534.8 - 535.3 m

7.2 GEOLOGICAL INTERPRETATIONS

Interpretations for each of four geological sections 7738920mN, 7739240mN, 7739320mN and 7739400mN (Figs.7.1-7.4) and a series of plan sections at 50m R.L. intervals (Figs.7.5-7.10) are described below. It is stressed that these are not intended as an exhaustive study of the primary zone. Much of the WMC core through the primary zone must be relogged to validate the geological and structural interpretations, particularly on the southern portion of the orebody. Further drilling may also be required in this area.

7.2.1 Section 7738920mN (Figure 7.1)

Six diamond drillholes for 3627m were drilled on section 8920mN, all of which were drilled by WMC in the FTCD series. This section comprises the most southerly of those fully drilled. A number of the holes were re-logged in February 1994 and the interpretation presented is that of the EHM team.

The geology is dominated by volcanics of probable intermediate composition. There are well- developed amygdaloidal units in the hanging wall sequence frequently associated with discrete porphyritic zones. The Hanging Wall Shear Zone is well developed above the ore zone on this section but shows significant displacement and rotation by late brittle faulting. The sequence passes down through mineralised volcanics with breccia textures and intercalated massive non-mineralised volcanics.

The footwall sequence is marked by intensely sheared volcanics, together with a distinctive metasomatic carbonate unit known as the Marble Matrix Breccia (MMB), (e.g., DDH FTCD 53 and 54). Intensely carbonate-veined FV2 volcanics, typical of the upper gradation into the MMB, is seen stratigraphically below the MMB on the west of the section (FTCD 52, 55). This is due to apparently reverse movement on the Revwood Fault. On the eastern portion of this section, the MMB and related carbonate veining are absent, due probably to steep, apparently normal, faulting within the Badj Kharkl Fault Zone which displaces the Footwall Shear Zone significantly down to the east.

At this northing the orebody is some 200m below the surface, thus there is no supergene ore development (Fig.7.1). However, up to 20m of weathered volcanics occurs just beneath the Mesozoic unconformity. Primary mineralisation, contoured at 0.5% copper, has two lenses in the eastern zone which coalesce up-section to the west, and seem to have largely shear- or fault- bounded upper and lower margins. The ore is terminated sharply on the eastern margin by the Badj Kharkl Fault Zone. On the western margin the ore appears to naturally lens out, but is also terminated by the Revwood Fault Zone. Within the 0.5% copper contour there are zones of > 2% copper which also appear to lie along or adjacent to high strain zones. These shears are sympathetic to the bounding shear zones. Holes' in the otherwise coherent 0.5% grade contour coincide with zones of massive volcanics (FV), where no brecciation has occurred and therefore no mineralisation introduced.

Within the primary zone, the copper to gold ratio is remarkably uniform at 2:1 (e.g., a split with 2% Cu will carry 1g/t Au, see Chapter 8 for detail); consequently, a separate gold contour plot was not produced for this section.

Structurally, three main styles of faulting are evident on this section:

i. generally low angle shears (30-40ø), parallel or sub-parallel to the bounding HW and FWSZ's. In a portion of the HWSZ between 9200E and 9350E, higher angle (60ø) layer-parallel foliation was recorded than elsewhere, which is interpreted to be due to rotation of the block by late brittle faulting;
ii. late, high angle (75-80ø) brittle faults, marked in core by rubble zones, usually with slickensided clasts of the pre-existing shear zones; the hanging wall amygdaloidal units are offset along these faults; and
iii. low angle, late brittle fault zones, which partly exploit the low-angle shear zones, but which may be genetically related to the high angle, extensional brittle zones of (ii) above. The very low-

angle <20ø fault at 350m depth on 9400E occurs in core just below a distinctive green sedimentary unit beneath the upper ore lens and is readily correlatable from FTCD53 to FTCD56.

7.2.2 Section 7739240 mN (Figure 7.2)

A total of 12 diamond drill holes have been completed on the 9240N section. This includes seven by Western Mining Company, one of which was subsequently deepened by Ernest Henry Mining, and five by Ernest Henry Mining. On the western margin the supergene zone comprises a narrow band extending from the Phanerozoic unconformity surface at 45 m to 80 m (FTCD43). No mineralisation of significance was noted in this zone by WMC. Within the primary zone the rocks are dominated by porphyritic felsic volcanics in both FTCD43 and FTCD44, which appear to be truncated by the steep, probably west-dipping, Revwood Fault Zone. Mineralisation appears similarly truncated by the Revwood Fault Zone, although the grade distribution suggests that copper mineralisation is pinching out towards the west of the section (as noted for 8920mN).

The Footwall Shear Zone and Marble Matrix Breccia units are encountered at 260m and 248m respectively in FTCD43, and have an apparent dip of 15ø E in section.

Broad intersections of mineralisation occur in the central part of the section between 9050mE and 9250mE, and include several high grade pods that appear to be approximately flat lying in cross-section. Mineralisation is exclusively hosted in magnetite-carbonate altered volcanics (FV2). Grades increase with an increase in the matrix: clast ratio.

The supergene profile is best developed slightly east of and above the principal primary mineralisation. The zone is dominated by incipiently altered rock (Frox), which is overlain by haematite and chlorite gangue zones (refer Fig.7.2 and refer to section 7.3). The supergene extends to a maximum depth of 155 m below the present surface on this section. Mineralisation is typically higher-grade, but somewhat more erratic than primary mineralisation. Manual contour plots show that supergene copper appears to correlate with the weakly oxidised transition zone (Frox) and the haematite gangue zone. Gold distribution decouples from copper, in contrast to primary mineralisation, and occurs immediately above high grade supergene copper.

An interpreted moderate- to steep-dipping fault penetrated by FTCD46 at 75m forms the eastern margin of the main mineralisation zone. To the east, a series of steep east-dipping normal faults form the Badj Kharkl Fault Zone which downthrows mineralisation eastward as a series of fault-bound blocks. The most easterly occurrence of the Marble Matrix Breccia occurs within FTCD46 at 312 m.

As noted for cross-section 8920mN, sub-horizontal shear zones are common, and are probably cross-cut by late and steep brittle faults.

7.2.3 Section 7739320 mN (Figure 7.3)

Twelve west-dipping and one vertical hole were completed on the 9320mN section. Nine holes were drilled by Western Mining Corporation and four by Ernest Henry Mining, including one metallurgical hole. The Phanerozoic unconformity surface lies between 35-40m.

A prominent feature is a series of foliation-parallel shear zones with a sectional dip of approximately 30ø E. Again, these are probably cross-cut by steep late brittle faults, which in plan display continuity between sections. Supergene weathering is best developed between 9200mE and 9400mE, reaching a maximum depth of 160m. The base of partial oxidation shows considerable topography and may reflect the effects of late brittle faults acting as conduits for oxygenated groundwaters. The alteration style is dominated by iron oxides, with haematite and lesser limonite. Chlorite gangue appears to rim the best developed supergene mineralisation.

Mineralisation is laterally displaced from the best supergene ore (c.f., 9240mN section). However, steep west-dipping faults which bound the mapped extent of the supergene may contribute to the deepening of the profile in this zone. In cross-section, the primary mineralisation forms a roughly oval shape, with a gradual pinching out of high grade zones on the western margin. The Revwood Fault on this section appears to displace pre-existing units (e.g., Marble Matrix Breccia) yet does not seem to offset mineralisation. At the eastern margin the mineralisation is truncated in part, suggesting that a steep late fault of unknown attitude and displacement is present. Until more information is available this remains speculative. Similarly, a large gap in drilling occurs between FTCD16 and EH141, an Eastern Lens exploration hole. A small window of mineralisation bounded by faults forming part of the Badj Kharkl Fault Zone reinforces the observations of the 9240mN section, viz., mineralisation is displaced in a series of downthrown normal faults to the east.

7.2.4 Section 7739400 mN (Figure 7.4)

Twelve holes were drilled on section 9400 mN, six by WMC and a further six by EHM at a 40m spacing to an average depth of 200m. One of the EHM holes, EHMET3, was drilled at PQ size as a metallurgical test hole. The base of partial oxidation varies across the section. It generally occurs at 100m below surface and deeper around major structures.

The Marble Matrix Breccia (MMB) is poorly developed and probably displaced by faulting. However, the Footwall Shear Zone (FWSZ) is well developed and relatively thick. The FWSZ is folded at the eastern end, and this together with the apparent thickness suggests kinking in the third dimension. At the western margin, the Revwood Fault Zone displaces rocks west-block down, whereas on the eastern margin the Badj Kharkl Fault Zone offsets mineralisation and host rocks east-block down. There are numerous other faults and ductile shears with minor displacements. As noted for the previous sections, the ductile shear zones are generally shallow dipping and the brittle faults steep dipping. The fault between holes FTCD41 and EH124 was interpreted from geological and Au-Cu patterns.

7.2.5 Sterilisation Drillhole Features

Most of the alteration styles identified within the immediate environs of Ernest Henry were also recognised in the northern portion of M.L.2671. Carbonate (vein and birdswing-style), muscovite and biotite alteration was noted in almost all of the holes. Intense carbonate alteration was observed at the bottom of EH145 with weak magnetite and minor chalcopyrite mineralisation. Red rock alteration was variable throughout the zone of sterilisation but notably intense in holes EH154 and EH150. Garnet porphyroblasts were observed throughout the area and were often seen to be rotated within the foliation. As garnets occur outside the immediate deposit it is concluded that they are a regional feature and, from overprinting relationships, predate the mineralising event. Magnetite is generally a minor component, however; in the two holes drilled to test the magnetic highs, significant local magnetite was recorded together with biotite alteration (e.g., EH150). Chalcopyrite occurs as veins and disseminations, locally with minor pyrite and pyrrhotite, but in sub-economic concentrations.

The main rock types in the sterilisation area comprise felsic volcanics and biotite-(mt) schists, but brecciated felsic volcanics (FV2) occurs less frequently than at Ernest Henry itself. The main zones of FV2 are in the southern region which is closest to the deposit while in the north, porphyritic felsic volcanics (FVp) and schistose felsic volcanics (FV3) are more common. Intense shearing is evident in several holes, e.g., EH147, 149, 151, which tends to FV3 and mylonitic felsic volcanics (FV4). Spotted Rock occurs only locally and there is a possible MMB equivalent in EH151. Rare amygdaloidal felsic volcanics (FVa) were logged in EH150.

It is concluded from the results of the above drilling that the northern portion of M.L.2671 does not contain economic mineralisation. Similarly, the NE trending magnetic ridge in that part of the M.L. does not host economic mineralisation.

7.3 SUPERGENE ZONE

The supergene drilling programme was largely focussed north of 7739100 mN, as the profile is poorly developed over the southern, deeper portion of the orebody (see Fig.7.1).

7.3.1 Gangue Zone Classification

A sequence of weathering zones with rapid lateral changes has been established for the supergene zone, but it is stressed that complex overprinting relationships and rapid lateral changes imply that a simple 'layer-cake' model is not appropriate for the supergene profile (see gangue zone diagrams in Figs.7.11 - 7.14). The zonation is presented schematically in Table 7.3.

TABLE 7.3 Supergene Gangue Zone Classification

1. CLAY ZONE	Pale grey/white, kaolinite-rich leached zone beneath the Mesozoic unconformity; better developed towards north of body. Frequently gold enriched cap. Rare relict fabric.
2. CHLORITE	Dark to medium green chlorite and septechlorites; frequently leached and vuggy in appearance; remnant felsic volcanic (Fv) clasts evident. Commonly interdigitated with lenses of haematite altered Fv. Coarse native copper and fine grained chalcocite/bornite frequently occur, +/- haematite/magnetite.
3. IRON OXIDE	Brownish- to purplish-red in colour; frequently leached and vuggy in appearance with remnant felsic volcanic clasts. Grossly haematitic in composition, but with complex sub-zones of goethite and/or chlorite. Native copper and chalcocite rich.
~~***Base of Complete Oxidation*** ~~~~~~~~~~~~~~~~~~~~~~~~~~~~	
4. PITTED SILICA	Grey siliceous zone at base of weathering profile, characterised Transition Zone' by pitting and vuggy cavities (≤ 1 - 5cm). Weak cpy-py, cc, Cu.
5. FR-OX	Fresh andesitic volcanics and primary ore with incipient oxidation (e.g., along joints, faults and broken zones)
~~***Base of Partial Oxidation*** ~~~~~~~~~~~~~~~~~~~~~~~~~~~~~~	

7.3.1 Gangue Zone - Sulphide Assemblage Relationships

The distribution of copper minerals and pyrite within the gangue zones (Table 7.3) is complex. WMC identified broad mineralogical associations within the supergene profile based largely on petrographic observations (brackets indicate minor component):

- chalcocite/pyrite (cc/py)
- chalcocite/ (native copper) (cc/(Cu))
- chalcopyrite/pyrite (cp/py)
- pyrite/ (chalcopyrite) (py/(cp))

The WMC scheme was applied and in the current study and expanded to allow for all combinations of sulphides and native copper (refer Table 3.3). Thus, all sulphides and native copper were recorded in terms of their relative abundances for each split of core. This information provides the basis for an examination of sulphide assemblage and gangue zone relationships.

The relative proportions of the different gangue zones are depicted in Figures 7.11-7.14, and also Figure 7.15, which is a bar chart of all assayed splits classified according to logged gangue zone and the observed sulphide assemblage.

The relative proportions of sulphide assemblages by gangue zone are highlighted in Figure 7.16. This diagram supports the simplified model of the supergene zone (Table 7.3) in that the proportions of sulphide-bearing splits decrease in successive gangue zones towards the surface (e.g., the uppermost clay zone is the most intensely weathered).

As might be expected, the transitional area between the bases of complete and partial oxidation contains proportionately the most total sulphide; and together with the silica zone, proportionately the most pyrite. Significantly, the relative proportions of native copper-bearing to chalcocite-bearing splits vary little throughout the supergene zone (Fig.7.16). This feature, as well as the relatively consistent proportion of pyritic splits in each gangue zone above the base of complete oxidation, indicates that the gangue zones of the supergene profile do not correspond to systematic changes in ore mineralogy.

7.3.3. Metal Distributions by Gangue Zone

A brief examination of the mean metal abundances of each gangue zone (refer Table 7.4) reveals :

a) a progressive increase in the Cu/Au ratio with depth from the clay zone at the top of the supergene profile to the silica zone; this feature reflects the greater susceptibility of Cu to supergene mobility and enrichment than Au.

b) that the Cu/Au ratio of the clay zone is distinctly lower than that for primary ore (÷2:1), indicating the preferential leaching of Cu relative to Au;

c) that Cu is relatively enriched and Au relatively depleted in the silica zone compared to the chlorite and iron oxide zones, indicating that Au mobility and enrichment was confined largely to above the silica zone; and

d) like Cu/Au, Cu/As ratios also increase with depth; the Co pattern is similar, except in the silica zone where mean Co levels are highest for the deposit; this feature reflects the local abundance of almost massive secondary pyrite in the silica zone.

Point (c) is emphasised by Cu/Au ratios of >200 in the Frox zone of DDH EH109 (section 7.3.4), a zone which, prior to supergene alteration, was probably not mineralised. Table 7.4 also shows how total iron varies sympathetically with copper, and more importantly, how mean iron levels vary by only 2 or 3

FIGURE 7.15 Sulphide distributions according to gangue zone

Gangue Zone	Chalcocitic	native Cu	Chalcopyritic	pyrite	no sulphide	totals
clay	14	12	0	16	67	109
chlorite	67	46	24	115	362	614
Fe-oxide	91	97	29	95	231	543
silica	33	34	31	75	82	255
Frox	50	51	255	317	180	853
Fresh	6	10	942	450	551	1959
				Total number of splits		4333

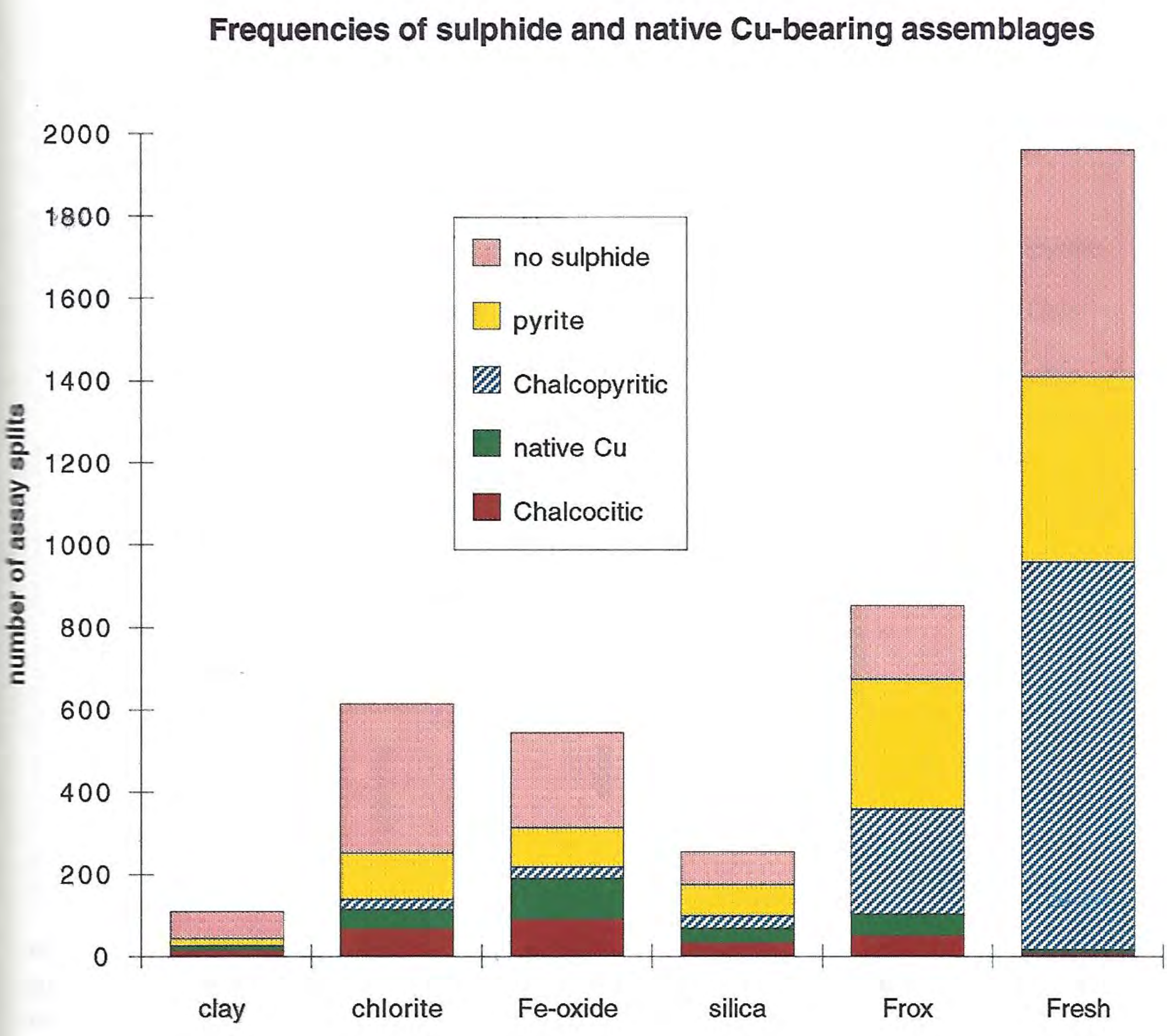

See Figure 7.16 for explanation of legend

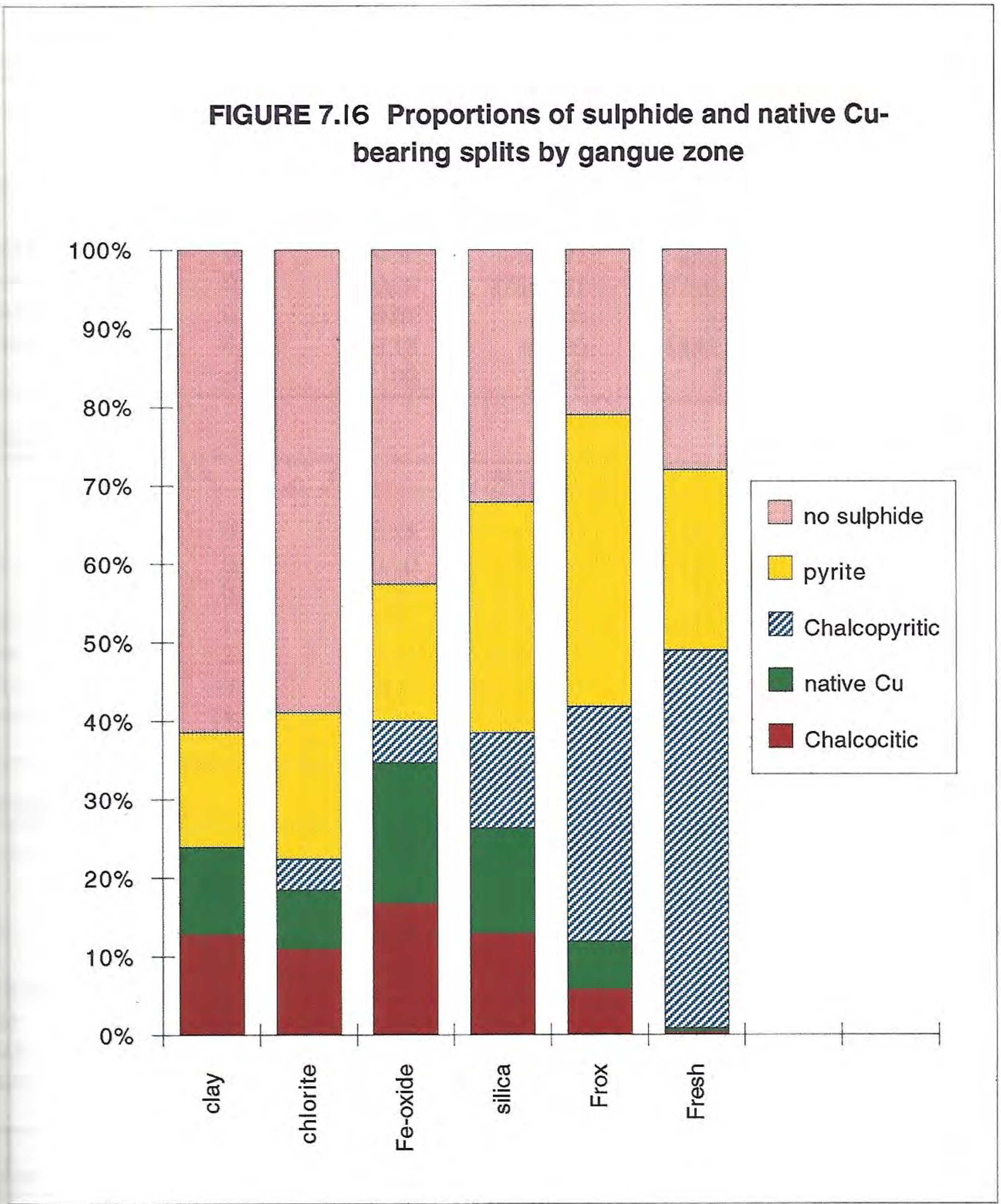

no sulphide	no observed (logged) sulphide or native Cu
pyrite	pyrite the only sulphide observed
chalcopyritic	observed chalcopyrite or (chalcopyrite + pyrite)
native Cu	native Cu observed alone or with chalcocite or pyrite
chalcocitic	observed chalcocite or (chalcocite + pyrite) or (chalcocite + chalcopyrite)

TABLE 7.4 Summary assay statistics by logged gangue zone

ay zone

	copper (%)	*gold (ppm)*	*arsenic (ppm)*	*cobalt (ppm)*	*manganese (ppm)*	*iron (%)*
ean	0.34	0.21	103.96	186.43	1197.06	14.10
edian	0.14	0.11	30.00	138.00	620.00	15.00
ode	0.07	0.01	10.00	40.00	50.00	15.00
ndard Deviation	0.65	0.30	166.97	222.98	1348.30	4.80
riance	0.42	0.09	27878.81	49720.86	1817919.08	23.02
nimum	0.01	0.01	10.00	5.00	30.00	2.07
ximum	4.31	2.13	760.00	1350.00	7450.00	26.10
unt	109	109	109	109	109	109

lorite zone

	Cu	*Au*	*As*	*Co*	*Mn*	*Fe*
an	0.81	0.44	125.94	252.31	1209.63	17.44
dian	0.21	0.10	50.00	160.00	575.00	16.65
de	0.03	0.01	10.00	70.00	110.00	17.00
dard Deviation	1.70	0.73	207.38	282.50	2035.85	7.74
ance	2.88	0.53	43005.18	79803.87	4144688.81	59.98
mum	0.01	0.01	5.00	5.00	10.00	3.00
imum	14.90	6.62	2400.00	2510.00	23400.00	40.80
t	613	614	610	614	614	614

nite/haematite zone

	Cu	*Au*	*As*	*Co*	*Mn*	*Fe*
	0.94	0.39	142.38	287.16	1060.03	18.53
ian	0.20	0.12	40.00	184.00	680.00	17.00
e	0.03	0.01	10.00	80.00	280.00	17.00
lard Deviation	1.98	0.58	293.38	270.62	1210.58	7.65
nce	3.92	0.34	86070.57	73233.21	1465496.47	58.49
num	0.01	0.01	5.00	12.00	30.00	4.00
num	19.90	5.06	3320.00	1610.00	12800.00	46.90
	543	543	543	543	543	543

a zone

	Cu	*Au*	*As*	*Co*	*Mn*	*Fe*
	0.75	0.24	136.56	392.23	1455.50	15.39
ian	0.38	0.12	60.00	284.00	850.00	15.00
e	0.10	0.01	10.00	140.00	310.00	16.00
rd Deviation	1.12	0.31	194.15	393.02	2393.26	5.45
nce	1.26	0.10	37695.29	154466.78	5727672.77	29.74
m	0.01	0.01	5.00	12.00	40.00	5.00
num	8.10	2.30	1710.00	3870.00	25500.00	36.00
	255	255	255	255	255	255

x zone (partly oxidised/pitted rock above BOPO)

	Cu	Au	As	Co	Mn	Fe
an	0.55	0.23	173.07	386.26	1434.74	16.97
dian	0.18	0.06	40.00	234.00	1000.00	16.00
de	0.05	0.01	10.00	80.00	300.00	15.00
dard Deviation	0.87	0.38	316.42	443.90	1474.46	7.30
iance	0.75	0.14	100124.23	197047.78	2174043.98	53.32
imum	0.00	0.01	5.00	5.00	5.00	2.00
imum	7.90	2.96	3200.00	4990.00	25870.00	50.00
nt	851	853	853	853	853	853

sh rock (below BOPO)

	Cu	Au	As	Co	Mn	Fe
	0.33	0.15	133.47	224.16	2027.15	14.57
an	0.08	0.03	20.00	94.00	1300.00	13.60
e	0.01	0.01	10.00	30.00	760.00	13.00
dard Deviation	0.57	0.28	358.72	284.67	2228.89	6.36
ce	0.32	0.08	128681.73	81038.65	4967949.00	40.39
num	0.00	0.01	5.00	4.00	90.00	2.00
num	6.70	4.32	7680.00	2540.00	22500.00	45.00
nt	1950	1959	1959	1959	1959	1959

wt.% throughout the supergene zone (excluding the volumetrically minor clay zone). This observation is consistent with those of section 7.3.2.

7.3.4 Differentiation of Gangue Zones

As part of the characterisation of supergene materials, pulps from DDH EH102 and 109 were systematically analysed by X-ray diffraction and for the major rock-forming elements. The primary aim of the investigation was to establish whether the observed gangue zones correspond to significant mineralogic and/or chemical changes that may influence the metallurgical treatment of ore, or possibly open-cut operations (see original proposal, Hannan, 1993a).

- ***Quantitative XRD analysis***

Calculation of the modal mineralogy of each assay split (Appendix IIIa) required both XRD analysis and major element and sulphur assays (also Appendix IIIa). Chemical analyses are also available on computer file for DDH EH113 and EH121; it was decided not to proceed with the XRD analysis of this material after treatment of the results from the first two drill holes.

The methodology and assumptions made for the calculations of the modal mineralogies tabulated in Appendix IIIa are outlined in two AMDEL reports (Till, 1994a, b).

Although the XRD results confirm that each gangue zone tends to be dominated proportionately by its mineral namesake, it also clearly demonstrates the gradational character, both mineralogically and chemically, between gangue zones. For example, the silica zone of EH109 has splits with modelled quartz contents of between 5 and 47%, the iron oxide zone 3 and 38% and the chlorite zone between 10 and 30%. For modelled haematite contents, each zone contains between 1 and 37%, 2 and 43%, and 1 and 39%, respectively.

An examination of the mean abundances of the more important major elements reveals clear differences in mean Si, Fe and K abundances between the chlorite zone and unweathered splits (Fr zone) of EH109 and, by contrast, a lack of change between the various gangue zones logged along DDH EH121 (Table 7.5). There are also contrasting mean K abundances in the iron oxide zone splits from EH109 and those from EH102, 113 and 121. Clearly, of the four drill holes, the chlorite zone is best developed in the core of EH109 which contains minimal K-feldspar.

Despite the generally inconclusive nature of the results, XRD analysis has emphasised, and to some extent quantified, the extreme chemical and mineralogical variability of the supergene zone at Ernest Henry. Such variability is consistent with the observed unpredictability of copper sulphide and native copper distributions in the supergene zone (section 7.3.2).

- ***Statistical analysis of whole rock geochemical data***

Descriptive statistics, by gangue zone, of major element, sulphur, copper nad gold assays of splits from DDH EH102 and 109, as well as the results of principal components analysis of the chemical compositions and inferred mineralogy of each gangue zone are available in Appendix IIIb.

A first pass examination of the principal components analysis follows.

Fr/Frox splits

Splits classified as unweathered (Fr) from EH109, and to a lesser extent the transitional (Frox) splits of EH102, have first components with opposing loadings that reflect an antipathetic relationship between the feldspathic host volcanics and carbonate-magnetite-sulphide mineralisation. That is, SiO_2, Al_2O_3, Na_2O and K_2O have loadings strongly opposed to CaO, FeO, CO_2, S, Cu and Au. Significantly, P_2O_5 has a mineralisation-like loading, albeit weaker.

The Fr splits of EH109 have a second principal component with a strong MgO and K_2O association, possibly indicating the influence of biotite.

TABLE 7.5 - MEAN MAJOR ELEMENT COMPOSITIONS OF GANGUE ZONES

	SiO_2	Al_2O_3	FeO	CaO	TiO_2	P_2O_5	Na_2O	K_2O
DDH EH 109								
Clay								
Chlorite	34.6	11.7	25.8	0.8	1.0	0.23	0.1	0.62
Fe Oxide	49.1	12.1	14.8	1.1	1.2	0.23	0.3	7.4
Silica	48.5	10.2	17.1	0.4	0.9	0.20	0.2	6.9
Fr	58.3	12.8	9.8	4.2	0.6	0.17	4.5	2.17
DDH EH 102								
Clay								
Chlorite	41.1	10.6	18.9	1.2	1.0	0.49	0.2	5.2
Fe Oxide	38.0	8.3	23.3	1.4	0.7	0.82	0.2	4.5
Silica	48.2	11.8	14.2	1.1	1.1	0.48	0.4	7.5
Fr	50.1	13.5	11.7	0.5	1.3	0.20	0.3	9.2
DDH EH 113								
Chlorite	47.8	12.5	22.2	1.2	1.1	0.28	0.2	4.7
Fe Oxide	55.5	12.4	15.8	0.7	1.0	0.30	0.3	8.3
Silica								
Frox	49.8	9.0	27.6	0.9	0.7	0.18	0.2	5.9
Fr	48.8	12.3	20.9	1.8	0.7	0.23	0.2	5.3
DDH EH 121								
Chlorite	49.6	13.5	19.4	0.84	1.4	0.13	0.3	9.0
Fe Oxide	49.3	13.0	19.9	0.9	1.3	0.13	0.3	9.4
Silica	50.0	13.0	20.2	0.5	1.2	0.13	0.3	9.8
Frox	47.5	13.0	20.8	1.7	1.2	0.23	0.3	9.6

Chlorite Zone

Component 1 comprises strongly opposed loadings between groups of elements associated with precursor feldspar (plagioclase, microcline) and sulphide-berthierine (i.e., Si-Al-Na-K versus Fe-Cu-Au-S).

The second component highlights opposing Ca-P-CO2-(Mg) and Cu-S associations which suggest that secondary carbonate- and apatite- (primary?) rich parts of the chlorite zone are less favourable sites for supergene sulphide (and Au in the case of EH109).

Iron Oxide Zone

These splits have similar multivariate characteristics to the chlorite zone, although loadings on Cu and Au are weaker. For EH109 splits, the loading of S is even weaker, suggesting the presence of native copper.

As observed for the chlorite zone, Au and S can have opposed loadings in the second component (EH109).

Silica Zone

The first component comprises opposing Ca-Fe-P-CO2-(Mg) and K-Al-Ti-Si associations, similar to the secondary carbonate factor calculated for chlorite zone splits. In other words, much of the chemical variability of silica zone splits reflect the effects of secondary carbonate (and residual apatite?) alteration of a rock dominated by feldspar.

7.3.5 Supergene ore mineralogy

This section aims to present a synthesis of observations in core and petrographic thin section. The reader is referred to the petrographic reports by WMC petrologists, Dr. Croxford and MIM petrologists for detailed descriptions and interpretations.

- ***Copper Mineralogy***

Petrographical studies by both WMC and EHM indicate that a series of oxidation/reduction events have affected the supergene profile leading to a complex overprinting pattern of sulphides (Clarke 1993, Knights 1993a, 1993b, Landmark 1993a,b, 1994).

The dominant copper species in the supergene profile are chalcocite (not djulerite - Knights 1993b), digenite and secondary bornite, and erratically distributed coarse native copper. Knights (1993b) observed that between 10-15% of chalcocite identified by the naked eye is fine-grained bornite. Clarke (1993) established a sequence of alteration, substantiated by Landmark and Knights (op. cit.), whereby the primary mineralogy was destroyed by oxidation and dissolution of sulphides, with subsequent volumetric changes opening up fractures and cavities, which were then partially filled by secondary minerals. Multi-generational fracture/fill sequences are observed in thin section.

As shown in sections 7.3.2 and 7.3.4 there is no predictable pattern of distribution for any of the copper minerals relative to host rock types (i.e., gangue zones). For example, native copper-rich intervals are present, but they show little continuity either vertically or horizontally.

- ***Iron Oxides***

The iron oxides in the supergene profile display similar complexity to the copper sulphides. The primary magnetite in the orebody is largely oxidised to haematite and/or goethite through a series of phases (refer to WMC reports by Clarke), which is reflected in the magnetic susceptibility values. Occasionally, primary magnetite remains above the base of partial oxidation (Table 7.3; and refer to Landmark 1993b).

- ***Carbonates***

Secondary carbonates as calcite and siderite are ubiquitous throughout the supergene altered rocks and locally act as favoured sites for the precipitation of chalcocite and bornite. It occurs as yellow filamentous webbing throughout the chlorite and iron oxide gangue zones. Copper carbonates are not observed in the supergene profile, which suggests that conditions of supergene development were too acidic for the stabilisation of malachite. The siderite is largely a manganoan variety. The presence of large amounts of carbonate will probably cause enhanced acid consumption during leach-processing of supergene ore.

7.3.6 Evolution of the supergene zone

As mentioned above, the development of the supergene profile at Ernest Henry is the result of several chemical alteration events affecting the ore body. Clarke (1993) describes a postulated evolution of the supergene weathering profile at Ernest Henry, and his work is drawn on here.

Exposure and weathering began prior to the Cretaceous transgression, although the timing of this event is poorly constrained. During the first phase, chalcopyrite was oxidised and later precipitated as chalcocite and other secondary copper species. The sulphidic character of the copper species and ferrous nature of the gangue infers that the fluids were still at least weakly reducing during weathering.

The onset of the Cretaceous transgression occurred with little erosion, as indicated by preservation of vadose textures (Clarke, 1993). Reduced sediments were laid down over the deposit. Phreatic fluids were able to pass through the sediments and into the ore body along fracture zones, in turn becoming reduced and further modifying the sulphides. This is manifested as overgrowths of carbonates and clays on the vadose textures and local reduction of chalcocite to secondary chalcopyrite (Clarke, 1993). Any native copper formed during the previous oxidation event was probably reduced to chalcocite.

After marine regression and Cainozoic uplift, further oxidation continued along faults and joints. This resulted in the development of broad bands of iron oxides, principally precipitating as haematite and goethite. This phase of oxidation also resulted in the formation of native copper from secondary copper sulphides within the iron oxide-rich gangue.

Primary features of the host rock are variably preserved within the supergene profile. Porphyritic bands and amygdales rarely occur, in contrast with the margins of the supergene zone, where correlation of such units can be made over 40-120 m (see cross-sections for details). Elsewhere, relict breccia clasts of the pre-existing magnetite-chalcopyrite felsic rock are apparent.

This above history of weathering of the Ernest Henry deposit clearly simplified. The local Eh-pH controls on the oxidation process at the time of the weathering were probably dependent on the fracture permeability and thus rock buffering effects. These fluctuated rapidly both laterally and vertically, and produced the complex supergene pattern observed today. The process may be summarised in the diagram below:

primary mineralisation	chalcopyrite + pyrite			
first oxidation phase	chalcocite		native copper	
burial, weak reduction	chalcocite	2° chalcopyrite	chalcocite	
second oxidation phase	native copper	chalcocite	chalcocite	native copper

7.4 THE PRIMARY ZONE

This study did not endeavour to rigorously investigate the nature of the primary mineralisation at Ernest Henry. The reader is referred to section 7.2 of this report and Hronsky (1993) for more discussion of the geology and primary ore of the Ernest Henry deposit. An extensive petrographic examination of primary zone ore and host rocks is reported in Croxford (1994), this information had not received due attention on the completion of this report.

7.4.1 Rock types

- ***Intermediate Volcanics***

The main rock type present in the orebody is altered, variably brecciated, porphyritic andesite with localised flow banding, amygdales and interbedded fine-grained sediments. A number of porphyritic and amygdaloidal units are correlatable in drill core, and may support evidence of high-angle late faulting (see below). The amygdaloidal units largely concentrate in the hangingwall sequence (see Fig.7.1), but do not form a single marker horizon as suggested in earlier work by WMC. The apparent concentration of amygdaloidal volcanics in the hanging wall may also reflect preservation of primary textures outside the zone of mineralisation, compared with their destruction in the mineralised sequence.

- ***Marble Matrix Breccia***

The Marble matrix Breccia (MMB) in the footwall sequence of the orebody is a granular, coarse-grained carbonate rock, interpreted as a metasomatic product developed along a shear zone. It locally contains volcanic clasts rimmed by biotite ñ magnetite ñ chlorite. Its precursor is considered to be a zone of intensely carbonate-veined volcanics and lesser sediments below the ore lenses. MMB is characterised by banded swirling textures and local folding, indicating that ductile deformation continued during its formation. This relationship to earlier veining is seen in numerous drillholes (Fig.7.1; FTCD53, FTCD56). A 10-12 cm wide carbonate-haematite vein was identified in a number of drillholes just above the MMB (e.g., FTCD5, FTCD15), and may prove useful as a marker unit. The MMB is intrinsically related to the footwall shear zone and ramps northwards to shallow depths subparallel to the shear zone (Fig.7.4, c.f. Fig.7.1).

- ***Footwall Siltstone***

This horizon was recorded by WMC at the base of the sequence, and is a distinctive marker unit. The siltstone is grey-green to pale grey in colour, thinly bedded and locally cross-laminated and frequently contains a shaley component. It is sometimes replaced by carbonate and therefore locally transitional, like the volcanics, to MMB

7.4.2 Structural Features of the Primary Zone

- ***Fabrics***

Mineralisation at Ernest Henry is developed in a south-easterly-plunging body of altered and variably brecciated intermediate volcanics. The deposit is bound, above and below, by two foliation parallel shear zones - the Hangingwall Shear Zone and the Footwall Shear Zone - which strike north-easterly and dip shallowly to the southeast, steepening at depth. The Hangingwall and Footwall Shear Zones probably represent an intensification of the dominant foliation and are annealed throughout. The north-easterly strike of these structures is evident in the magnetic images of the area. Throughout the deposit, away from the main shear zones, are numerous smaller-scale and similarly oriented zones of intense foliation. All show kinematic evidence of reverse shearing (i.e., south block up to the north). All reverse-sense shearing in the deposit environs, both in the Hangingwall and Footwall Shear Zones and that distributed throughout the deposit in smaller-scale shear zones, is therefore likely to be synchronous and kinematically linked.

Mawer (1993) documented two tectonic foliations in the Ernest Henry rocks. The earlier foliation is weak and only very sporadically developed (or preserved). If this foliation was originally pervasive, it has been overprinted or destroyed by subsequent deformation. It is associated with a high-grade metamorphic event, during which garnet and fibrolitic (?) sillimanite aggregates grew, but its overall significance is unknown. The later foliation is pervasive and moderately- to well-developed throughout the entire lithological package, except in massive porphyritic andesites which preserve primary textures. This foliation is sympathetic to, and probably synchronous with, the major shear zones described above, although Mawer does not explicitly correlate the foliation with major structures. It is also pointed out that Hayward (1992) described the weak foliation as postdating and crenulating the dominant foliation.

In many places, there is also a weak- to moderately-developed extension lineation on the main foliation. The foliation dips moderately to the south-east, and the extension lineation plunges moderately to the south-east within this foliation. The Ernest Henry ore body is roughly parallel to the extension lineation. Mawer concluded that this strongly suggests a causal link between the strong foliation and lineation, and formation of the Ernest Henry ore deposit.

In long section the ore lenses are broadly parallel to the Footwall and Hangingwall Shear Zones, while in cross-section the ore lenses are often bound by narrower zones of intense foliation. This suggests that ductile structures were critical to the emplacement of mineralisation. Later brittle zones of unknown sense of movement, sub-parallel to the shear zones and with strongly slickensided clasts in the fault rubble, are interpreted to postdate these shears (e.g., Fig.7.1).

It is suggested that the reverse sense Hangingwall and Footwall Shear Zones formed in an overall extensional regime, within a locally developed low-angle compressional zone, reversing an earlier low angle extensional fault close to the roof zone of an igneous intrusive (Fig.7.17). To the south of Ernest Henry there is evidence in outcrop (Paul Pearson, pers. comm. 1994) at Courtenay Creek that low angle reverse sense shears occur in Corella Formation calcsilicates, just above the contact with Naraku aged granites. Thus, compressional regimes may co-exist in the essentially extensional regimes of granite emplacement. A reverse sense shear may have developed a zone of dilation (or jog) in the main structure at Ernest Henry, causing brecciation in the enclosed zone. Sub-parallel shears developed within the dilatant zone, enclosing separate lozenges' of brecciated host rock in which mineralising fluids could precipitate copper, gold and iron oxides (also Fig. 7.17).

The entire package was then faulted by late, high angle brittle fault zones which offset the mineralisation and explain rapid decreases in grade on the eastern margin (see section 7.2 for descriptive details). The east-dipping Badj Kharkl Fault Zone has an apparent normal displacement of at least 200m. The displacement and sense of movement on the western Revwood Fault Zone is unknown. Clearly, these late brittle structures have modified the morphology of the deposit to some extent, as well as being important in geotechnical management of pit design (c.f., Hronsky, 1993).

The paragenetic sequence of structures at Ernest Henry and their relationship to regional structures and deformation fabrics needs to be fully investigated in order to fully understand the deposit and aid the search for, and discovery of, more copper-gold deposits.

- ***Textures***

The overall progression from massive volcanics (FV) through to altered and breccia-textured volcanics (FV2) is largely a chemical effect (i.e., metasomatic) rather than a mechanical brecciation. Although FV1 (crackled felsic volcanics) represents a brittle fracturing of the rock, no significant rotation of clasts is observed in the progression through to brecciated volcanics (FV2). The hairline fractures developed in FV1 acted as conduits for mineralising fluids, which in turn digested the clasts to the varying degrees seen in core. The degree of digestion is critical, because increasing matrix to clast ratios generally correspond to higher grades of copper and gold.

There are no consistent overprinting relationships between carbonate-dominated veining and breccia matrix development of FV2; this, together with observed textural progressions from veined rock to

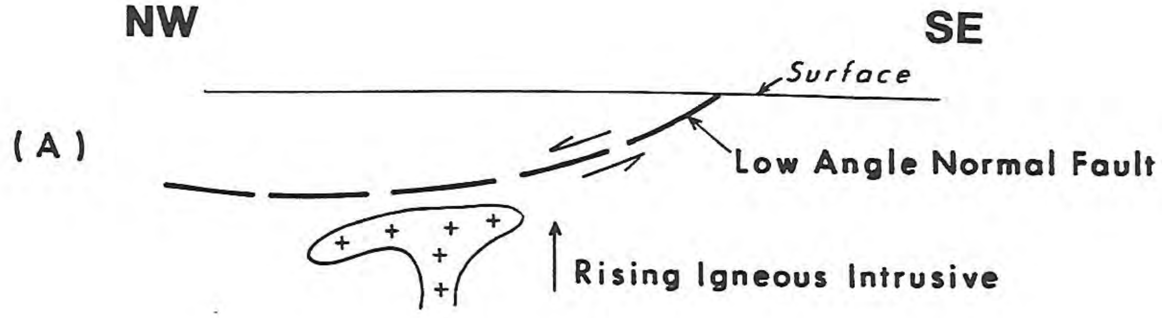

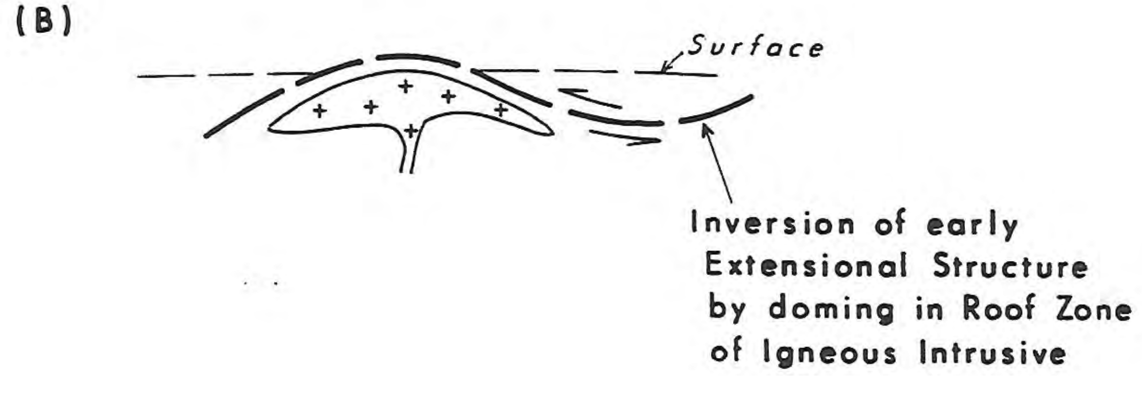

Figure 7.17

STRUCTURAL MODEL FOR DEVELOPMENT OF LOW ANGLE REVERSE–SENSE SHEARS

(After Pearson)

Drg.No. 43198

matrix-supported breccia, is a strong indication that veining and brecciation are due to the same processes, operating at the same time.

In the same way that a textural continuum is observed between FV and FV2, there is a continuous and complete gradation from weakly-veined volcanics through increasing degrees of veining to carbonate-matrix-supported volcanics logged as Marble Matrix Breccia. There is no indication of any original protolith to the `marble matrix breccia' other than the host volcanics, and locally, minor sediment. The only differences between what is logged as volcanic rock on the one hand and `marble matrix breccia' on the other are the greater degree of carbonate introduction, the stronger alteration, and the more intense and concentrated ductile deformation in the `marble matrix breccia'. The latter has undergone pervasive ductile deformation, and represents a shear zone with unknown but potentially large displacement.

- ***Other discussion***

Mawer (1994) argues that early normal faulting associated with igneous intrusion assisted in emplacement of the mineralisation and predates the ductile shears (in contrast to Mawer, 1993, see above). The extension associated with this normal faulting caused brecciation of the host rock (FV1-FV2; Table 3.3). However, Mawer (1994) acknowledges that there is little evidence for such extensional bounding structures. As noted above, the reverse sense shear zones are observed in core to represent a gradual increase in strain from volcanics through to mylonitised volcanics (FV4; Table 3.3), and there is little evidence in this sequence of textures to indicate pre-existing brittle faults. If the early normal faults did exist, there have been at least two later phases of reactivation: the first marked by the compressional sinistral shears parallel to the bounding hanging wall and footwall shear zones and the second another brittle phase of unknown sense of movement.

Mawer (1993) observed that in some parts of the core, the sulphide mineralisation is foliated and folded, indicating that some ductile deformation post-dated mineralisation. As this textural relationship is identical to relationships seen in unmineralised core (i.e., some ductile deformation prior to veining and brecciation, the majority syn-veining and -brecciation, and some post- the majority of brittle deformation), it is concluded that the deposit does not seem to have suffered major post-mineralisation ductile deformation.

7.4.3 Mineralogy of the Primary Zone

- ***Ore Assemblage***

The ore assemblage is dominated by chalcopyrite within a magnetite-carbonate gangue. Pyrite is locally abundant, but typically decreases volumetrically in proportion to increasing chalcopyrite. Gold is chiefly contained within chalcopyrite, although detailed microprobe analyses have indicated that pyrite and haematite may locally be important sites of gold mineralisation (Clarke, 1993). No other sulphides or oxides of economic importance have been noted within the ore zone, although systematic analysis for rare earth elements (REE) or platinoids has not been carried out. REE's associated with locally abundant apatite may add credits to the concentrates.

Mineralisation is located almost exclusively in altered and brecciated volcanics (FV2), but occurs locally in higher strain (FV3) zones. The copper and magnetite-carbonate are considered to be coeval. High-grade intersections may occur with or without carbonate, although away from the highest grade ore, chalcopyrite is rarely seen without carbonate. It is important to note, however, that carbonate alteration (birdswing'-style) with little or no sulphide is commonly observed in the sterilisation drillholes of ML2671.

- ***Magnetite***

Magnetite is significant in that, as mentioned above, the copper grade increases with increased matrix, percentage of magnetite and therefore specific gravity. Average magnetite contents in the primary ore range from 12-15% (Lockwood, 1994). In the MMB, magnetite also occurs as a minor component with low-grade chalcopyrite mineralisation. No investigations have been carried out to date on the viability of magnetite as an economic commodity. Calculation of the magnetite resource may be possible from the magnetic susceptibility readings made routinely during the logging of drill core (refer to section 10.1).

- ***Pyrite***

Pyrite is present throughout the orebody but decreases markedly in proportion to chalcopyrite in the higher grade zones. Locally coarse-grained, globular pyrite was recorded forming intervals of up to 0.5m of massive sulphide. Pyrite and chalcopyrite often occur as intergrowths, but may also occur separately. From a limited number of microprobe analyses pyrite was found to contain an average of 1.4 wt.% cobalt and 0.78 wt.% arsenic (Clarke, 1993). Detailed mineralogical studies have failed to identify discrete cobalt mineralisation recoverable by physical beneficiation; thus, any cobalt extraction must be by chemical means which would incur high capital costs. Test work is underway to examine the possibility of leaching cobaltiferous pyrite concentrate to get the cobalt into solution (Munro 1994).

- ***Gangue Assemblage***

Gangue refers to the non-economic minerals of the ore assemblage, and therefore includes magnetite as well as carbonate. A number of other minerals comprise the gangue assemblage, and are discussed separately below. Two texturally destructive gangue assemblages were recorded as being particularly useful for correlation:

i. dark rock' refers to those zones which comprise dominantly biotite-magnetite, but with fine grained carbonate invariably present in the dark rock' matrix (caution: the term dark rock' also refers in some drill logs to biotite ñ amphibole ñ chlorite ñ garnet zones in footwall areas and the eastern lens).
ii. the descriptive term spotted rock' was used for carbonate-dominated rocks with only minor magnetite, and variable chalcopyrite contents.

- ***Red Rock Alteration (RRA)***

K-feldspar is ubiquitous in the district, primarily as a regional, potash metasomatism characterised by adularia-microcline that predated brecciation and therefore mineralisation. This locally overprints an earlier sodic (albite) metasomatism. A later intense potassic alteration, represented by an intensification of RRA, was noted with a strong spatial relationship to mineralisation, viz., observed at ore margins and in volcanic clasts within the ore zones. Later microcline-rich veins are observed, which cross-cut the foliation and are themselves undeformed. Occasionally, coarse-grained K-feldspar is seen in the carbonate-magnetite matrix or rimming clasts (FV2 texture within ore zone) and is locally overgrown by pyrite (DDH EHMet4: 158m, 167m).

In the footwall, RRA is absent where the sequence becomes dominated by the metasomatic MMB, from which it might be concluded, that the RRA predates the destructive metasomatic event that formed the MMB.

- ***Biotite***

Biotite is ubiquitous at Ernest Henry as selvedges on veins and relict volcanic clasts', and within the dominant foliation. WMC documented at least two generations of biotite, but further petrographic work by EHM is required to ascertain the significance of biotite in the system. The first generation may be related to an early intense potash metasomatism, which predates brecciation (Croxford, 1994), while the second generation may reflect potassic alteration associated with intrusion (therefore mineralisation?) of the 1500ma Naraku granite. As indicated above, the second generation of biotite may represent a reaction front between the Ca-Mg-Fe and potassic parts of the alteration sequence (viz., selvedges between FV clasts and matrix).

- ***Pegmatites***

Pegmatites with the same mineralogy are seen both as discordant and concordant features with sharp margins, indicating that they were emplaced late in the deformational history.

- ***Garnet***

Garnet was observed in the geological sequence in three forms:

- as subhedral porphyroblasts ó 2cm in diameter
- as cross-cutting garnet-quartz-carbonate veins
- as large, ≤ 5cm, with irregular ragged edges, being overprinted by a variety of other minerals, including chalcopyrite (Fig.7.18).

The large irregular garnets clearly predate mineralisation, and suggest that mineralisation postdates the peak regional metamorphic event. The garnet is not strictly part of the ore alteration assemblage as it is seen up to 800 m from the orebody margins in sterilisation drillholes (EH145; see section 7.2.5).

Spatially, the garnets tend to occur below the ore package (e.g., Figs.7.1, 7.3), but above the MMB. However, in the 9240mN section (Fig.7.3), garnet also occurs above the ore package on the eastern downthrown side. This suggests they may have existed in the ore zone (as in EH127, 143.5m), but have been largely destroyed by the mineralising event.

- ***'Green Spot' occurrences***

This refers to distinctive, subcircular, chloritised amphibole clots which generally occur in the footwall of the ore zone, usually with garnet. Green spot' occurrences intensify towards the north end of the orebody, but is also seen at least as far south as 8920mN in FTCD53 below the upper mineralised lens. Its occurrence with garnet away from the principal mineralised areas suggests that it is formed with garnet during pre-mineralisation regional metamorphism.

- ***Muscovite***

Muscovite occurrences in core were also recorded. It occurs as a pale-yellow, soft wispy mineral, usually aligned in the foliation, but also, locally, as slender decussate prisms in massive grey-green andesite. There are indications that some occurrences of the foliated muscovite may represent the remnants of an earlier fabric, preserved locally in dark zones within red rock altered clasts. By contrast, the prismatic muscovite masses may pseudomorph peak-metamorphic (?) sillimanite porphyroblasts.

The spatial significance is unclear, but the muscovite alteration is commonly observed just outside the ore package in the eastern holes (e.g., on the 7739240mN section, Fig.7.2), in the northernmost holes in the FWSZ and to the northeast in the sterilisation holes over ML2671. It is locally correlatable from hole to hole and if documented carefully, could form a useful marker horizon.

- ***'Satin Mica'***

This term refers to a very soft, satin-sheened, waxy, pale green mica (or talc?), which was observed in the footwall sequence, just below the ore package. It is locally related to foliation-controlled muscovite occurrences, but not categorically so.

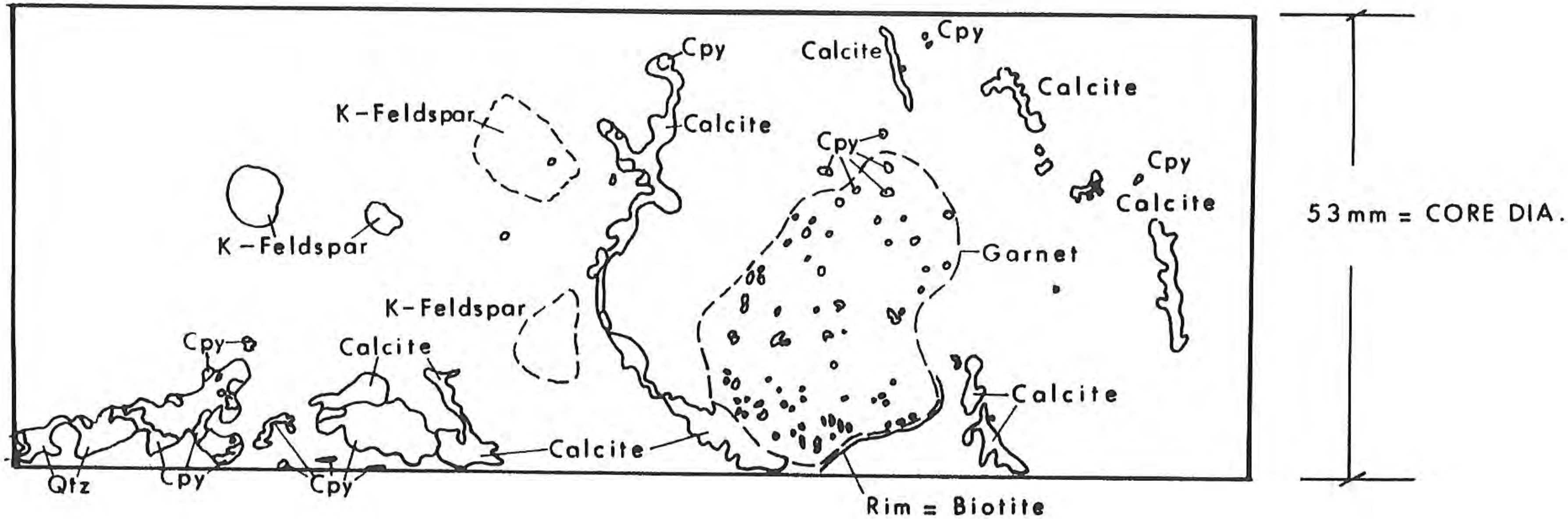

Figure 7.18

SKECTH SHOWING CHALCOPYRITE REPLACING GARNET
ERNEST HENRY PROJECT EH127 (143.5m)

Drg.No. 43199

8. GEOCHEMISTRY & METAL DISTRIBUTIONS

In this chapter, the procedures employed for core sampling, assaying, and quality control of lab assays are described, followed by an examination of copper, gold, cobalt and arsenic distributions in the supergene zone of the Ernest Henry deposit.

8.1 SAMPLING AND QUALITY CONTROL

8.1.1 Sample Preparation and Trial Assays

Core samples selected for assay were diamond split at the EHM camp. Most samples were less than 2 m in length, and correspond, where appropriate, to logged rock type changes.

After diamond-saw splitting, a total of 4762 half core samples was manually broken up into numbered calico bags, catalogued, and sent in pelletised batches of several hundred to Australian Laboratory Services (Townsville) for assay. Table 8.1 lists all assayed drill holes and the number of assay splits from each hole.

Laboratory Sample Preparation
Routine preparation at ALS involved :

1) drying of each sample (~60ºC);
2) crushing of each 5-6 kg sample to -5 mm (Jacques 8" x 5", Cr-Steel);
3) splitting of the -5 mm chips by a vertically-fed splitter;
4) 50% of chips retained as coarse rejects (cryovacced using nitrogen, stored at ALS)
5) 50% of chips (2-3 kg) pulverised for 7 minutes (Lab Technic LM5);
6) 1 kg of pulp taken to analytical stage;
7) ~2 kg of pulp stored in plastic bags, now mostly discarded.

By pulverising for 7 minutes, >95% of each sample, except those with considerable native copper, passed 75 microns and ensured thorough mixing. This procedure was critical to minimising the native copper nugget effect in many supergene samples.

- ***Routine Analytical Procedures***

Gold was routinely determined by fire assay (method PM208, 30g sample).

Copper, cobalt, iron, manganese and nickel were determined by the digestion of a 0.25g pulp aliquot in HCl/HNO3, made up to a final volume of 50 ml and an AAS finish (method A101).

For silver, arsenic, lead and zinc, 0.25g of pulp was digested in perchloric acid for 90 minutes, made up to 10 ml and finished by AAS (method G001). This procedure was also followed for samples with low copper and/or cobalt (e.g., cobalt <300 ppm). Lead and zinc were not determined routinely.

Drill core splits with logged visible native copper were also analysed for copper by screen assay (method PM212). This involved the treatment of about 100 g of pulp as two size fractions: (a) >75 microns, and often native copper rich; and (b) <75 microns, generally native copper poor. The coarse fraction was totally digested (HNO3/HCl) for determination by AAS. The fine fraction was treated as a routine copper determination (i.e., A101 described above).

TABLE 8.1

LISTING OF ASSAYED DRILL HOLES

DDH	From (m)	To (m)	No. of Assay Splits
EH 100	48.7	91.1	26
EH 100a	56.3	201.2	82
EH 101	50.6	138.0	44
EH 102	48.8	276.0	147
EH 103	50.9	192.2	74
EH 104	47.5	168.3	60
EH 105	47.5	162.0	65
	191.0	211.0	10
	368.0	380.0	5
	495.0	504.0	3
EH 106a	47.6	648.5	298
EH 107	47.6	110.0	33
EH 108	47.5	187.2	101
EH 109	50.6	224.7	83
EH 110	47.6	144.2	53
EH 111	41.9	132.3	42
EH 112	43.1	122.0	43
EH 113	41.9	210.3	79
EH 114	41.7	150.1	55
EH 115	47.9	185.7	56
EH 116	41.7	171.5	61
EH 117	36.4	207.0	88
EH 118	38.2	159.1	58
EH 119	41.7	158.5	62
EH 120	42.0	210.2	125
EH 121	41.0	300.2	182
EH 122	34.8	162.0	85
EH 123	33.4	179.0	72
EH 124	34.4	222.0	95
EH 125	37.6	126.2	59
EH 126	37.3	98.8	34
EH 127	35.7	207.3	187
EH 128	31.3	132.5	103
EH 129	38.7	138.0	103
EH 130	49.9	600.0	281
EH 131	31.0	108.0	85
EH 132	36.1	132.0	98
EH 133	35.3	200.0	133
EH 134	37.0	111.0	59
EH 135	30.6	155.0	131
EH 136	36.0	203.8	175
EH 137	45.0	420.0	244
EH 139	30.0	114.2	82

DDH	From (m)	To (m)	No. of Assay Splits
EH 140	27.3	109.2	88
EH 141	42.1	447.3	236
EH 142	27.3	102.3	77
EH 143	33.0	102.3	68
EH 145			51
EH 151	229.0	249.4	10
EH 153	118.0	251.5	72
EH 154	101.8	252.4	64
FTCD 60 ex	472.0	606.0(?)	70
FTCD 52	396.0	525.2	65
TOTAL			4762

- ***Trial Assays and Standards***

Test work was carried out at the beginning of the programme to determine an optimal analytical scheme. As part of this work, the pulps from DDH's EH100, FTCD60 ext, and FTCD49 (WMC samples) were comprehensively analysed by ALS, *viz*.:

- Cu, Co, Fe, Mn, Ag, Bi, Pb, Zn, Ni, As (A101, Townsville Laboratory)
- Au (Fire Assay, PM208, Townsville Laboratory)
- Cu (Screen, PM212, Townsville Laboratory)
- S (Leco Furnace, G013, Brisbane Laboratory)
- U, As, Mo, Sb (XRF1, Brisbane Laboratory)
    - Fluorine (peroxide/carbonate fusion, G006)
- Si, Al, Fe, Ca, Mg, Ti, K, P, Mn, Sr, S, Cu, LOI (ICP-OES, M275)

A full analysis of the data was not possible, although some of it was used as part of the quality control process (e.g., the screen assays and repeat analysis of WMC pulps). The fluorine, manganese (2 methods) and sulphur (2 methods) data may be of metallurgical interest. Sulphur assays are also available for DDH's EH102, EH109, EH113 and EH121.

Three metallurgical standards prepared by WMC and stored at AMDEL Laboratories (Adelaide) were pulped and prepared as internal standards for the assay programme (refer Table 8.2). Both AMDEL and ALS have kept these standards for any future work on Ernest Henry samples.

The upper part of Table 8.2 shows how the calculated head grades of the composite cores for each standard are unrealistic, given the bulk assays for contributing drill holes; thus a weighted grade, based on core length (but not density), was calculated from the bulk assays for comparison with the replicate analyses during the assay programme.

An aliquot of each pulped standard (about 5 kg) was initially analysed repeatedly by AMDEL, ALS and ANALABS to determine accurate Cu and Au abundances and to provide an indication of the internal precision of each laboratory. The lower part of Table 8.2 summarises some of that test work as well as the ALS results from the ensuing routine assay programme. The following observations are noted from Table 8.2:

a) The ANALABS assays are closest to the "weighted" grades deduced from WMC bulk assays produced by AMDEL (Adelaide) for WMC. Given the uncertainty in the "weighted" grade calculation it is not implied that ANALABS produced the most accurate assays.
b) The mean ANALABS Cu assays are unusually precise (viz., very low standard deviations). This was presumably achieved by very thorough mixing and grinding prior to analysis.
c) The mean AMDEL Cu assays are almost unacceptably imprecise (particularly for MET 12, standard deviation = 0.34) and biased low for MET 19 and MET 21. ALS mean Cu values from the main assay programme are also relatively imprecise.
d) The precision of Au assays for each laboratory is similar, and that assays of primary ore sample MET 12 are consistently less precise than those of MET 19 (transitional ore) and MET 21 (supergene ore). A batch-by-batch breakdown of the ALS standard replicate results for all elements as well as a statistical summary of Cu and Au results for all laboratories is available in Appendix IIa and IIb.

TABLE 8.2

INTERNAL STANDARDS FOR ASSAY PROGRAMME

Standard	Origin	WMC Bulk Assay		WMC Calculated Head Grade		This Report Weighted Grade	
		Cu	Au	Cu	Au	Cu	Au
MET 12	Primary Ore FTCD 23, 240.5-270.5 m	2.46	1.18	-	-	2.46	1.18
MET 19	Transitional Ore FTCD 76, 75-91 m FTCD 59, 110-120 m	1.79 1.69	1.02 0.99	1.78	1.14	1.75	1.01
MET 21	Supergene Ore (native Cu) FTCD 59, 74-112 m FTCD 77, 50.3-55 m	1.94 1.66	0.48 1.10	1.84	1.05	1.91	0.55

	Testwork ANALABS (Perth) n = 20				Testwork ALS (Townsville) n = 110				Testwork AMDEL (Adelaide) n = 20			
	Cu		Au		Cu		Au		Cu		Au	
	Mean	σ	Mean	σ	Mean	σ	Mean	σ	Mean	σ	Mean	σ
MET 12	2.52	0.03	1.18	0.14	2.42	0.16	1.27	0.13	2.44	0.34	1.19	0.09
MET 19	1.77	0.02	0.90	0.08	1.67	0.10	0.88	0.06	1.45	0.11	0.87	0.07
MET 21	1.93	0.02	0.05	0.03	1.81	0.22	0.61	0.05	1.71	0.14	0.62	0.07

8.1.2 Assay Quality Control

- ***Repeatability of Copper and Gold Assays***

Within laboratory precision (repeatability) was monitored at ALS by replicate analysis of the internal MET standards (1 MET standard every 15 unknowns) and by duplicate analysis of every tenth unknown pulp. All of this data is available in computer files (refer listing in Appendix Ib).

Copper

In an analysis of the matched data pairs from the 10-in-1 duplicate assays, Birnbaum (1994a) concluded that the ALS copper values are reported without internal bias, with an analytical precision (s) of ± 0.053 wt% and within a 95% confidence interval of ± 1.96 s = ± 0.104% Cu. Figure 8.1 graphically emphasises the satisfactory internal variability of ALS copper assays.

Relative precisions at 95% confidence levels calculated from the MET standard replicates are generally higher than for the 1-10-pulp duplicates (see Table 8.3); indicating that the MET standard pulps were not well mixed for the main assay programme. (See also Fig.6, Hannan, 1993b).

Gold

For the 1-in-10 duplicate gold assays, Birnbaum (1994a) concluded that the individual ALS gold values are reported without internal bias, with an acceptable analytical precision (s) of ± 0.064 g/t and a 95% confidence interval of ± 1.96s = ± 0.125 g/t. Lower precisions were achieved for the MET standard replicates (Table 8.3), a pattern consistent with the Cu results.

Precision of Au assays tends to decrease with increasing Au content (see Fig.8.2, this report, and Fig.7 of Hannan, 1993b; also Birnbaum, 1994a for a statistical treatment).

- ***Reproducibility of Copper and Gold Assays***

Between laboratory precision (i.e., reproducibility or accuracy) estimates were achieved by the analysis at AMDEL (Adelaide) of every 10th pulp (EA numbers ending in zero) assayed as part of the supergene project by ALS. Unfortunately, this work was not carried out until after ALS had completed all batches of pulps from Ernest Henry. Ideally, batches should have been sent, as originally requested, to AMDEL periodically for maximum quality control.

Copper

Birnbaum (1994a) concluded that although the AMDEL Cu results are almost 6% higher than ALS, the two labs report Cu assays with nearly the same analytical precisions (Table 8.3). Figures 3 and 4 of Hannan (1994) display graphically the bias of AMDEL to slightly higher Cu assays than ALS, and how the bias is not dependent on Cu grade. It is not possible to determine from the available data which laboratory has produced the most accurate results.

Gold

Gold assays at AMDEL, like copper, were found to have acceptable precision levels of less than ± 0.2 g/t (95% confidence, Table 8.3). However in contrast to copper, AMDEL assays of the 1-in-10 pulps reported some 12.5% lower than ALS for grades greater than 0.2 g/t (Birnbaum 1994b; and see also, Figs.7 and 8 of Hannan, 1994).

Unfortunately, it is not possible to confidently assume that AMDEL assays consistently under-report relative to ALS because they were found to over-report in an earlier batch of pulps selected to test the reproducibility of WMC assays (viz., pulps for FTCD76, refer Figs.5 and 6 of Hannan, 1993b). Furthermore, the precision calculations for the AMDEL labs by (Birnbaum, 1994b) were calculated for a much smaller dataset (21 MET standards) and not the 380 1-10-pulp checks used for the equivalent copper calculation.

Thus, gold has proven to be difficult to assay accurately, and for this reason 25 samples were selected from the 1-in-10 pulp batch for umpire analysis in the U.K. (results not available yet).

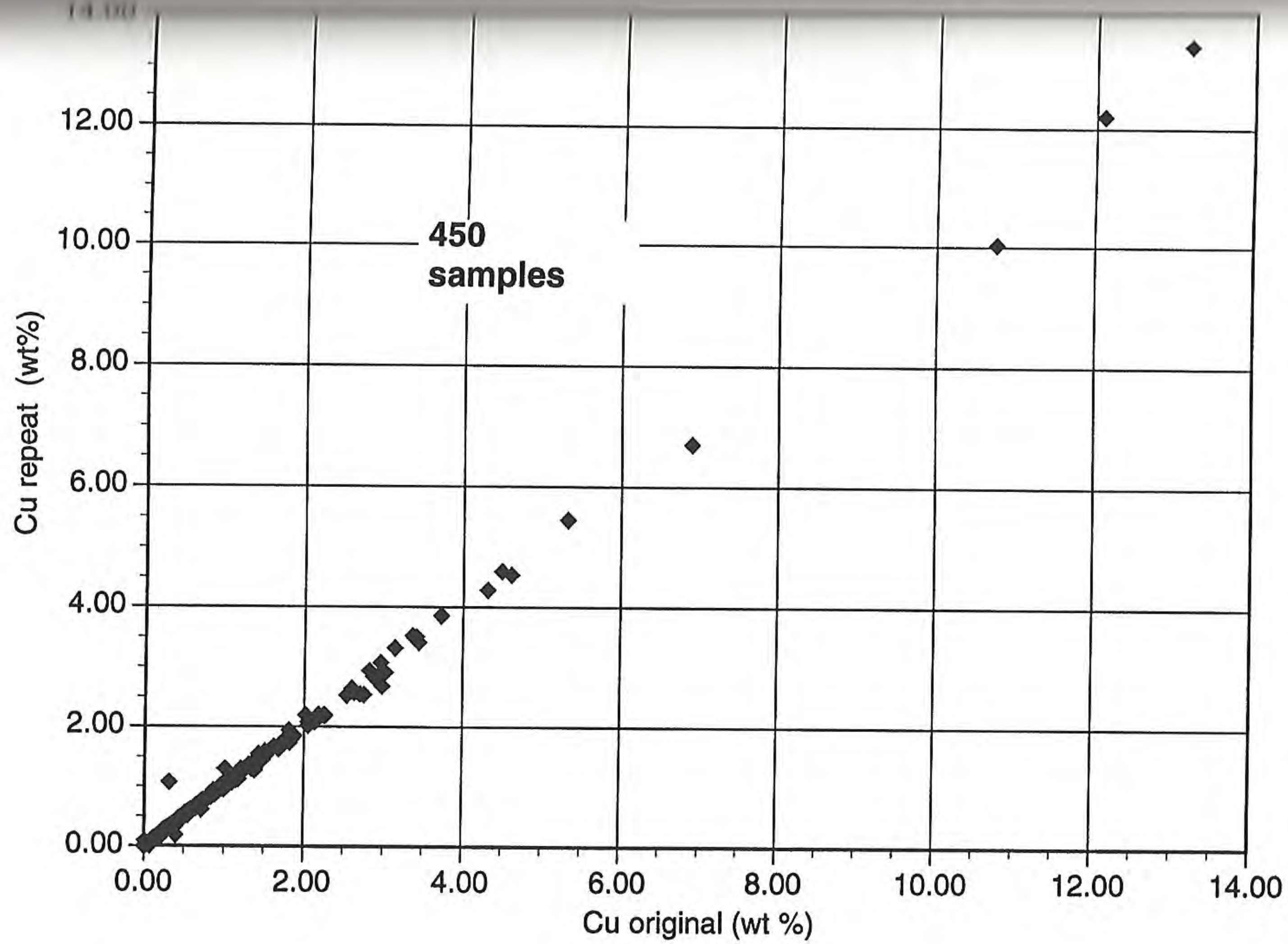

FIGURE 8.1 Cu Assay Repeatability
Comparison of ALS first and repeat results for about every tenth sample

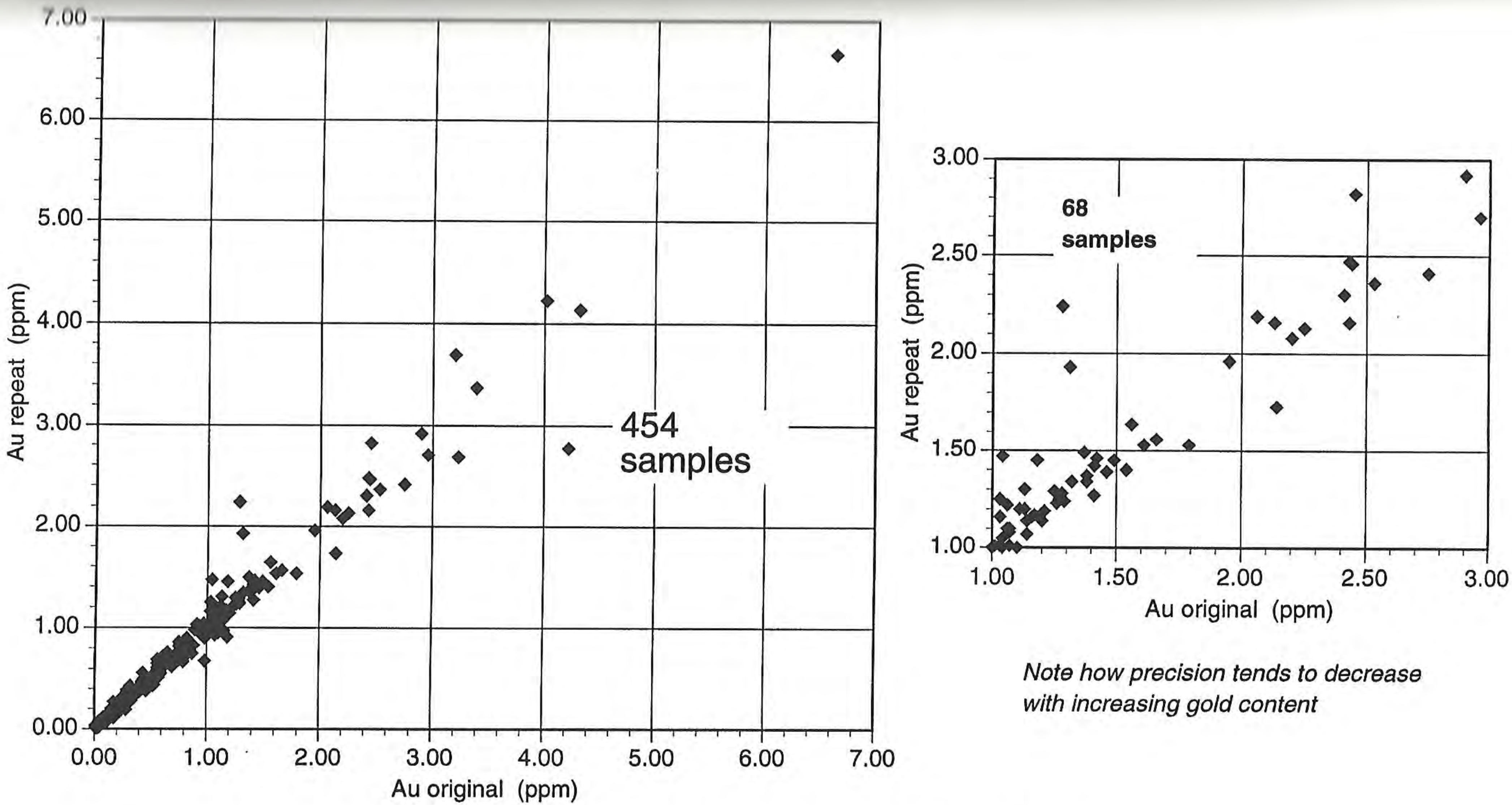

FIGURE 8.2 Au Assay Repeatability
Comparison of ALS first and repeat results for about every tenth pulp.

TABLE 8.3

ALS ASSAY PRECISIONS (weight % with 95% confidence)

	Original vs Duplicate		MET 12		MET 19		MET 21	
Laboratory	Cu	Au	Cu	Au	Cu	Au	Cu	Au
ALS	0.104*	0.125*	0.129	0.20	0.118	0.13	0.239	0.16
AMDEL	0.093*	0.178*	0.272	0.15	0.149	0.16	0.161	0.22
ANALABS			0.024	0.23	0.022	0.17	0.020	0.11
ALL LABS			0.131	0.19	0.118	0.13	0.229	0.15

* from Birnbaum (1994)

- ***Native Copper-Bearing-Samples***

As described in section 8.1.3, all visibly native copper-bearing samples were screen assayed to monitor nugget effects. Analysis of the first 132 screen and A101 assays indicated that the nugget effect is minimal:

- most screen assays repeat within ñ 0.2 wt% of the A101 assay (Fig.8.3); and
- although repeatability by screen assay is reduced for nugget rich samples (i.e., pulps with >40% total Cu in the +75 micron fraction), there is no observed bias to higher screen assays relative to the A101 method results, as might be expected of a systematic nugget effect (refer Fig.2, Hannan, 1993b)

The high within lab precision of copper assays (section 8.1.2), most of which apply to supergene ore samples, emphasises how native copper nuggeting should not detract from ore grade calculations and modelling based on A101 assays.

Finally, it is stressed that less than half of the available screen assays have been examined. Furthermore, there is scope, given the systematic geological - mineralogical logs available, to examine in detail the control of copper mineral species on the precision of both copper and gold assays.

8.2 METAL DISTRIBUTIONS VERSUS SULPHIDE MINERALOGY

In this section, relationships of copper, gold, cobalt and arsenic abundances to logged sulphide (± native copper) assemblages are investigated. At the time of this analysis, 4383 of a possible 4762 splits had been assayed and logged according to visible sulphides. The missing data apply mostly to splits from sterilisation holes (DDH's EH 144, 145, 151, 153, 154).

8.2.1 Copper and Gold

In the supergene zone, unlike the primary mineralisation, gold largely decouples from copper and distinctive distribution patterns are observed in the contoured grade sections. This suggests that the weathering of copper sulphide liberates gold in the secondary zone. Indeed, WMC's microprobe analyses of secondary copper minerals show scant presence of gold (Clarke, 1993). However, free gold is not seen in the supergene zone with the naked eye. Knights asserts that the gold is extremely fine grained (≤ 1-2 microns) and reports to interstitial gangue sites. One occurrence of gold has been identified as electrum, containing ~14% wt% Ag, enclosed in pyrite in a quartz vein (Knights, 1993b).

- ***Splits with only chalcocite visible***

Figure 8.4 (upper) shows that:

a) Assay splits logged as containing visible chalcocite can have negligible copper; this emphasises the difficulty of identifying disseminated chalcocite in Ernest Henry core.
b) Gold levels bear little relationship to copper levels, e.g. splits with only traces of chalcocite (Cu <0.1%) can have up to 3.5 g/t gold; this indicates that free gold may be common in splits with chalcocite-only splits.

- ***Splits with only native copper visible***

Figure 8.4 (middle) shows:

a) How gold levels are generally <1 g/t.
b) That copper levels are generally <2 wt%.

Thus, sulphide-free, native copper-bearing zones are relatively copper- and gold-poor parts of the supergene profile (see also summary statistics of Table 8.4).

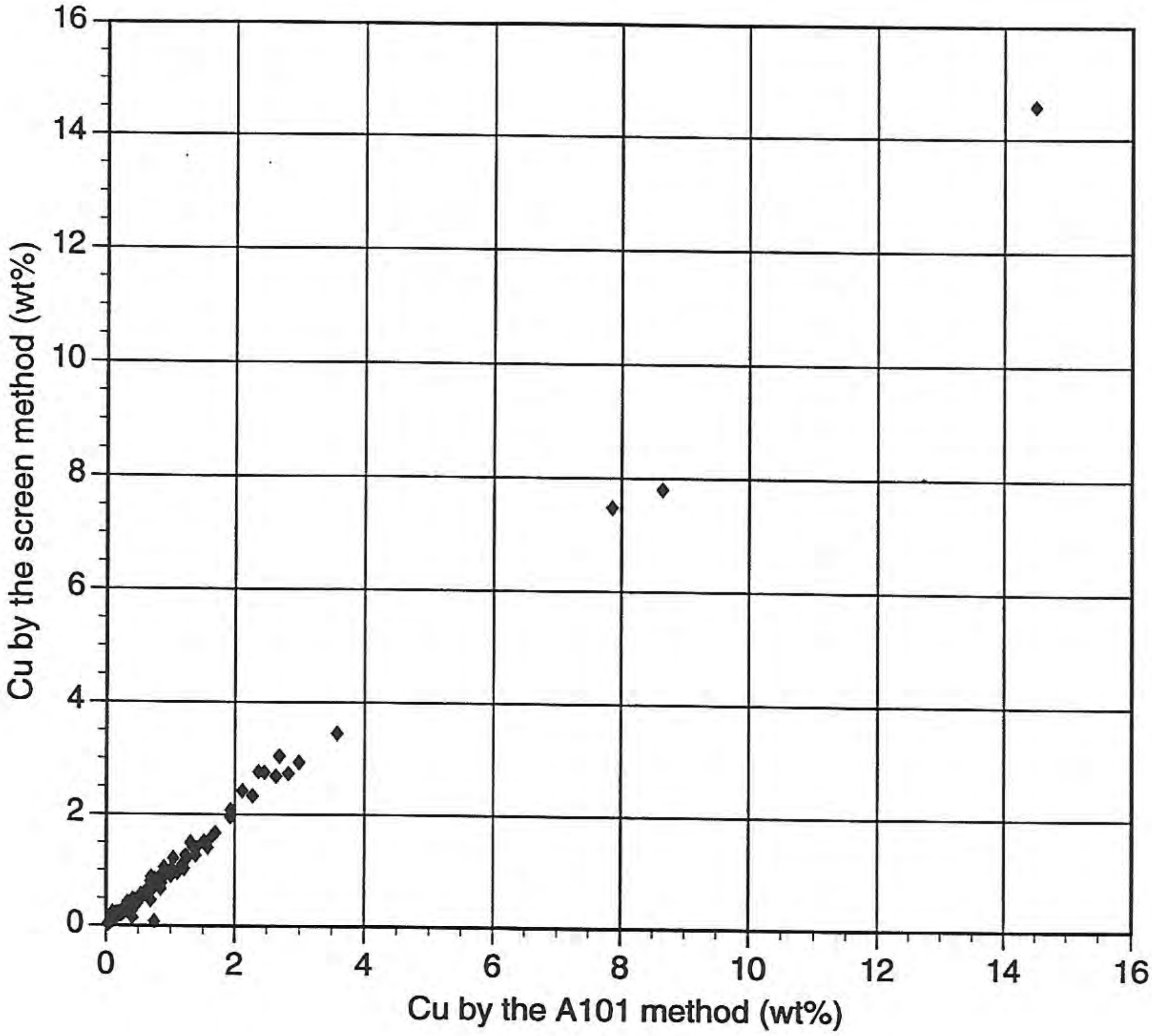

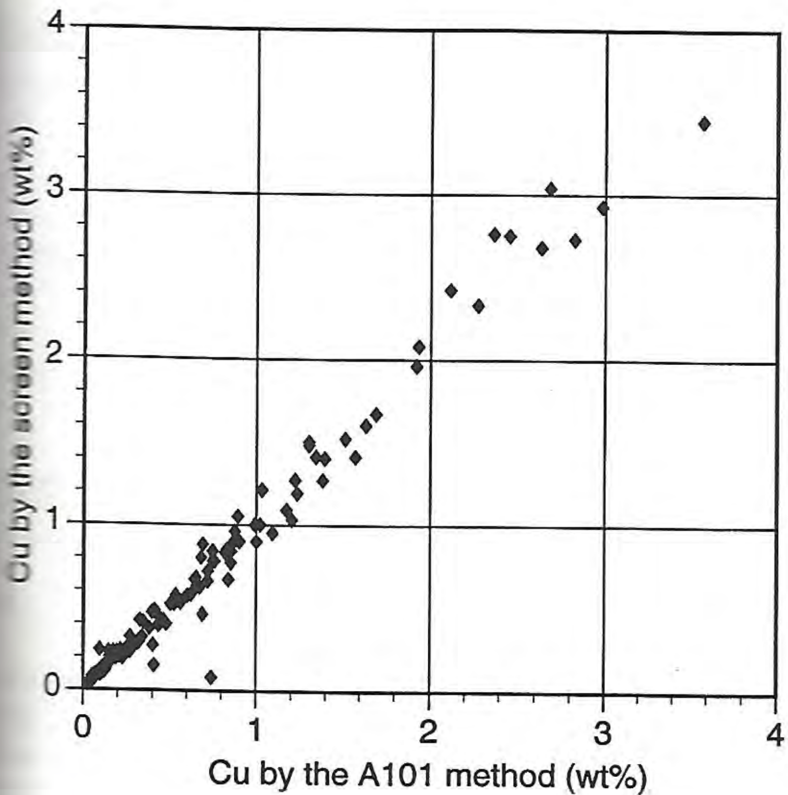

FIGURE 8.3

Upper plot: comparison of 132 Cu assays using the A101 and screen (total) methods

Left plot: as above, close-up of 129 assays below 4 wt% Cu

All data from ALS, Townsville; samples from DDH EH100, EH104-115, FTCDext'd

…ABLE 8.4 Summary assay statistics - by sulphide assemblages

No Visible Sulphides

…ary - no visible sulphides

	Cu	*Au*	*As*	*Co*	*Mn*	*Fe*
…an	0.08	0.04	59.19	76.87	1906.02	11.82
…dian	0.02	0.01	10.00	40.00	1420.00	11.90
…e	0.01	0.01	10.00	38.00	1030.00	13.00
…dard Deviation	0.21	0.11	297.05	138.96	1995.81	4.87
…ance	0.04	0.01	88236.80	19309.39	3983258.07	23.71
…mum	0.00	0.01	8.00	4.00	90.00	2.00
…mum	2.19	1.37	4120.00	2090.00	22500.00	41.00
…nt	543	551	551	551	551	551

…ergene - no visible sulphide or native Cu

	Cu	*Au*	*As*	*Co*	*Mn*	*Fe*
…an	0.31	0.25	87.82	179.24	1382.08	15.61
…dian	0.10	0.05	23.50	124.00	794.00	15.00
…e	0.03	0.01	10.00	40.00	110.00	16.00
…dard Deviation	0.87	0.48	209.52	185.70	2143.87	6.67
…ance	0.75	0.23	43899.70	34482.88	4596193.77	44.49
…mum	0.00	0.01	5.00	5.00	10.00	2.00
…mum	19.90	4.22	3320.00	1940.00	25870.00	40.00
…nt	935	937	934	936	936	936

Pyritic splits

…e (primary and supergene zone splits)

	Cu	*Au*	*As*	*Co*	*Mn*	*Fe*
…an	0.40	0.16	117.98	282.10	1241.97	15.53
…dian	0.13	0.04	30.00	176.00	810.00	14.80
…e	0.01	0.01	10.00	60.00	650.00	11.00
…dard Deviation	0.76	0.37	332.80	307.49	1416.60	6.45
…ance	0.58	0.13	110757.25	94551.17	2006761.44	41.62
…mum	0.00	0.01	5.00	5.00	5.00	2.00
…mum	12.20	3.23	7680.00	2950.00	13700.00	42.00
…nt	1085	1086	1086	1086	1086	1086

… with visible pyrite only and Cu<0.1% (primary and secondary)

	copper	*gold*	*arsenic*	*cobalt*
…an	0.05	0.03	36.07	112.45
…dian	0.04	0.01	10.00	85.00
…e	0.01	0.01	10.00	40.00
…dard Deviation	0.03	0.08	94.59	107.61
…ance	0.00	0.01	8947.55	11579.11
…mum	0.00	0.01	5.00	5.00
…mum	0.10	1.57	1940.00	1430.00
…nt	495	495	495	495

Chalcocite-bearing Splits

alcocite/chalcocite+pyrite/chalcocite+chalcopyrite

	copper (%)	gold (ppm)	arsenic (ppm)	cobalt (ppm)	manganese (ppm)	iron (%)
an	1.98	0.65	218.52	482.97	958.61	18.76
dian	0.93	0.37	80.00	306.50	620.00	18.00
de	0.07	0.01	10.00	100.00	40.00	17.00
dard Deviation	2.75	0.82	307.57	494.62	1066.81	8.52
ance	7.58	0.67	94597.03	244644.66	1138082.84	72.55
imum	0.01	0.01	5.00	22.00	16.00	4.00
imum	14.90	6.62	1710.00	3870.00	8200.00	42.00
	519.60	170.49	57253.00	126537.00	251156.00	4914.48
nt	262	262	262	262	262	262

s with visible chalcocite only

	copper (%)	gold (ppm)	arsenic (ppm)	cobalt (ppm)
	1.29	0.58	237.83	353.54
ian	0.32	0.27	90.00	190.00
	0.20	0.01	10.00	100.00
dard Deviation	2.01	0.68	295.37	360.04
ance	4.04	0.47	87245.22	129626.66
um	0.02	0.01	5.00	30.00
num	10.76	3.36	1120.00	1480.00
	123	123	123	123

s with chalcocite with either native Cu or pyrite

	copper	gold	arsenic	cobalt
	2.27	0.56	200.88	497.64
ian	1.12	0.21	66.00	356.50
	0.07	0.01	10.00	80.00
dard Deviation	3.04	0.82	319.65	469.02
nce	9.25	0.68	102174.17	219975.98
um	0.01	0.01	5.00	22.00
um	14.90	6.62	1800.00	3870.00
	200	200	200	200

Native Copper-bearing Splits

tive Cu/Cu+chalcocite/Cu+pyrite

	Cu	*Au*	*As*	*Co*	*Mn*	*Fe*
ean	0.89	0.21	121.49	276.44	1361.51	17.17
dian	0.25	0.06	40.00	218.00	920.00	16.00
de	0.06	0.01	10.00	120.00	400.00	18.00
ndard Deviation	1.75	0.33	245.12	180.85	1881.89	6.19
iance	3.07	0.11	60084.91	32706.52	3541522.60	38.26
imum	0.03	0.01	10.00	26.00	120.00	5.00
imum	14.50	2.37	1800.00	980.00	16100.00	46.90
nt	253	253	251	253	253	253

ts with visible native copper only (i.e. no sulphides)

	copper	*gold*	*arsenic*	*cobalt*
an	0.58	0.19	102.11	241.42
dian	0.18	0.03	25.00	189.50
de	0.06	0.01	10.00	240.00
ndard Deviation	1.29	0.33	228.41	147.98
ance	1.66	0.11	52171.52	21896.78
um	0.03	0.01	10.00	49.00
mum	9.55	2.37	1520.00	678.00
nt	150	150	148	150

Chalcopyritic Splits

lcopyrite/chalcopyrite+pyrite (i.e., primary zone splits with visible sulphide))

	Cu	*Au*	*As*	*Co*	*Mn*	*Fe*
	0.69	0.32	218.72	390.78	2147.04	17.50
an	0.37	0.16	80.00	262.00	1420.00	16.00
	0.04	0.01	10.00	40.00	760.00	13.00
dard Deviation	0.87	0.41	352.00	405.77	2281.56	7.42
nce	0.75	0.17	123907.39	164649.34	5205518.97	55.04
um	0.01	0.01	10.00	13.00	50.00	3.00
um	8.53	5.06	6110.00	4990.00	22500.00	50.00
	1280	1282	1282	1282	1282	1282

ergene splits with only chalcopyrite visible

	copper (%)	*gold (ppm)*	*arsenic (ppm)*	*cobalt (ppm)*
	1.04	0.70	317.77	477.85
	0.51	0.30	120.00	300.00
	0.55	0.01	10.00	30.00
ard Deviation	1.27	0.97	502.20	687.37
nce	1.60	0.94	252208.49	472483.96
um	0.02	0.01	10.00	30.00
um	5.90	5.06	2970.00	4170.00
	47	47	47	47

...mary zone splits with only chalcopyrite visible

	Copper	*gold*	*arsenic*	*cobalt*
...ean	0.44	0.21	109.45	180.85
...edian	0.18	0.05	60.00	79.00
...ode	0.03	0.01	10.00	81.00
...ndard Deviation	0.55	0.30	129.03	192.40
...iance	0.30	0.09	16649.07	37019.26
...imum	0.02	0.01	10.00	32.00
...ximum	1.64	1.10	480.00	646.00
...unt	33	33	33	33

- ***splits with visible chalcocite-native-copper or chalcocite-pyrite***

Figure 8.4 (lower) and Table 8.4 show that :

a) Gold `spikes' occur in low copper samples of the chalcocite-pyrite subset (i.e. free gold?).
b) Chalcocite-bearing assemblages are the most gold- and copper-rich of the Ernest Henry deposit (Table 8.4).

- ***Splits with visible chalcopyrite-pyrite and visible chalcopyrite only***

This subgrouping applies mostly to splits from the primary zone (chalcopyrite-pyrite subset), where Cu/Au ratios are markedly uniform (Fig.8.5). Gold spiking to 3 or 4 g/t occurs with splits from the supergene zone, and indeed, the Au grade for this subgroup is higher relative to copper than any other sulphide assemblage (Table 8.4).

- ***Splits with only pyrite visible (and Cu <1%)***

This subset is dominated by primary zone splits. Those pyritic samples with anomalous gold (spikes of Fig.8.6) are mostly from gold-rich intervals of DDH's EH100a, 107 and 117 from the supergene zone. Significantly, these intervals are succeeded immediately below by chalcocite zones, at or just above the BOCO, with some of the highest copper assays of the programme. It is suggested that such intervals correspond to zones of the most intense supergene enrichment, and that gold spiking in pyritic splits indicates either the presence of free gold or its enrichment relative to copper on primary pyrite or within secondary pyrite.

8.2.2 Cobalt

Cobalt occurs largely in solid solution with pyrite in the primary ore zone (Knights, 1993a; Clarke, 1993; Munro, 1994). However, it has also been sighted as isolated grain occurrences enclosed in magnetite/pyrrhotite/chalcopyrite as cobaltite ((Co,Fe)AsS), cobaltian pentlandite ((Fe,Ni)9S8 and carrollite (CuCo2S4) in the primary zone and once as cobalt violarite in the supergene (Knights 1993b). Its general occurrence therefore is complex and may pose metallurgical problems in extraction. Tests are underway to examine whether cobalt can be leached from a cobaltiferous pyrite concentrate to recover cobalt in solution (Munro 1994).

Bulk cobalt abundances rarely exceed 1300 ppm in both supergene and primary ore splits (Figs.8.7 and 8.8). Microprobe analysis indicates that supergene pyrite contains at least 1 wt.% cobalt, and other sulphides less than 500ppm (Clarke, 1993). Cobalt in a few micro-probed primary zone pyrites ranges from 1-8 wt.% (Clarke, 1992) and was not detected in chalcopyrite.

There is no evidence of cobalt enrichment in specific sulphide assemblages of the supergene zone. Indeed, the dominant chalcocite-bearing and native copper-bearing assemblages have lower Co/Cu ratios than pyrite- or chalcopyrite-bearing assemblages (derived from Table 8.4).

It is also not possible to determine, using this approach, how cobalt is partitioned between pyrite and chalcopyrite in primary ore. The pyritic subgroup of Table 8.4 certainly has the highest mean Co/Cu ratio of any sulphide assemblage. However, it is clear from the right-hand side of Figure 8.8 that cobalt abundances correlate very strongly with copper in splits that contain chalcopyrite without visible pyrite. Thus, cobalt probably occurs in both mineral phases (c.f., Clarke, 1992).

Figure 8.4 Au and Cu distributions (by visible Fe-Cu sulphides)

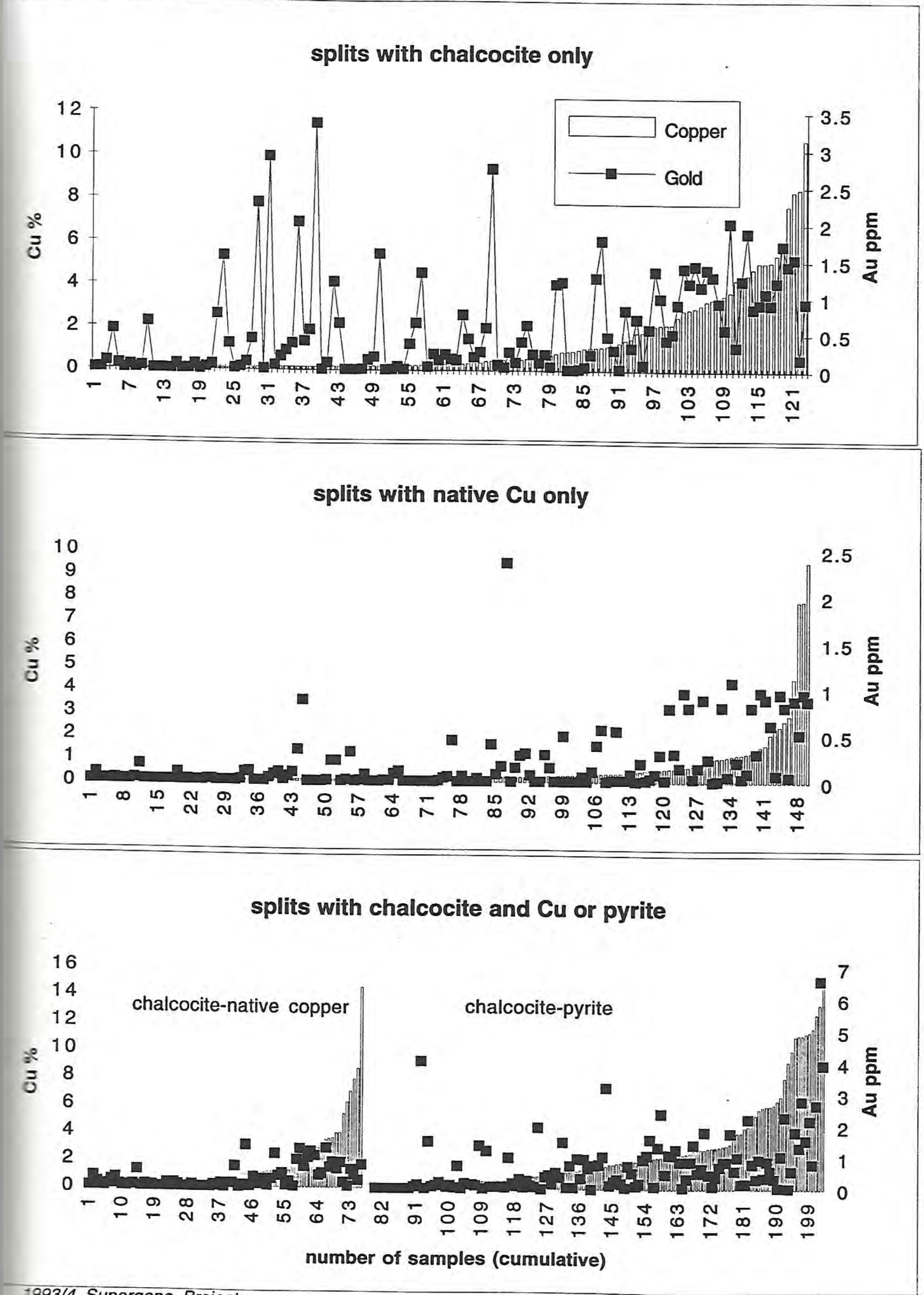

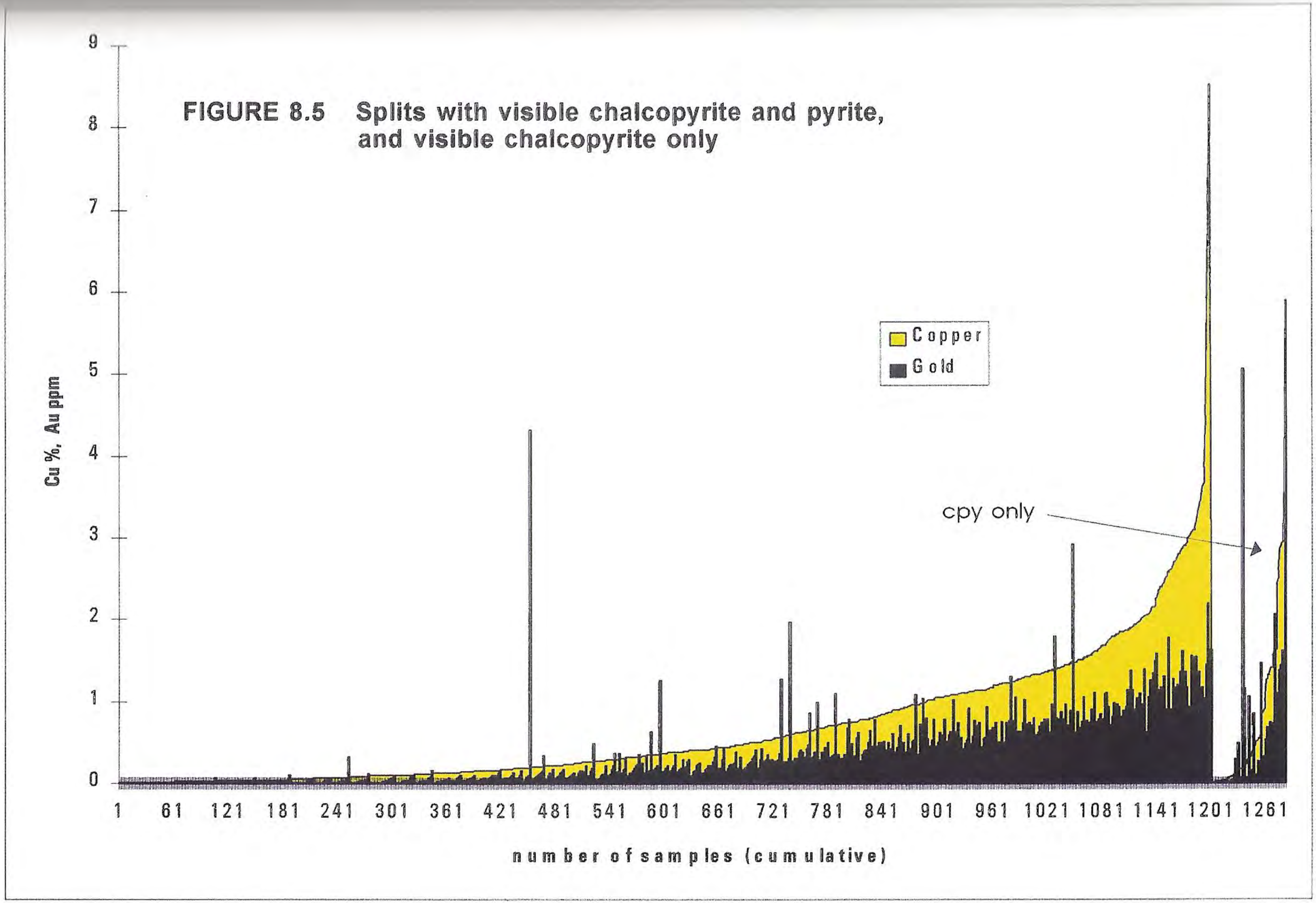

FIGURE 8.5 Splits with visible chalcopyrite and pyrite, and visible chalcopyrite only
Copper
Gold
cpy only
Cu %, Au ppm
0
1
2
3
4
5
6
7
8
9
1 61 121 181 241 301 361 421 481 541 601 661 721 781 841 901 961 1021 1081 1141 1201 1261
number of samples (cumulative)

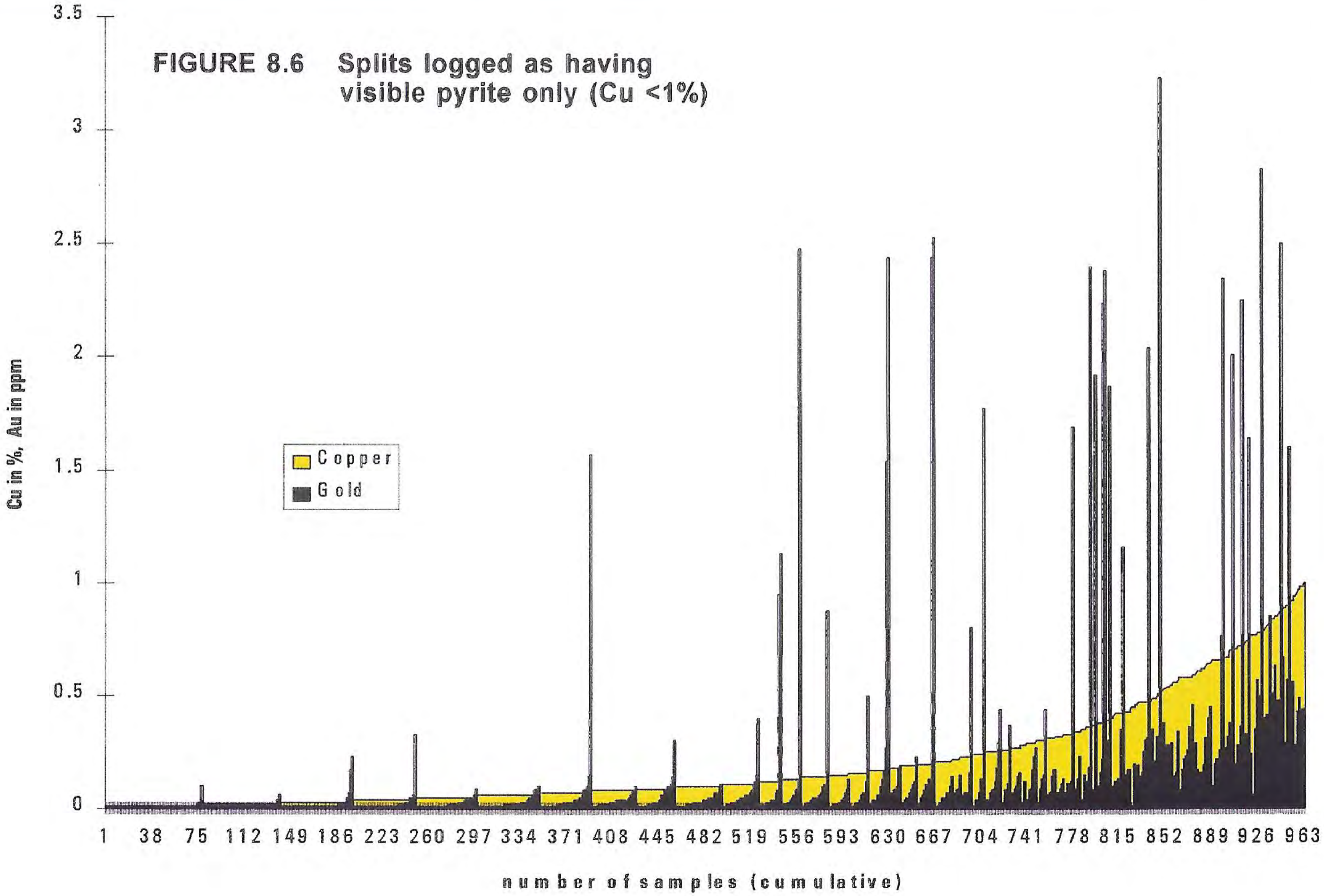

FIGURE 8.6 Splits logged as having visible pyrite only (Cu <1%)
Copper
Gold
Cu in %, Au in ppm
3.5
3
2.5
2
1.5
1
0.5
0
1 38 75 112 149 186 223 260 297 334 371 408 445 482 519 556 593 630 667 704 741 778 815 852 889 926 963
number of samples (cumulative)

FIGURE 8.7 Co and Cu distributions (by visible Fe-Cu sulphides)

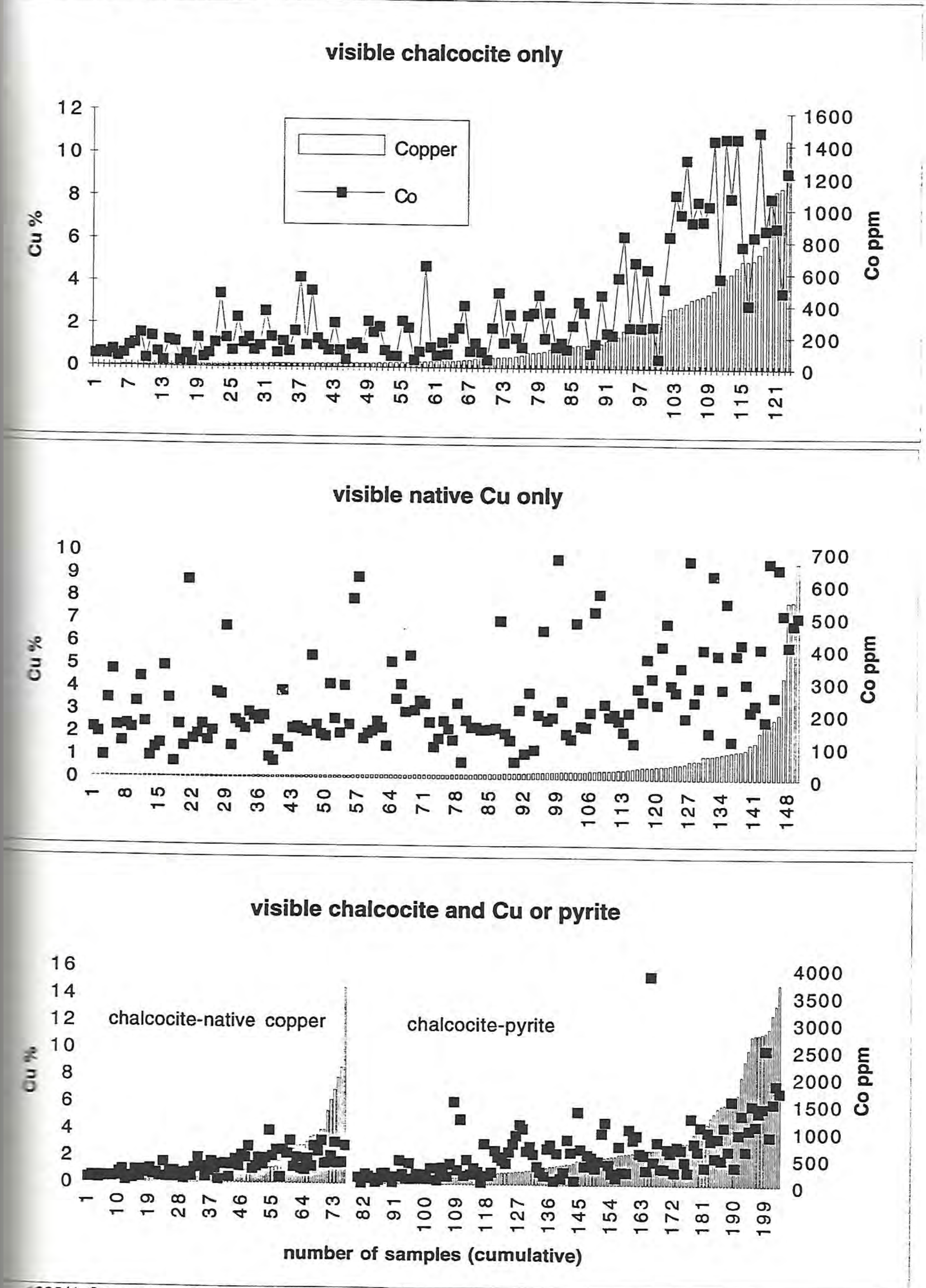

FIGURE 8.8 splits with visible cpy-py and visible cpy only

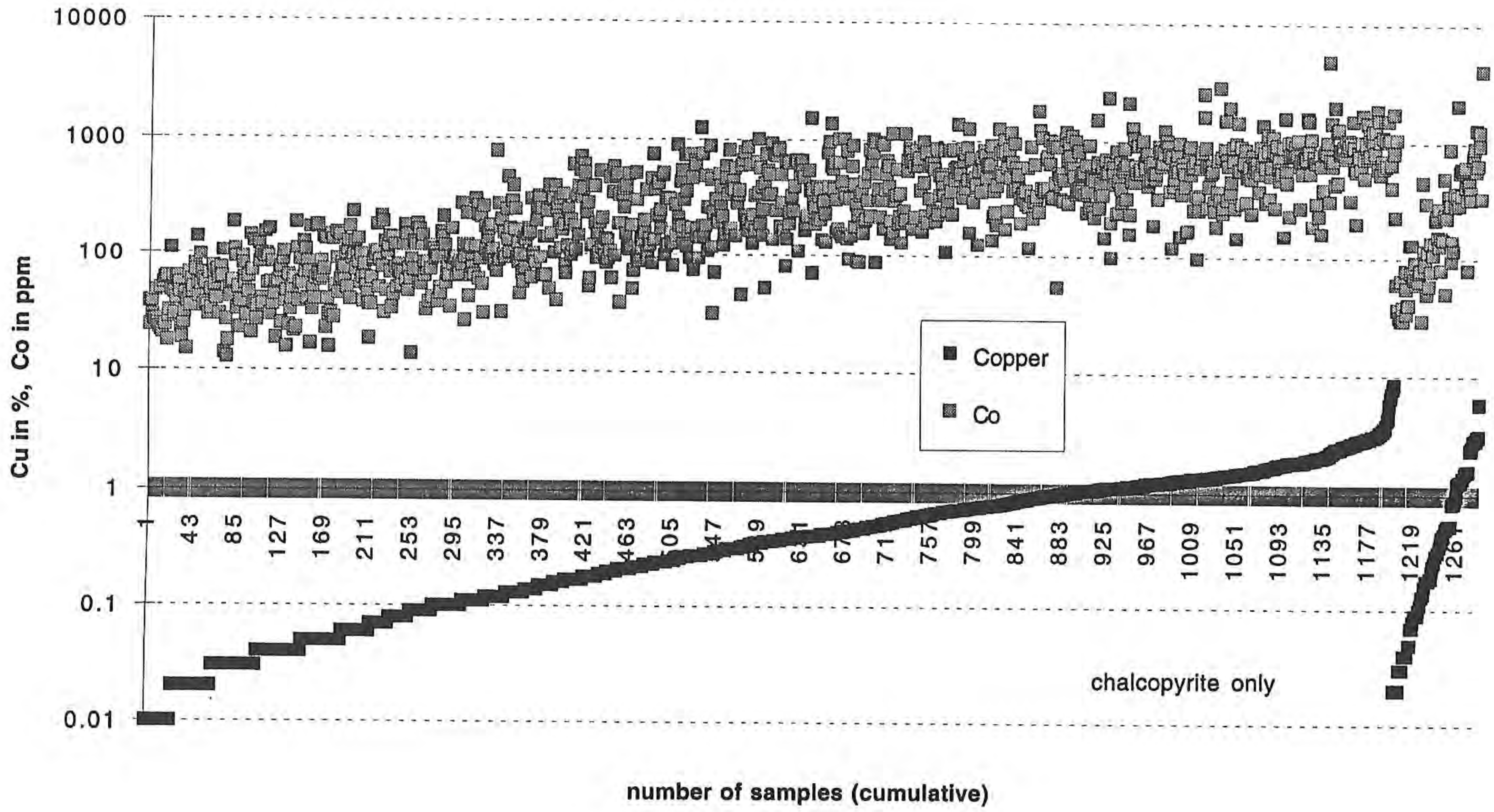

8.2.3 Arsenic

In the primary zone, arsenic occurs in pyrite and rarely as arsenopyrite. In the supergene zone it is partly decoupled from pyrite and occurs, at least in part, within secondary chalcopyrite (Clarke, 1993). Arsenic-bearing native copper in the form of whitneyite grading to algondonite was identified as a minor constituent in the supergene zone section of DDH EH109 (Knights, 1993b).

Microprobe analyses of a few sulphide grains indicate that primary zone pyrite contains up to 8 wt.% arsenic, and supergene pyrite less than 1%; and in the case of primary zone chalcopyrite, less than 1 wt.% (Clarke, 1992; 1993).

This study shows that bulk arsenic abundances are highest in assemblages dominated by the copper sulphides chalcopyrite and chalcocite. In primary ore, and in contrast to cobalt, arsenic has an obviously stronger association with chalcopyrite than pyrite. For example, pyrite-only splits with <0.1% Cu have a mean arsenic value of only 37 ppm (Table 8.4).

Of possible metallurgical interest are the contrasting relationships of Co and As to chalcocite. A comparison of Figures 8.7 and 8.9 would seem to suggest that arsenic occurs more independently (as a separate sulphide?) of chalcocite than Co.

As observed for cobalt, As/Cu ratios are lower in chalcocite-bearing and native copper-bearing splits than pyrite- or chalcopyrite-bearing splits (Table 8.4). Thus, arsenic is not enriched in a particular assemblage of the supergene zone relative to primary ore (Fig.8.10).

8.2.4 Molybdenum

Molybdenum is present in both supergene and primary mineralisation as minor quantities of molybdenite and is the best preserved of the primary sulphides in the supergene zone (Clarke, 1993). Anomalous quantities of molybdenite may occur locally (e.g., DDH EH100, 169m; (Croxford, pers. comm. 1994), and secondary (?) molybdenite has been observed on joint planes.

8.2.5 Uranium, Barium, Fluorine

Uranium was not routinely assayed for this study, although it is clear that Ernest Henry mineralisation has anomalously high uranium levels (often 50-100ppm). Uranium was detected in trace galena and acanthite, and also as inclusions in fluorite and biotite. It is not likely to cause serious metallurgical problems (see Clarke, 1992).

Barium abundances are consistently in excess of 200ppm and often between 0.1 and 0.8 wt.% in both primary and supergene ore. Barite ($BaSO_4$), rather than celsian feldspar, is therefore probably a common accessory mineral of the Ernest Henry deposit.

Given the occurrence of visible fluorite in core, fluorine assays were acquired from the initial trial assay batch (section 8.1.1). Supergene zone splits assayed 100-3000ppm and primary zone splits 250-3000ppm fluorine.

FIGURE 8.9 As and Cu distributions (by visible Fe-Cu sulphides)

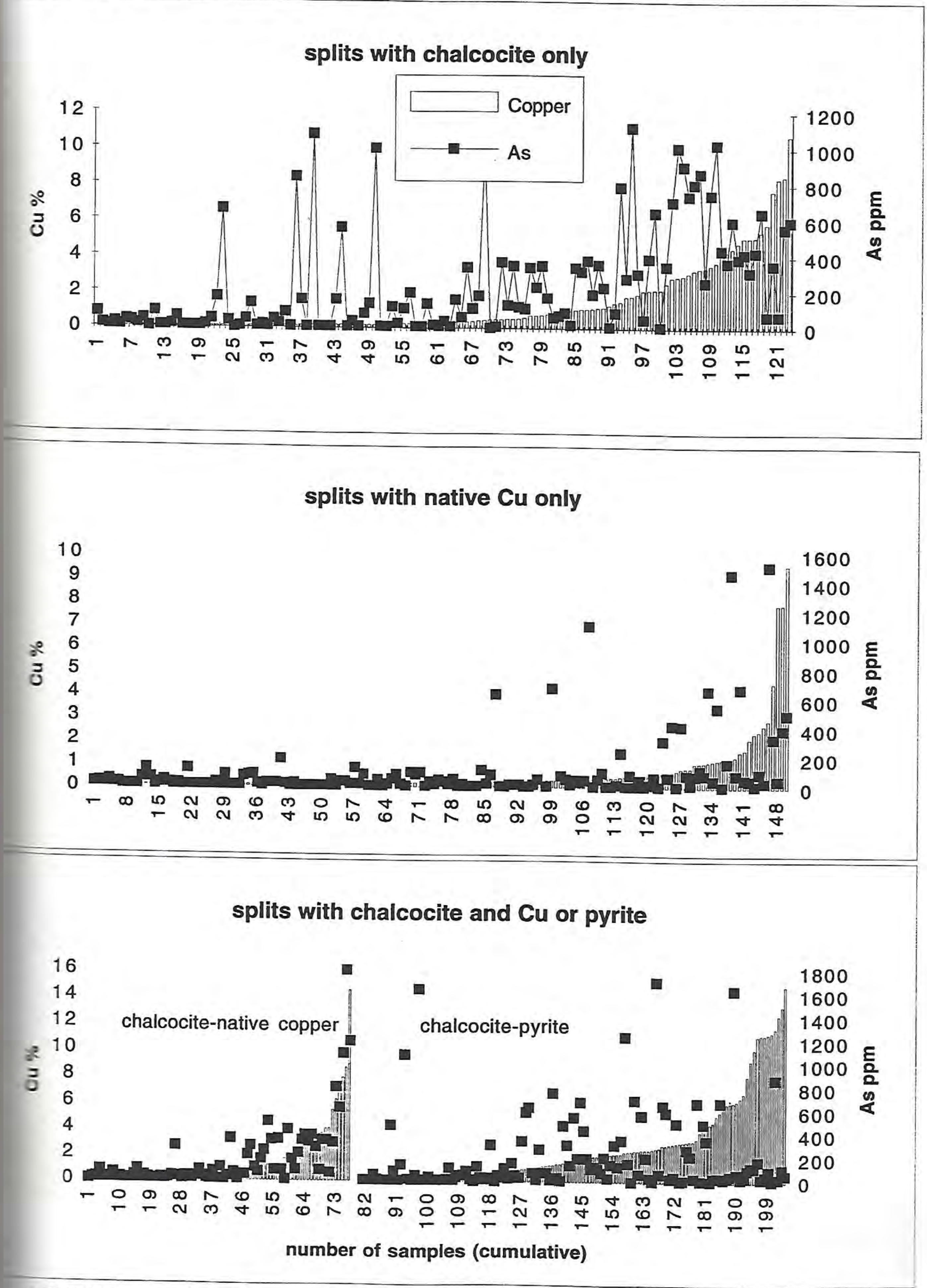

FIGURE 8.10 splits with visible cpy-py, and visible cpy only

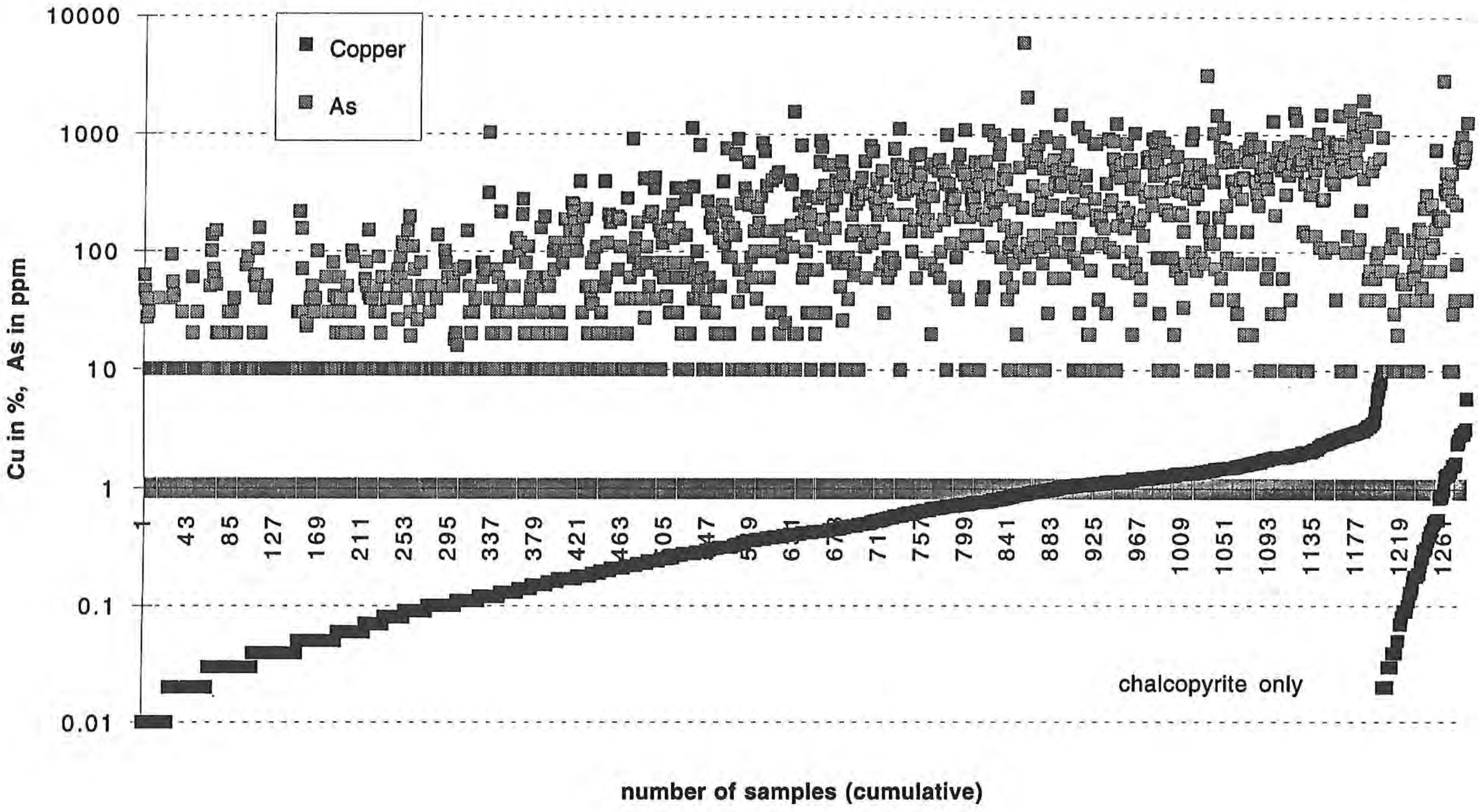

9. METALLURGY

9.1 METALLURGICAL BEHAVIOUR OF SUPERGENE ORE

Petrographical and X-ray diffraction studies were carried out by the Minerals Research team at MIM (Mount Isa) to predict the likely metallurgical behaviour of the sulphides and gangue minerals in supergene drillholes EH102 and EH109 (Knights, 1993a,b,c; Landmark, 1993a,b, 1994). The details of the petrographical and XRD studies are beyond the scope of this study and the reader is referred to the original reports for more information.

Knights (1993c) highlighted those features within the supergene which are most likely to limit efficient ore recoveries:

- The berthierine-rich ‘chlorite’ zone (Table 7.3) contains ultra-fine chalcocite/bornite. Berthierine is an iron-rich septechlorite belonging to the kaolin-serpentine group. It may cause potential loss of minerals with high intrinsic copper content by raised reagent consumption (Knights, 1993b).
- Ultrafine disseminations of chalcocite/bornite are frequently enclosed in siderite and calcite; loss of minerals with high intrinsic copper content is predicted.
- Carbonate will cause enhanced acid consumption during leaching (modelled siderite abundances as high as 30% in some assay splits, refer Appendix IIIa).
- Visible stringer pyrite is frequently overprinted by secondary chalcocite, producing complex boxwork replacements of intergrown chalcocite-bornite-pyrite and replacement-rimming chalcocite/pyrite binaries. Copper recoveries may be reduced in such material.
- Secondary chalcopyrite invariably generates a high proportion of finely disseminated chalcopyrite within the gangue matrix; this may incur significant metal losses.
- Flotation recovery of native copper to the copper concentrate will incur higher background arsenic levels (section 8.2.3).

9.2 METALLURGICAL TEST WORK

Subsequent to the Supergene' drilling programme, four PQ holes were drilled to specifically address metallurgical issues in both the supergene and primary zones (refer to section 4.3). The holes were logged using the EHM scheme (Table 3.3) and also a method based on meso- and micro-textural relationships (e.g., Marcault, 1994). The applicability of the textural approach remains to be determined, but it appears to take little account of gangue mineralogy in well-developed supergene profiles and thus the potential difficulties outlined above. Refer to section 3.3.2 for other comments on this approach .

Early metallurgical tests on the PQ drill core have achieved 90% Cu recoveries and production of a 27% Cu concentrate from primary ore (Munro 1994). Gold within the primary zone is anticipated to exceed yields obtained from test work carried out by WMC. For supergene ore, a minimum 30% Cu concentrate is expected, with 80% recovery. No figures are yet available on the metallurgical performance of supergene Au.

10. GEOPHYSICS

The following is a summary of work carried out by MIM Exploration to determine geophysical signatures of the Ernest Henry orebody.

10.1 MAGNETIC SUSCEPTIBILITY RECORDS

MIM Exploration staff contracting to Ernest Henry Mining Pty. Ltd. routinely sampled apparent susceptibility on core for all holes drilled in the EH series. Readings were taken at approximately 1-2m intervals (i.e., equivalent to each assay split) with a GeoInstruments GMS II susceptibility meter and results were merged into the MS Access Database.

In order to calibrate the apparent susceptibility results with true susceptibilities and then potentially to volume percent magnetite, samples of core were sent to Dr. Dave Clark of CSIRO. Intensity and orientation of any remanent magnetisation was also specifically requested on four oriented core samples from holes EH108 and EH132. Final reporting is still pending on the results of these studies; however, interim results are available and are presented in Table 10.1.

The conversion factor (as determined from the 21 samples) between apparent and true susceptibilities, correcting for instrument response and finite core volume would be of the order of twice (1.833 from linear regression) the measured susceptibilities. This is widely variable in the more inhomogeneous core where the meter has been placed on the more magnetic parts of the sample.

The magnetic mineral has been found to be stoichiometric magnetite (Fe_3O_4) with negligible substitution of other cations; thus, the percentage of the mineral should be able to be approximated well from the susceptibility of the sample using published formulae. The main error in any conversion would lie with the self-demagnetisation of the sample and the accuracy of the apparent susceptibility to true susceptibility conversion. As there is a 40% standard error associated with calculating true susceptibility from the apparent susceptibilities (using a conversion factor of 1.833), this conversion would obviously be the most significant contributor to the error in calculating the magnetite resource.

10.2 DOWNHOLE TEM

Six holes were logged in six days at the Ernest Henry deposit by Solo Geophysics and Co. contracting for MIM Exploration Pty. Ltd. Axial transient response was recorded for WMC holes FTCD41 and -62 and EHM holes EH105, -109, -130 and -141 for a total of 5 hole kilometres of logging. Each hole was logged with 2 loops powered by a SATX transmitter and with responses recorded generally in composite times by a Mk III Sirotem (Rowston 1994). A loop, drilltrace and conductor location diagram is presented in Figure 10.1. Plots of Axial TEM response are contained in Appendix IV.

The responses have been rudimentarily interpreted using the modelling software Multiloop II. Initially, modelling was undertaken without reference to known geology in an attempt to avoid "preconception" of conductive zones. After modelling, a comparison with drillhole intersections was made. An interpretation of each hole follows;

- ***FTCD41***

Little anomalous response is apparent for either loop. The relatively minor intersection response at 130m corresponds to an intersection of 10% chalcopyrite. The weak response indicates that the intersection does not have a large electrically continuous areal extent.

Table 10.1 Magnetic Properties of Drillcore Samples
Ernest Henry Project

SAMPLE	N	k(G/Oe)	k(SI)	APPARENT k(SI)	NRM Int.	NRM Dec.	NRM Inc.	Qn	Q50	A
EH108-154.2m	5	0.0647	0.813	0.45	9070	272°	-72°	0.27	0.07	1.18
EH108-182.0m	5	0.1498	1.88	1.0	27,880	266°	-58°	0.36	0.07	1.31
EH132-101.1m	4	0.0949	1.19	0.81	36,640	259°	-41°	0.76	0.07	1.51
EH132-117.1m	4	0.2607	3.28	1.3	195,200	249°	-42°	1.5	0.16	1.27
EH132-100.8m (S5)	3	0.000588	0.00739	0.0036	135		-54°	0.45		
EH113-137.0m (S7)	5	0.0258	0.324	0.130	2280		-15°	0.17		
EH113-177.6m (P6,TR2)	5	0.0944	1.19	0.379	7130		-76°	0.15		
EH113-190.5 (P1)	4	0.00407	0.0512	0.071	235		-58°	0.11		
EH113-201.3m (P4)	5	0.0797	1.00	0.459	11,840		-22°	0.29		
EH113-205.9m (P2)	4	0.00647	0.0813	0.054	1,510		-4°	0.46		
EH114-70.0m (S2, TR4)	5	0.0318	0.400	0.228	6,260		-68°	0.39		
EH114-78.0m (S3)	3	0.0290	0.364	0.122	9,070		-69°	0.61		
EH114-96.0m (S4)	5	0.0143	0.192	0.0747	3,780		-68°	0.52		
EH114-141.3m (P7, TR1)	4	0.137	1.72	0.991	6,950		-56°	0.10		
EH114-148.8m (P9)	5	0.0682	0.857	0.987	3,320		-65°	0.10		
EH111-41.9m (S6)	4	0.00930	0.117	0.049	142		-60°	0.03		
EH111-47.1m (S1)	4	0.00645	0.0811	0.338	570		-64°	0.17		
EH111-110.0m P3, TR3)	4	0.00887	0.111	0.0544	1,230		-74°	0.27		
EH111-113.0m (P10)	5	0.0256	0.322	0.125	4,410		-24°	0.34		
EH111-126.2m (P8)	4	0.0216	0.272	0.520	6,160		-70°	0.56		
EH111-129.2m (P5)	4	0.120	1.505	0.460	7,450		-39°	0.12		

N = no. of specimens measured

k = bulk susceptibility (mean of susceptibilities along three mutually orthogona directions), corrected for self-demagnetisation, inn cgs units (G/Oe) and SI.

Apparent k is raw measurement with hand-held susceptibility meter (carried out by MIM personnel). Note that some inconsistencies in correction factors between laboratory and field measurements occur for samples that are very inhomogeneous. In some cases the meter has clearly been placed on the most magnetic portion of the sample.

NRM = natural remanent magnetisation

Int = remanence intensity in_μG or mA/m

Dec = remanence declination, positive clockwise from TN

Inc = remanence inclination, positive downwards

Q_n = Koenigsberger ratio for NRM = NRM Int/kF, where Int is in_μG, k is in_μG/Oe and F = 0.51 Oe (51,000 nT)

Q_{50} = Koenigsberger ratio for remanence remaining after alternating field demagnetisation in 50 Oe.

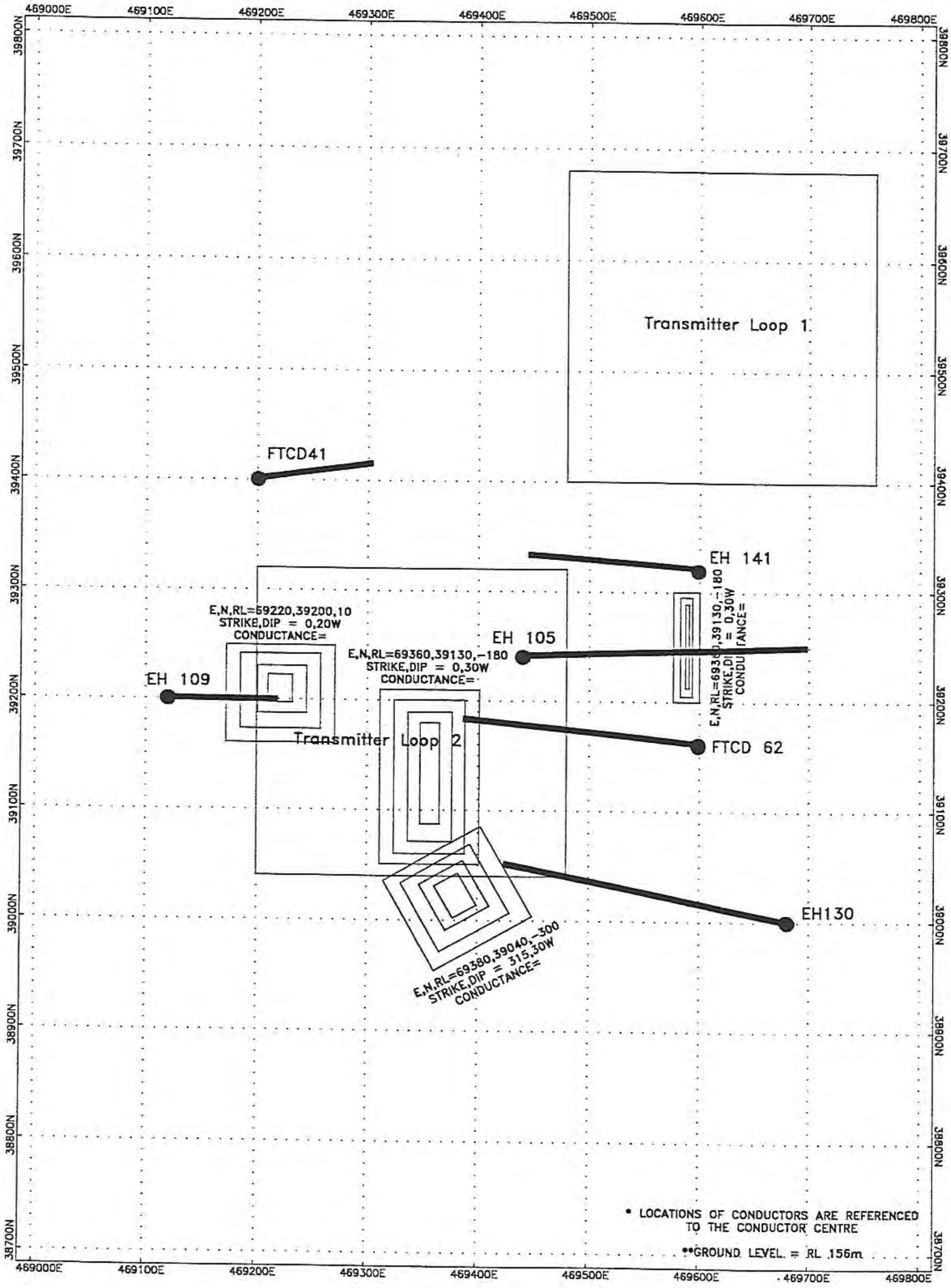

MIM EXPLORATION PTY. LTD.

ERNEST HENRY PROJECT
ERNEST HENRY LEASE
ERNEST HENRY DHTEM 1993

Figure 10.1

- ***FTCD62***

Intersection style responses are visible for both loops between 215m and 265m. These are associated with massive magnetite/carbonate veining and minor pyrite/chalcopyrite. An in-hole response centred at 400m downhole, with a significant, confined off-hole component (i.e., an intersection close to the edge of the conductor) is observed in both loops. The interpreted source lies to the west of the drillhole trace in plan section and has its centre at approx. 69360E, 39130N and -180m RL. The conductor as modelled has a shallow dip to grid west. The four drillholes which come closest to intersecting this zone are FTCD10, FTCD12, FTCD50 and FTCD51. Of these holes FTCD50 intersects the model close to its interpreted centre. FTCD51 is the most removed from the interpreted source whilst FTCD10 intersects the interpreted source at the models outer edges and FTCD12 narrowly misses the modelled conductor. FTCD50 intersects the interpreted conductor at 320m downhole. This is a zone of good sulphide mineralisation with visual estimates of a 15-20m zone of 5-6 % chalcopyrite and 4-5% pyrite. FTCD10 just wings the interpreted conductor at depths downhole of between 360m and 400m.This is a zone averaging > 6% pyrite with trace chalcopyrite. While FTCD 12 narrowly misses the modelled conductor but its projected intersection is coincident with a zone of 6% cp and 4% py. This zone is also a strong conductor in the downhole resistivity logging. FTCD51 has only trace sulphides throughout.

- ***EH105***

An intersection response with an off hole component is visible between 300m and 400m in the loop 2 data. A much diminished intersection response occurs in the loop 1 logs at 400m. The modelled source is a steeply dipping conductor with the majority of the model being above the intersection. The intersection itself occurs at 400m and can be explained by an intersection of 15-20% pyrite between 398 and 400m. The relatively weak nature of the decays within this zone indicates the conductor is not arealy extensive.

- ***EH109***

A very large in-hole response centred at approx. 180m downhole is observed with both loops. This response can be characterised by a decay constant of 28 milliseconds. An exponential decay of this magnitude is indicative of very conductive lithologies. The conductor has been modelled as a gently dipping plate. The modelled conductor is coincident with intersections of native copper between 185 to 192m. The continuation of this conductor or a similar occurrence of native copper is responsible for the anomalies recorded in the first and second phases of the WMC's moving loop work.

- ***EH130***

An in-hole response characteristic of intersection on the extremities of a conductive zone is noted. The in-hole response can be attributed to mineralisation intersected between approx. 500 to 550m (abundant pyrite and locally abundant chalcopyrite - up to 8%) and extending beyond the hole. FTCD53 comes quite close (the closest of all holes) to intersecting the modelled conductor. The sulphide mineralisation between 480 and 500m down FTCD53 (4% cp and 6% py) may form part of the conductive system from which the response is derived.

- ***EH141***

Intersection style responses are visible in this log, although no modelling has been undertaken. The causative lithology once again appears to be primary mineralisation. In this case the "Eastern Lens" mineralisation recorded between 330 and 340m is coincident with the inferred source. The response is less strong than those occurring in holes FTCD62 and EH130. This would imply that the mineralisation is less conductive (lesser grades?) and/or less arealy extensive than the sources of the other two responses.

10.3 GRAVITY

Spectral analysis of the magnetic and gravity data in the immediate vicinity of the deposit indicates the depths to top of the magnetic and gravity sources are distributed between approximately 50 and 140m. The radially averaged Power Spectrum of the two datasets is presented in Figure 10.2. In this plot the gradient of the spectral decay is proportional to the depth of source. Gradients of 140m and 50m are

Figure : 10.2 Ernest Henry : Radially Averaged Power Spectrum
WMC Ground Magnetics and Gravity

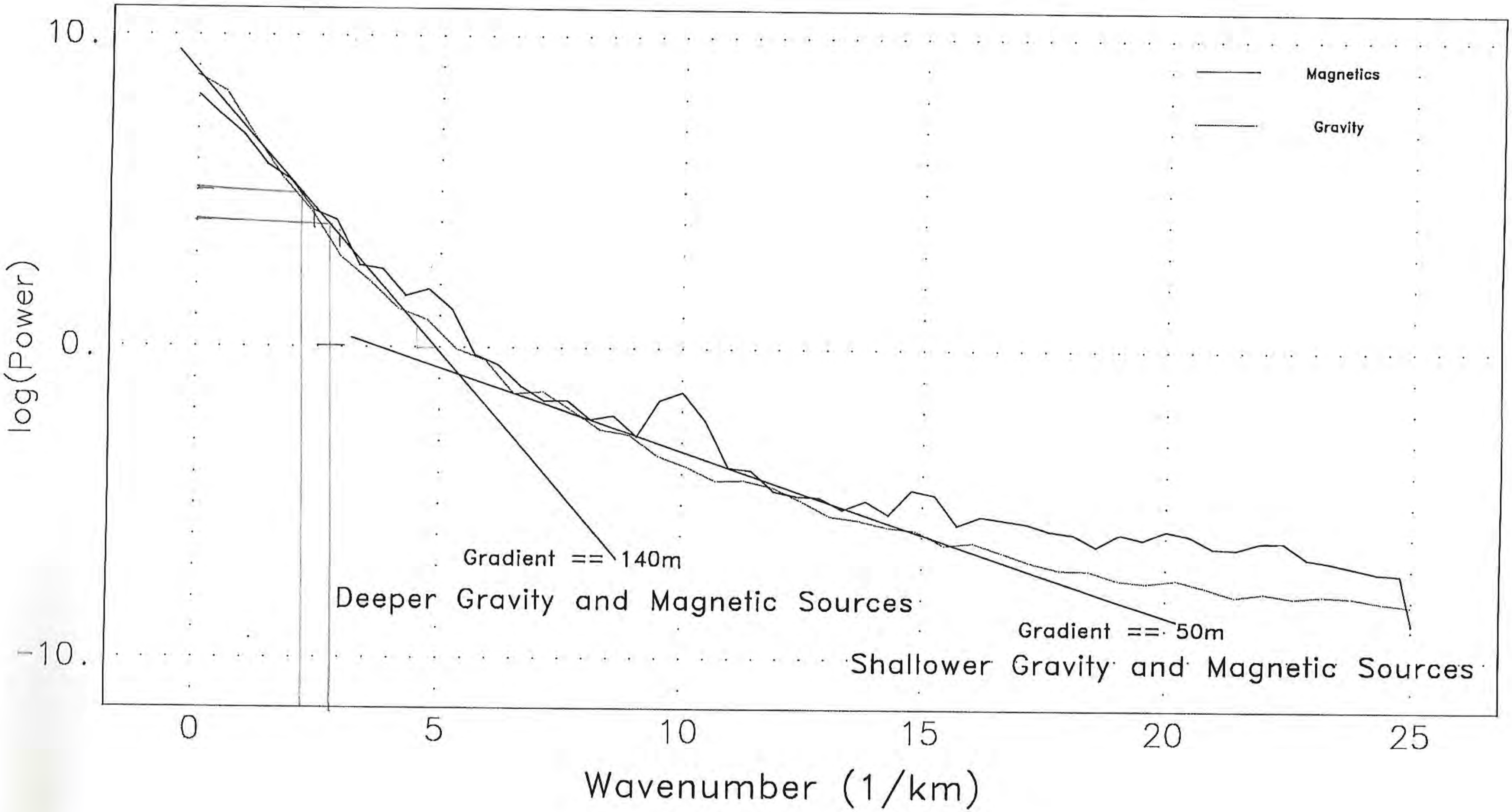

plotted. The close spatial correlation of the gravity and magnetic (returned to pole) datasets seen in plan is thus also seen in the third dimension of depth to source (Rowston 1994). Indeed the spectral characteristics of both datasets are nearly identical.

Population and regression studies of the Cu and Au grades against Archimedes density and susceptibility indicate a stronger correlation between susceptibility and density than between grade and density. Grade and susceptibility are so strongly cross-correlated however as to make further statistical analysis difficult.

It is therefore concluded that the gravity response is sourced primarily and inseparably from the magnetic sources, i.e., the magnetite is the dominant source of the anomalous mass giving rise to the gravity response.

10.4 INDUCED POLARISATION

The strongest IP anomaly produced from WMC's work was interpreted to have the shallowest source and was a direct indicator of supergene mineralisation, namely pyrite/chalcopyrite and possibly native copper. However most IP lines (two lines with no anomalous response) have what were considered to be anomalous responses. Some of these can be attributed to off-section responses from the secondary mineralisation. No definitive primary ore responses are seen from the surface work. This is attributed to the conductive overburden and masking of the shallow primary ore by secondary mineralisation rather than a lack of IP response of the primary mineralisation. The primary ore's response is clearly visible downhole (for example FTCD12 between 210 and 250m).

10.5 CONCLUSIONS

- The strong EM anomaly drilled by WMC leading to the discovery of the Ernest Henry deposit was sourced by native copper occurring within supergene mineralisation.

- The notion that the primary ore does not form an EM target is dependent upon a frame of reference:

  From MIMEX's down-hole work, it is known that some higher grade sulphidic zones generate significant EM responses up to at least 80m off-hole. These conductive zones however, in the limited logging to date, all occur at depth. The logging through the shallower sections only exhibit responses sourced from the secondary mineralisation. It may however, be possible to detect from surface some of the conductive zones delineated by the downhole work. This would require higher transmitter loop currents and different transmitter loop geometries to than used in WMC's work. Indeed, if some of these zones occurred at depths comparable to the supergene mineralisation then they would likely form EM targets. Furthermore, no direct magnetite sourced EM responses (minor intersection style responses only) were noted down-hole.

- The factors affecting surface geophysical recognition of the primary ore at Ernest Henry are the geometry of the orebody, the conductive overburden, the masking qualities of the secondary mineralisation and the fact that possibly, the shallowest primary ore is neither an EM conductor nor IP responder.

- Primary ore geophysical targets do exist, but are too deep for surface resolution with galvanic IP methods and even possibly for EM methods. It must be recognised that deposits of similar origin and grade could be both EM and IP targets, contingent upon the depths to source. It must also be recognised that supergene mineralisation is obviously a definitive indicator of the primary mineralisation at Ernest Henry and it provided an obvious, strongly anomalous response to both of the electrical methods used.

11. IMPLICATIONS FOR EXPLORATION

Based on our current knowledge of the spatial distribution of interpreted controls on mineralisation at Ernest Henry deposit, there is considerable scope for increasing the current resource and locating new orebodies.

11.1 DISTRICT EXPLORATION

Several prominent late brittle faults, inferred from drill core and R.L. plans, occur within the environs of the deposit. These faults trend roughly north-northwest and dip steeply to the east and west. At the southwest end of the deposit, the Revwood Fault terminates mineralisation, but the sense of movement is not known. Given that the western margin of mineralisation (defined by the >0.5% Cu contour) appears to have a natural termination controlled by the extent of brecciation towards the north and west, the size of possibly displaced mineralisation is not likely to be significant.

At the eastern edge of the main resource block, the Badj Kharkl Fault Zone comprises a series of steep, probably east-dipping, normal faults that commonly cut mineralisation, resulting in a slicing of the resource east block downwards. We believe that this is the origin of the eastern lens. Western Mining geologists inferred a fault in this zone, although they were unclear about its position and indicated a westerly dip. The fault was called Hoffman's Fault, after the driller who drilled the discovery hole (Hronsky, 1993). From the cross-sections constructed to date, the Eastern Lens represents a valid target. However, a number of points need to be considered prior to engaging in high cost exploration of the area:

- as a result of probable multiple faulting, resource blocks rarely appear wider than 40-50 m in cross-section;
- the down-throw to the east will mean costly drilling because the resource is predicted to lie 500-700m below the present surface;
- no increase in grade is apparent from information to date that would improve the economics of exploiting a deep resource.
- there is evidence for a gradual decrease in ore grades, reflecting less intense alteration and brecciation, on the western margin of the deposit.

Mawer (1994) suggested that significant mineralisation may occur beneath the marble matrix breccia unit. Examination of some of the Western Mining core which penetrated beneath the marble matrix breccia zone (e.g., FTCD73, 9440 mN cross-section) indicates sub-economic disseminated chalcopyrite + pyrite within fractured and weakly brecciated felsic volcanics. Based on a genetic model involving formation of tension gash and en echelon mineralised lenses, potential exists for mineralisation beneath the marble matrix breccia, which is commonly assumed to be the footwall boundary to mineralisation. This represents a high priority exploration target for district-scale exploration.

The Marshall Shear Zone to the south is poorly understood and may also represent a valid target. Mawer (1994) suggests that movement on this shear zone may be very late, with top down to southeast movement. This would displace any extensions of the Ernest Henry resource down to the southeast. Clearly further district exploration drilling is required to address these issues.

11.2 REGIONAL EXPLORATION

Regional exploration for Ernest Henry-style targets remains an important focus for future work in the Eastern Succession and elsewhere. A number of geophysical and geochemical techniques have been tested over the deposit by both WMC and MIMEX to examine their effectiveness in detecting the blind orebody. Summary results of these surveys are presented below.

- ***Transient EM***

Western Mining carried out a Sirotem survey in 1990 which identified a weak anomaly centred over the as yet undiscovered orebody. Follow-up work defined a strong late-time anomaly, which on drilling was found to correspond to supergene native copper mineralisation.

Downhole EM work carried out by WMC confirmed the presence of a strong conductor in the supergene zone. Ernest Henry Mining conducted downhole TEM in six holes across the mineralised body. Anomalies ranged from weak off-hole responses corresponding to holes peripheral to mineralisation (e.g., FTCD62), to highly anomalous responses (28msec decay constant) in holes penetrating the orebody where supergene development is extensive (e.g., EH109). All modelled data from TEM work reflects a strong correlation between anomalous EM and mineralisation, with the best and most consistent anomalies developed in native copper zones.

- ***Induced Polarisation***

The strongest and shallowest I.P. responses across the Ernest Henry grid correspond to supergene mineralisation on line 9350mN. No definitive primary ore responses are seen from the surface work.

- ***Potential Field Methods***

Total magnetic intensity and Bouguer gravity datasets both exhibit regionally anomalous responses in the vicinity of the Ernest Henry deposit. The magnetic data has obvious utility in isolating significant magnetite occurrences, and therefore potential Cu-Au-magnetite resources of the Ernest Henry type. The 2 mgal gravity response over at Ernest Henry is probably caused by the high concentration of magnetite in the deposit. However, it is possible that deposits of a similar style may occur without a significant density contrast with country rocks.

- ***Physical Properties***

Natural gamma logging shows a strong correlation with copper grade. Low magnetic susceptibility readings within the supergene zone reflect the destruction of magnetite during weathering, whereas readings from the primary zone are typically high (800 x 10-3 SI). A calibration factor that relates apparent magnetic susceptibility to true susceptibility has been determined. This factor can be used to calculate percentage magnetite from the apparent susceptibility readings.

- ***Gas Vapour Phase Geochemistry***

A gas vapour phase geochemical survey was carried out over the Ernest Henry deposit in late 1993 to determine whether any anomalous vapour emissions from the underlying mineralisation could be detected. Results show that an anomalous zone exists across the area of strongest mineralisation. However, it must be noted that each GVP survey is effectively internally calibrated and as such is not readily applicable to other areas. Nonetheless, with further development and studies, GVP represents a potentially powerful tool in the detection of blind' orebodies.

- ***Partial Extraction***

Samples of the overlying black soils were collected to determine whether a subtle geochemical response over buried mineralisation (> 40m) could be detected. The results were somewhat unexpected in that anomalous values were detected at the margins of rather than over the orebody. Testing of partial extraction methods will continue as they offer a potentially effective means of ranking geophysical targets in covered regions.

In summary, the most definitive signatures of mineralisation observed at Ernest Henry are related to gravity and TEM anomalies. The projected outline of mineralisation closely corresponds to the coincident response of strongly anomalous Sirotem with peak gravity /magnetic signatures. The TEM is strongest over supergene mineralisation, although more powerful transmitters may detect the primary mineralisation response in late times. Similarly, the best response from IP is returned from the supergene zone, with little evidence to date that IP/EM would detect 'blind' primary mineralisation. Thus, it may be possible to have magnetic and gravity signatures similar to Ernest Henry in orebodies without a supergene zone and IP/EM response.

GVP and partial extraction surface geochemical methods are sensitive to local geological and hydrologic variability. Persistence in the refinement of such techniques may provide us with a powerful means of ranking geophysical targets at the district scale.

REFERENCES

Brinbaum, P.M., 1994a. Reliability of Ernest Henry Mining Drill Core Assays. Mineral Sampling Consultants Pty Ltd, 23pp.

Birnbaum, P.M., 1994b. Precision and Bias of Ernest Henry Mining Drill Core Copper and Gold Assays reported by ALS and AMDEL. Amendment to Birnbaum, 1994a, 4pp.

Blake, D.H., 1987. `Geology of the Mount Isa Inlier and environs, Queensland and Northern Territory'. Bulletin 225, Bureau of Mineral Resources, Canberra, 83 pp.

Blake, D.H., Etheridge, M.A., Page, R.W., Stewart, A.J., Williams, P.R., and Wyborn, L.A.I., 1990. Mount Isa Inlier - Regional geology and mineralisation. In: `Geology of the Mineral Deposits of Australia and Papua New Guinea', edited by F.E. Hughes, Australian Institute of Mining and Metallurgy Monograph 14, Volume 2, The Australasian Institute of Mining and Metallurgy, Melbourne, 915-925.

Blake, D.H., and Stewart, A.J., 1992. Stratigraphic and tectonic framework, Mount Isa Inlier. In: `Detailed Studies of the Mount Isa Inlier', edited by A.J. Stewart and D.H. Blake, Bulletin 243, Australian Geological Survey Organisation, Canberra, 1-11.

Clarke, J., 1992. Further studies of samples from Ernest Henry Prospect. Internal Memorandum XMP92/68, Western Mining Corporation Limited, 79 pp. EHM code SV100.

Clarke, J., 1993. Studies of the Supergene Profile at Ernest Henry. Internal Memorandum XMP 93/04, Western Mining Corporation Limited, 31pp. EHM code SV134.

Clemens, J.D., and Mawer, C.K., 1992. Granitic magma transport by fracture propagation. Tectonophysics, 204, 339-360.

Croxford, W., 1994. Summary Petrographic on EH Samples (with photographs)

Hannan, K.W., 1993a. Characterisation of the Ernest Henry Supergene Zone. MIMEX Memorandum, 2pp.

Hannan, K.W., 1993b. Quality Control of Ernest Henry Assays. MIM Exploration Memorandum, 3 pp text, 11 pp Figures and Tables.

Hannan, K.W., 1994. Quality Control of Ernest Henry Drill Core Assays. MIM Exploration Memorandum, 1pp text, 8 Figures.

Hayward, N., 1992a. Analysis of Ernest Henry structural orientation data. Internal memorandum XTV92/038, Western Mining Corporation Limited (unpublished), 13 pp.

Hayward, N., 1992b. Foliation and shear zone development at the Ernest Henry Au-Cu deposit and formation of footwall marble breccia. Internal memorandum XTV92/041, Western Mining Corporation Limited (unpublished), 11 pp.

Hill, E.J., Loosveld, R.J.H., and Page, R.W., 1992. Structure and geochronology of the Tommy Creek Block, Mount Isa Inlier. In: `Detailed Studies of the Mount Isa Inlier', edited by A.J. Stewart and D.H. Blake, Bulletin 243, Australian Geological Survey Organisation, Canberra, 329-348.

Holcombe, R.J., Pearson, P.J., and Oliver, N.H.S., 1991. Geometry of a Middle Proterozoic extensional d,collement in northeastern Australia. Tectonophysics, 191, 255-274.

Hronsky, J.M.A., 1993. The geology of the Ernest Henry copper-gold deposit, Cloncurry, Queensland. Internal report K/3535, Western Mining Corporation Limited (unpub.), 49 pp.

Knights, J., 1993a. Comments on Random Samples from Ernest Henry. Unpublished Internal Memorandum from Minerals Processing Research Manager to the Ernest Henry Project. MIM Exploration.

Knights, J., 1993b. Ernest Henry Mineralogical Investigations. Description of Collected DDH Samples (EH102, EH109).Mineral Services Report No. 6214. Unpublished Internal Report to the Ernest Henry Project. MIM Exploration.

Knights, J., 1993c. Suggestions re: Defining Metallurgical Classification of Ernest Henry Supergene Ore. Unpublished Internal Memorandum to the Ernest Henry Project. MIM Exploration.

Landmark, V.J., 1993a. Ernest Henry Mineralogical Investigations. Description of Collected Supergene Ore DDH Samples, EH102, EH109. Mineral Services Report No. 6215. Unpublished Internal Report to the Ernest Henry Project. MIM Exploration.

Landmark, V.J., 1993b. Ernest Henry Mineralogical Investigations. Description of Supergene Ore DDH Samples, EH102 & EH109. Mineral Services Report No. 6227. Unpublished Internal Report to the Ernest Henry Project. MIM Exploration.

Landmark, V.J., 1994. Ernest Henry Mineralogical Investigations. Description of Supergene Ore DDH Samples, EH102. Mineral Services Report No. 6231.Unpublished Internal Report to the Ernest Henry Project. MIM Exploration.

Lockwood, A., 1994. Correlation of Downhole Geophysics and Assay Data, Ernest Henry Drillholes. Unpublished Internal Report, MIM Exploration.

Marcault, L., 1994. Ernest Henry Textural Investigation. (Description of logging and samples taken from Metallurgical Holes). Unpublished Internal Report to the Ernest Henry Project, MIM Exploration.

Mawer, C.K., 1992a. Kinematic indicators in shear zones. In: `Basement Tectonics 8: Characterisation and Comparison of Ancient and Mesozoic Continental Margins - Proceedings of the 8th International Conference on Basement Tectonics (Butte, Montana, 1988)', edited by M.J. Bartholomew, D.W. Hyndman, D.W. Mogk, and R. Mason, Kluwer Academic Publishers, Dordrecht, 67-81.

Mawer, C.K., 1992b. Tick Hill structural study. Internal technical report, MIM Exploration (unpublished), 48 pp.

Mawer, C.K., 1993. Structure of drill core, Ernest Henry deposit. Internal technical report, MIM Exploration (unpublished), 151 pp.

Mawer, C.K., 1994. Structural interpretation, Ernest Henry deposit. Internal technical report, MIM Exploration (unpublished), 60 pp.

Munro, P., 1994. Ernest Henry Metallurgical Progress Report II. Unpublished Internal Memorandum, MIM Holdings.

Nesbitt, B.W., and Williams, C.R., 1993. Geological interpretation of aeromagnetic, radiometric and gravity data on the Clonagh 100,000 sheet area, Cloncurry district, with implications for mineralisation and suggested targets. Consultant's report to joint venture partners, Western Mining Corporation and MIM Exploration (unpub.), 27 pp.

Oliver, N.H.S., 1992a. Origin, timing, and evolution of Ernest Henry Au-Cu mineralisation and related alteration, Mount Fort Constantine, Mount Isa Inlier. Consultant's report to joint venture partners, Hunter Resources Ltd. and Western Mining Corporation (unpub.), 25 pp.

Oliver, N.H.S., 1992b. Regional structural, metamorphic, and stratigraphic setting of the Tick Hill gold deposit, with implications for ore genesis and exploration. Consultant's report, MIM Exploration and Carpentaria Gold (unpublished), 30 pp.

Oliver, N.H.S., Holcombe, R.J., Hill, E.J., and Pearson, P.J., 1991. Tectono-metamorphic evolution of the Mary Kathleen Fold Belt, northwest Queensland: a reflection of mantle plume processes? Australian Journal of Earth Sciences, 38, 425-455.

Page, R., 1993. Geochronological results from the Eastern Fold Belt, Mount Isa Inlier. Australian Geological Survey Organisation Research Newsletter, Number 19.

Page, R.W., 1988. Geochronology of Early to Middle Proterozoic fold belts in northern Australia: a review. Precambrian Research, 40/41, 1-19.

Page, R.W., and Bell, T.H., 1986. Isotopic and structural responses of granite to successive deformation and metamorphism. Journal of Geology, 94, 365-379.

Pearson, P.J., Holcombe, R.J., and Page, R.W., 1992. Synkinematic emplacement of the Middle Proterozoic Wonga Batholith into a mid-crustal extensional shear zone, Mount Isa Inlier, Queensland. In: `Detailed Studies of the Mount Isa Inlier', edited by A.J. Stewart and D.H. Blake, Bulletin 243, Australian Geological Survey Organisation, Canberra, 289-328.

Stewart, A.J., and Blake, D.H. (Eds.), 1992. `Detailed Studies of the Mount Isa Inlier'. Bulletin 243, Australian Geological Survey Organisation, Canberra, 374 pp.

Till, M., 1994a. Quantitative mineralogy of 92 samples. Report G175/94 to MIMEX, AMDEL Mineral Services Laboratory (Adelaide), 5pp.

Till, M., 1994b. Quantitative mineralogy of 83 samples. Report G2315pp./94 to MIMEX, AMDEL Mineral Services Laboratory (Adelaide), 5pp.

Western Mining Corporation Engineering Services Limited, June 1993. Cloncurry Copper Project: Ernest Henry Prospect. Draft Prefeasibility Study. Unpublished Internal Report.

Wyborn, L.A.I., Page, R.W., and McCulloch, M.T., 1988. Petrology, geochronology and isotope geochemistry of the post-1820 Ma granites of the Mount Isa Inlier: mechanisms for the generation of Proterozoic anorogenic granites. Precambrian Research, 40/41, 509-541.

Appendices

incomplete - this is a scanned selection from each Appendix with bias to chemical & mineralogical data - K Hannan, Oct, 2015

APPENDIX Ia - Micromine Files from the Ernest Henry Supergene Project

Data files in MIMDATA

ALLASSAY	EHMETSAM	WMCSG
ALLCOLLS	EHOXIDA	
ALLCOMP2	EHPETROL	
ALLGEOL	EHPZGEOL	
ALLMETZN	ERNEML	
ALLSURVS	LEGEND1	
EHGANGUE	WMCGEOL	
EHGEOTEC	WMCOXDA	

The above are contained in Micromine project 'MIMDATA'; details of variables and data contained are given below. The data is a mixture of material collected by MIM Exploration during the supergene evaluation program and that inherited from WMC.

ALLASSAY : Holes EH100 - EH154 incl.

EHMET1 - EHMET4, FTCD 2 - FTCD 91.

Includes all geochemical assays, supergene gangue zones, metallurgical zones and sulphide occurrences.

No. of records = 17106

ALLCOLLS : Collar file for holes

EH100 - EH163 incl. EHMET1 - EHMET4
(includes terrain holes)
FTCD 2-FTCD 92

No of records = 154

ALLCOMP2 : Holes EH100 - EH154 incl.

EHMET1 - EHMET4, FTCD2 - FTCD 91

2m composites of most data contained in ALLASSAY.

No. of records = 18603

ALLGEOL	:	Holes EH100 - EH154 incl. EHMET 1 - EHMET 4, FTCD 2 - FTCD 77 Geological splits with lithology and other qualifiers. Data from WMC holes is a conversion from their logging codes; inaccuracies may occur. No. of records = 8815
ALLMET Z	:	Holes EH100 - EH154 incl EHMET1 - EHMET4, FTCD2 - FTCD 77 Includes metallurgical zones and copper species occurrence No. of records = 8815
ALLSURVS	:	Holes EH100 - EH163 (terrain holes) incl. EHMET1 - EHMET4 FTCD 2 - FTCD 91 Survey measurements for all listed holes. No. of records = 1520
ALNEWCOL	:	Holes EH100 - EH163 incl. EHMET 1 - EHMET4. FTCD 2 - FTCD 92. Collar file for above holes with coordinates transformed to a new grid. No. of records = 154

Project MIMDATA File allsurvs.dat Fri Mar 18 11:06 1994

RECORD	FIELD_NAME	TYPE (C/N)	WIDTH<136	DEC
1	HOLE	C	10	0
2	SDEPTH	N	7	2
3	AZIM	N	7	2
4	DIP	N	7	2
5	GYRO(Y/N)	C	2	0

Project MIMDATA File alnewcol.dat Fri Mar 18 11:07 1994

RECORD	FIELD_NAME	TYPE (C/N)	WIDTH<136	DEC
1	HOLE	C	10	0
2	NORTHING	N	10	0
3	EASTING	N	10	0
4	RL	N	10	0
5	TDEPTH	N	10	1
6	AZIM	N	10	2
7	DIP	N	10	2
8	STATUS	N	3	1

Project MIMDATA File ehgangue.dat Fri Mar 18 11:07 1994

RECORD	FIELD_NAME	TYPE (C/N)	WIDTH<136	DEC
1	HOLE	C	10	0
2	FROM	N	10	1
3	TO	N	10	1
4	NORTHING	N	10	2
5	EASTING	N	10	2
6	RL	N	10	2
7	GANGUE	C	10	0

Project MIMDATA File ehgeotec.dat Fri Mar 18 11:07 1994

RECORD	FIELD_NAME	TYPE (C/N)	WIDTH<136	DEC
1	HOLE	C	6	0
2	FROM	N.	5	1
3	TO	N	5	1
4	DIST	N	4	1
5	REC	N	4	1
6	DOW	C	2	0
7	RS	C	2	0
8	RQD	N	2	0
9	FEAT	C	2	0
10	FREQ	N	3	0
11	FILL	C	10	0
12	SHAPE	C	1	0
13	ROUGH	C	1	0
14	FAULT	N	5	0
15	THICK	N	5	0
16	BETA	N	3	0
17	ALPHA	N	3	0
18	TYPE	N	1	0
19	COMMENTS	C	10	0
20	SYMBOL	N	3	0
21	J4	N	10	0
22	DEP	N	10	2

Appendix Ib - MacIntosh Files from the Supergene Drilling Project

	File Size in Kilobytes
Routine Assays ALS	
• Routine EH Assay ALS (all elements, excludes repeats and Met standards)	992
Routine Repeat Assays ALS	
• Repeats and Originals Cu ALS	155
• Repeats and Originals Au ALS	62
• Repeats Au + Checks + Metals	93
• Repeats ALS (metals excluding Au)	93
1 in 10 Check Assays at AMDEL	
• Repeats 1 in 10 AMDEL	93
• Repeats 1 in 10 ALS vs AMDEL	155
Check of WMC Assays	
• FTCD76 AMDEL	31
• FTCD76 ALS	31
Screen Copper Assays by Batch Number	
• H93001 Cu Scn	31
• H93008 Scn TXT	31
• H0301100 Scn TXT	31
• H93012 Cu Scn	31
• H93013b Cu Scn	31
• H93013c Cu Scn	31
• H93018 Scn TXT	31
Met Standards	
• MET STDS Study ALS) Metals	31
• MET STDS Study AMDEL) Major +	31
• MET STDS Study ANALABS) Trace Elements	31
• Routine Met Std Assays (A)) (ALS)	62
• Routine Met Std Assays (D)) (AMDEL)	31
XRD Work	
• XRD + gangue.1 (EH 102)	62
• XRD + gangue.2 (EH 109)	62
• XRD + gangue.3 (EH 113, 121)	93

Appendix IIa - Cu Internal Standard Replicate Summary

BATCH	MET 12		MET 19		MET 21	
	Mean	σ	Mean	σ	Mean	σ
ANALABS (G115 Test, n = 20)	**2.52**	0.03	**1.77**	0.02	**1.93**	0.02
AMDEL (AA7 Test, n = 20)	**2.44**	0.34	**1.45**	0.11	**1.71**	0.14
	(1.92, 3.05)		(1.06, 1.63)			
ALS (Screen Test, Townsville, n = 5)	**2.37**	0.08	**1.63**	0.03	**1.67**	0.05
ALS (Screen Test, Brisbane, n = 5)	**2.31**	0.01	**1.53**	0.00	**1.77**	0.02
ALS (A101 Test, Townsville, n = 5)	**2.44**	0.02	**1.73**	0.03	**1.81**	0.07
ALS (A101 Test, Brisbane, n = 5)	**2.42**	0.07	**1.67**	0.03	**1.78**	0.08
Batch 1 (n = 3)	**2.56**	0.20	**1.64**	0.10	**1.85**	0.48
Batch 5 (n = 9)	**2.27**	0.05	**1.75**	0.05	**1.95**	0.20
Batch 6 (n = 7)	**2.36**	0.07	**1.65**	0.05	**1.83**	0.06
Batch 8 (n = 9)	**2.31**	0.10	**1.64**	0.07	**1.72**	0.14
Batch 11 (n = 11)	**2.59**	0.12	**1.76**	0.14	**2.10**	0.26
Batch 12 (n = 15)	**2.56**	0.12	**1.73**	0.10	**1.78**	0.18
	(2.44, 2.84)				(1.40, 2.16)	
Batch 13a (n = 6)	**2.37**	0.08	**1.63**	0.07	**1.78**	0.18
Batch 13b (n = 18)	**2.49**	0.22	**1.66**	0.08	**1.66**	0.16
			(1.52, 1.79)			
Batch 13c (n = 4)	**2.33**	0.04	**1.69**	0.04	**1.77**	0.04
Batch 18 (n = 14)	**2.36**	0.07	**1.62**	0.06	**1.76**	0.15
	(2.18, 2.48)				(1.58, 2.11)	
Batch 20a (n = 9)	**2.39**	0.06	**1.72**	0.06	**1.83**	0.14
	(2.26, 2.48)					
Batch 20b (n = 9)	**2.36**	0.09	**1.54**	0.05	**1.76**	0.18
Batch 22 (n = 5)	**2.33**	0.23	**1.55**	0.02	**1.64**	0.11
	(2.15, 2.78)					
Batch 25 (AMDEL, ICP, n = 6)	**2.53**	0.08	**1.81**	0.04	**1.93**	0.09

Batch 1-22 : routine analyses by A101 at ALS, Townsville
Batch 25 : 1 in 10 checks by ICP at AMDEL, Adelaide
Mean = number of analyses; σ = first standard deviation
Values in parenthesis refer to batch minimum and maximum

Appendix IIa - Au Internal Standard Replicate Summary

BATCH	MET 12		MET 19		MET 21	
	Mean	σ	Mean	σ	Mean	σ
ANALABS (Fire Assay Test, n = 20)	**1.18**	0.14	**0.90**	0.08	**0.55**	0.08
	(0.66, 1.38)					
ANALABS (G115 Test, n = 2)	**1.05**	0.10	**0.75**	0.09	**0.65**	0.08
	(0.86, 1.26)		(0.60, 0.90)			
AMDEL (AA7 Test, n = 20)	**1.19**	0.09	**0.87**	0.07	**0.62**	0.07
	(1.06, 1.36)		(0.76, 1.06)		(0.54, 0.78)	
ALS (PM203 Test, n = 5)	**0.94**	0.08	**0.82**	0.22	**0.63**	0.10
ALS (PM208 Test, n = 5)	**1.30**	0.06	**0.95**	0.03	**0.71**	0.09
Batch 1 (n = 3)	**1.29**	0.06			**0.64**	0.04
Batch 5 (n = 7)	**1.30**	0.05	**0.94**	0.04	**0.61**	0.04
	(1.25, 1.41)					
Batch 6 (n = 7)	**1.33**	0.18	**0.90**	0.03	**0.63**	0.03
Batch 8 (n = 9)	**1.24**	0.14	**0.86**	0.05	**0.61**	0.05
	(1.03, 1.42)					
Batch 11 (n = 11)	**1.31**	0.13	**0.89**	0.04	**0.62**	0.04
	(1.19, 1.67)		(0.83, 0.96)			
Batch 12 (n = 15)	**1.27**	0.08	**0.88**	0.04	**0.62**	0.04
	(1.14, 1.41)					
Batch 13a (n = 6)	**1.22**	0.05	**0.82**	0.04	**0.58**	0.02
Batch 13b (n = 10)	**1.10**	0.04	**0.80**	0.03	**0.55**	0.04
	(1.03, 1.16)		(0.76, 0.85)			
Batch 13c (n = 4)	**1.20**	0.02	**0.91**	0.03	**0.56**	0.01
Batch 18 (n = 14)	**1.29**	0.12	**0.91**	0.07	**0.63**	0.04
	(1.10, 1.65)		(0.79, 1.08)			
Batch 20a (n = 9)	**1.29**	0.20	**0.85**	0.06	**0.59**	0.07
	(0.92, 1.67)					
Batch 20b (n = 9)	**1.28**	0.08	**0.89**	0.05	**0.61**	0.04
	(1.14, 1.41)					
Batch 22 (n = 5)	**1.29**	0.08	**0.90**	0.04	**0.64**	0.02
Batch 25 (AMDEL, n = 6)	**1.25**	0.04	**0.93**	0.06	**0.66**	0.06

Batch 1-22 : routine analyses Fire Assay, ALS, Townsville
Batch 25 : 1 in 10 checks by Fire Assay, AMDEL, Adelaide
Mean = number of analyses; σ = first standard deviation
Values in parenthesis refer to batch minimum and maximum

APPENDIX IIb

Replicate Analyses of the Internal Standards at ALS

KEY for replicate #: MET12A/6.3 indicates third replicate of MET12 in Batch 6 (ALS, T'VLLE)

Replicate #	Cu %	Co	Au	Fe %	Mn %	Ag	As	Ni	Pb	Zn
MET 12A/1.1	2.76	550		25.5	0.31	5	280	60	<10	30
MET 12A/1.2	2.66	570		26.9	0.40	3	360	70	<10	20
MET 12A/1.3	2.28	560		27.5	0.39	4	280	60	<10	40
MET 12A/1.4	2.36	560		26.9	0.38	5	360	50	<10	40
MET 12A/5.1	2.32	540	1.2	27.2	0.42	4		60	<5	22
MET 12A/5.2	2.38	560	1.77	24.7	0.38	4		50	<5	21
MET 12A/5.3	2.28	570	1.27	29.4	0.39	4		50	8	21
MET 12A/5.4	2.44	550	1.23	24.7	0.39	5		50	6	28
MET 12A/5.5	2.32	530	1.31	27	0.34	3		70	<5	24
MET 12A/5.6	2.47	540	1.29	27.9	0.36	5		70	<5	24
MET 12A/5.7	2.32	540	1.28	28.2	0.32	4		60	<5	17
MET 12A/5.8	2.34	540	1.25	26.5	0.34	3		60	<5	21
MET 12A/6.1	2.30	545	1.29	26	0.36	5		45	9	22
MET 12A/6.2	2.24	556	1.41	26.2	0.33	4		53	<5	21
MET 12A/6.3	2.26	527	1.27	28.6	0.35	5		49	6	20
MET 12A/6.4	2.32	542	1.27	28.6	0.35	5		49	<5	22
MET 12A/6.5	2.18	510	1.33	23.8	0.34	4		45	11	20
MET 12A/6.6	2.25	564	1.29	29.6	0.31	4		70	<5	20
MET 12A/8.1	2.30	530	1.03	28.6	0.40	4	480	70		
MET 12A/8.2	2.42	590	1.14	29.3	0.42	3	440	70		
MET 12A/8.3	2.17	580	1.14	29.5	0.41	4	280	70		
MET 12A/8.4	2.33	550	1.12	31.3	0.39	4	320	70		
MET 12A/8.5	2.54	620	1.37	31.3	0.56	3	280	100		
MET 12A/8.6	2.22	580	1.36	31.8	0.49	5	520	50		
MET 12A/8.7	2.25	560	1.42	30.8	0.47	<1	360	60		
MET 12A/8.8	2.28	540	1.41	32	0.46	4	360	60		
MET 12A/8.9	2.27	580	1.21	31.9	0.44	4	480	60		
MET 12A/10.1	2.49	570	1.31	30	0.38	3		52	<5	18
MET 12A/10.2	2.34	580	1.29	27.8	0.35	2		44	<5	15
MET 12A/10.3	2.40	560	1.29	30.9	0.38	1		43	<5	20
MET 12A/11.1	2.63	585	1.32	27.4	0.52	3	210	39		
MET 12A/11.2	2.61	553	1.29	24.4	0.45	4	250	55		
MET 12A/11.3	2.71	599	1.36	26.9	0.48	4	280	52		
MET 12A/11.4	2.50	557	1.19	30	0.42	4	270	55		
MET 12A/11.5	2.77	598	1.23	32.1	0.45	4	250	100		
MET 12A/11.6	2.80	577	1.29	32.7	0.47	4	230	66		
MET 12A/11.7	2.47	511	1.67	30.3	0.40	4	230	80		
MET 12A/11.8	2.53	533	1.31	31.6	0.44	3	190	64		
MET 12A/11.9	2.47	515	1.19	32	0.44	4	210	116		
MET 12A/11.10	2.50	560	1.25	30.6	0.44	4	240	41		
MET 12A/11.11	2.46	542	1.3	30.8	0.43	4	260	52		
MET 12A/12.1	2.46	550	1.27	28.2	0.42	3	260	40		
MET 12A/12.2	2.65	560	1.31	29.9	0.41	3	300	80		
MET 12A/12.3	2.59	490	1.27	31.8	0.42	4	280	60		
MET 12A/12.4	2.44	540	1.14	23	0.35	3	210	50		
MET 12A/12.5	2.56	507	1.37	26.2	0.37	2	280	60		

Routine Met Std Assays(A)

Replicate #	Cu %	Co	Au	Fe %	Mn %	Ag	As	Ni	Pb	Zn
MET 12A/12.6	2.84	492	1.23	30.6	0.42	5	220	70		
MET 12A/12.7	2.56	569	1.33	23.9	0.35	3	230	40		
MET 12A/12.8	2.70	548	1.21	26.2	0.41	4	280	90		
MET 12A/12.9	2.48	513	1.23	25.7	0.43	2	250	66		
MET 12A/12.10	2.44	525	1.41	27.2	0.46	4	260	71		
MET 12A/12.11	2.67	607	1.27	27.4	0.47	4	240	67		
MET 12A/12.12	2.44	561	1.14	26.1	0.43	4	300	55		
MET 12A/12.13	2.44	570	1.36	32.3	0.42	4	210	82		
MET 12A/12.14	2.65	630	1.31	29.4	0.42	4	200	76		
MET 12A/12.15	2.48	530	1.23	26.4	0.42	3	210	75		
MET 12A/13a.1	2.53	570	1.31	30.2	0.42	3	250	90		
MET 12A/13a.2	2.29	570	1.23	28.6	0.39	2	250	70		
MET 12A/13a.3	2.29	550	1.19	28	0.38	3	280	80		
MET 12A/13a.4	2.38	570	1.23	27.9	0.39	3	280	50		
MET 12A/13a.5	2.33	530	1.19	27.1	0.39	3	290	60		
MET 12A/13a.6	2.42	590	1.17	31.3	0.41	3	260	90		
MET 12A/13b.1	2.30	550	1.1	29.8	0.43	4	260	80		
MET 12A/13b.2	2.28	550	1.03	28.6	0.41	3	260	90		
MET 12A/13b.3	2.30	540	1.16	28.4	0.40	3	260	100		
MET 12A/13b.4	2.24	540	1.15	29.9	0.42	4	260	80		
MET 12A/13b.5	2.28	560	1.1	29.9	0.40	4	240	80		
MET 12A/13b.6	2.56	590	1.08	28	0.38	4	190	70		
MET 12A/13b.7	2.60	540	1.07	30	0.44	4	260	80		
MET 12A/13b.8	2.78	549	1.11	28.9	0.42	1	210	40		
MET 12A/13b.9	2.71	569	1.14	25.2	0.41	3	310	40		
MET 12A/13b.1(	2.82	571	1.08	28.7	0.41	3	310	60		
MET 12A/13c.1	2.27	533	1.17	29	0.44	4	290	80		
MET 12A/13c.2	2.32	549	1.18	29.1	0.44	4	260	50		
MET 12A/13c.3	2.38	540	1.22	29	0.45	4	280	70		
MET 12A/13c.4	2.33	541	1.22	28.8	0.43	4	230	60		
Met 12/18.1	2.32	550	1.16	30.4	0.44	3	260	72		
Met 12/18.2	2.35	550	1.1	30	0.43	3	320	42		
Met 12/18.3	2.38	510	1.29	30.2	0.41	2	250	69		
Met 12/18.4	2.38	510	1.29	30.1	0.44	2	250	62		
Met 12/18.5	2.33	540	1.31	25	0.41	3	180	71		
Met 12/18.6	2.35	520	1.25	27.1	0.42	3	260	50		
Met 12/18.7	2.37	500	1.3	27.6	0.43	5	240	68		
Met 12/18.8	2.31	570	1.2	28	0.40	4	280	80		
Met 12/18.9	2.44	560	1.65	28.7	0.40	4	300	60		
Met 12/18.10	2.18	530	1.22	27.8	0.40	3	330	70		
Met 12/18.11	2.29	580	1.36	28.6	0.40	3	310	60		
Met 12/18.12	2.41	580	1.36	26.9	0.40	5	300	40		
Met 12/18.13	2.48	620	1.29	28.1	0.41	4	310	60		
Met 12/18.14	2.41	570	1.3	29.2	0.37	3	280	50		
Met 12/20a.1	2.41	530	1.18	30.3	0.37	4	320	50		
Met 12/20a.2	2.41	550	1.23	30.8	0.39	3	330	49		
Met 12/20a.3	2.38	580	0.92	30.4	0.37	3	330	37		
Met 12/20a.4	2.38	540	1.48	27.1	0.43	4	240	36		
Met 12/20a.5	2.48	550	1.29	26.8	0.43	3	250	39		
Met 12/20a.6	2.37	540	1.67	26.1	0.40	2	270	42		
Met 12/20a.7	2.42	530	1.27	24.1	0.43	2	270	46		

Routine Met Std Assays(A)

Replicate #	Cu %	Co	Au	Fe %	Mn %	Ag	As	Ni	Pb	Zn
Met 12/20a.8	2.26	510	1.23	29.8	0.42	4	280	49		
Met 12/20a.9	2.42	530	1.41	30.2	0.41	3	270	45		
Met 12/20b.1	2.33	560	1.29	33.1	0.38	4	300	43		
Met 12/20b.2	2.16	520	1.22	27.8	0.37	3	310	43		
Met 12/20b.3	2.46	600	1.21	33.7	0.44	4	290	37		
Met 12/20b.4	2.45	550	1.14	30	0.42	2	240	45		
Met 12/20b.5	2.32	570	1.36	29.7	0.40	3	270	44		
Met 12/20b.6	2.44	600	1.27	34	0.40	3	280	42		
Met 12/20b.7	2.37	510	1.27	25	0.37	3	270	51		
Met 12/20b.8	2.38	600	1.41	30.6	0.42	4	300	51		
Met 12/20b.9	2.31	580	1.37	30	0.41	4	250	48		
Met 12/22.1	2.18	508	1.14	29.9	0.39	4	220	47		
Met 12/22.2	2.78	686	1.37	32.9	0.55	4	250	46		
Met 12/22.3	2.28	522	1.3	30.9	0.42	4	250	40		
Met 12/22.4	2.15	513	1.36	25.6	0.43	4	250	47		
Met 12/22.5	2.25	526	1.29	25.1	0.44	5	230	50		
MET 19A/1.1	1.80	960		26.4	0.11	2	660	90	<10	30
MET 19A/1.2	1.57	920		26.7	0.10	3	640	110	<10	40
MET 19A/1.3	1.57	860		27.3	0.11	3	660	110	<10	60
MET 19A/1.4	1.60	860		27.9	0.10	2	600	80	<10	40
MET 19A/6.1	1.66	796	0.87	24.4	0.09	2		105	5	39
MET 19A/6.2	1.79	879	0.97	24.5	0.09	2		135	<5	42
MET 19A/6.3	1.78	842	0.93	30.7	0.08	1		113	<5	39
MET 19A/6.4	1.73	812	0.98	25.2	0.10	1		106	6	40
MET 19A/6.5	1.71	808	0.96	26.4	0.10	1		96	<5	42
MET 19A/6.6	1.82	880	0.91	28.3	0.10	1		142	5	40
MET 19A/5.1	1.55	850	0.85	27	0.11	1	nalyses	110	5	43
MET 19A/5.2	1.69	870	0.96	28.4	0.12	2	nalyses	110	7	43
MET 19A/5.3	1.68	860	0.91	26	0.11	1	nalyses	120	8	41
MET 19A/5.4	1.70	820	0.91	28.5	0.10	1	nalyses	120	8	41
MET 19A/5.5	1.62	870	0.89	29.9	0.12	2	nalyses	140	8	42
MET 19A/5.6	1.62	850	0.91	27.7	0.10	2	nalyses	130	6	40
MET 19A/5.7	1.69	860	0.87	29.3	0.10	1	nalyses	120	10	40
MET 19A/5.8	1.67	840	0.89	28.2	0.09	2	nalyses	150	8	39
MET 19A/8.1	1.64	910	0.9	31.9	0.12	2	880	130		
MET 19A/8.2	1.58	930	0.84	29.4	0.11	1	800	130		
MET 19A/8.3	1.58	850	0.85	27.6	0.11	1	760	120		
MET 19A/8.4	1.68	900	0.8	31.5	0.11	1	720	140		
MET 19A/8.5	1.79	960	0.83	31.6	0.15	1	1040	150		
MET 19A/8.6	1.59	820	0.83	31	0.14	1	760	120		
MET 19A/8.7	1.56	820	0.95	32.9	0.14	1	640	130		
MET 19A/8.8	1.64	860	0.93	30.1	0.15	1	880	150		
MET 19A/8.9	1.69	90	0.84	35.2	0.14	1	920	160		
MET 19A/10.1	1.86	960	0.87	32.5	0.11	1		109	5	34
MET 19A/10.2	1.67	930	0.91	29.9	0.11	1		108	5	31
MET 19A/11.1	1.66	849	0.93	25.7	0.15	2	520	90		
MET 19A/11.2	1.95	920	0.91	27.3	0.15	1	560	110		
MET 19A/11.3	1.73	829	0.87	26	0.14	1	640	105		
MET 19A/11.4	1.64	833	0.89	30.9	0.12	1	540	116		
MET 19A/11.5	1.98	918	0.85	32.5	0.12	2	540	121		
MET 19A/11.6	1.86	925	0.96	33.8	0.11	1	540	148		

Routine Met Std Assays(A)

Replicate #	Cu %	Co	Au	Fe %	Mn %	Ag	As	Ni	Pb	Zn
MET 19A/11.7	1.54	827	0.91	30.2	0.14	1	540	107		
MET 19A/11.8	1.68	816	0.87	31	0.12	1	490	132		
MET 19A/11.9	1.64	797	0.83	30.8	0.12	1	510	167		
MET 19A/11.10	1.88	922	0.9	33.3	0.13	1	590	120		
Met 19A/12.1	1.62	840	0.81	29.3	0.11	2	580	110		
Met 19A/12.2	1.75	830	0.84	29.9	0.11	1	650	130		
Met 19A/12.3	1.60	840	0.88	28.8	0.10	2	550	130		
Met 19A/12.4	1.63	860	0.87	25.2	0.11	1	530	140		
Met 19A/12.5	1.61	860	0.91	27.9	0.10	2	520	120		
Met 19A/12.6	1.63	833	0.9	28.2	0.09	2	520	130		
Met 19A/12.7	1.68	885	0.96	26.6	0.12	2	520	146		
Met 19A/12.8	1.81	929	0.9	27.7	0.11	1	560	140		
Met 19A/12.9	1.74	867	0.88	27.3	0.12	1	550	135		
Met 19A/12.10	1.89	825	0.84	28.9	0.14	1	490	135		
Met 19A/12.11	1.83	880	0.84	28.5	0.10	2	460	125		
Met 19A/12.12	1.87	900	0.87	29.6	0.12	2	470	140		
Met 19A/12.13	1.79	920	0.89	27.1	0.12	1	480	136		
Met 19A/12.14	1.78	900	0.91	27.6	0.13	1	500	144		
MET 19/13a.1	1.50	780	0.88	27.2	0.11	1	600	190		
MET 19/13a.2	1.64	900	0.85	28.5	0.12	1	660	130		
MET 19/13a.3	1.60	840	0.83	25.5	0.11	2	610	110		
MET 19/13a.4	1.63	840	0.79	27.9	0.11	2	660	110		
MET 19/13a.5	1.71	910	0.79	28.7	0.12	1	660	110		
MET 19/13a.6	1.72	910	0.75	29.1	0.11	1	630	140		
MET 19/13b.1	1.61	870	0.85	28.6	0.11	1	440	110		
MET 19/13b.2	1.67	990	0.8	30.8	0.13	1	600	120		
MET 19/13b.3	1.55	1000	0.76	30.3	0.12	1	600	140		
MET 19/13b.4	1.52	890	0.77	29.9	0.12	1	600	90		
MET 19/13b.5	1.66	870	0.81	28.3	0.10	1	600	160		
MET 19/13b.6	1.65	850	0.82	30.6	0.13	2	570	120		
MET 19/13b.7	1.73	840	0.78	29.5	0.13	1	590	150		
MET 19/13b.8	1.79	974	0.83	30	0.14	1	520	150		
MET 19/13b.9	1.66	892	0.82	28.3	0.12	1	640	110		
MET 19/13b.10	1.75	862	0.77	27.3	0.11	1	630	140		
MET 19/13c.1	1.64	866	0.89	28.5	0.13	1	620	100		
MET 19/13c.2	1.68	840	0.96	28.7	0.13	2	650	160		
MET 19/13c.3	1.67	866	0.89	28.7	0.12	1	640	140		
MET 19/13c.4	1.76	860	0.9	29.4	0.13	1	640	160		
Met 19/18.1	1.74	890	0.79	31.3	0.14	1	620	132		
Met 19/18.2	1.70	880	0.91	32.3	0.14	1	700	139		
Met 19/18.3	1.66	860	0.84	31.7	0.14	1	680	123		
Met 19/18.4	1.68	790	0.84	29.6	0.13	1	650	119		
Met 19/18.5	1.56	770	0.91	26.9	0.12	1	580	112		
Met 19/18.6	1.53	750	0.85	26.8	0.12	1	660	114		
Met 19/18.7	1.64	910	0.96	28.4	0.11	1	610	160		
Met 19/18.8	1.57	910	0.91	28.8	0.11	1	640	110		
Met 19/18.9	1.56	890	0.91	29.4	0.11	2	670	140		
Met 19/18.10	1.56	890	1.08	29.3	0.12	2	690	160		
Met 19/18.11	1.62	910	0.98	29.6	0.12	1	660	110		
Met 19/18.12	1.66	880	0.83	28.3	0.11	1	660	130		
Met 19/18.13	1.57	870	0.96	28.9	0.11	2	720	140		

Routine Met Std Assays(A)

Replicate #	Cu %	Co	Au	Fe %	Mn %	Ag	As	Ni	Pb	Zn
Met 19/20a.1	1.74	870	0.82	30.8	0.11	1	710	116		
Met 19/20a.2	1.70	900	0.85	31	0.12	1	650	99		
Met 19/20a.3	1.78	910	0.82	30.5	0.11	1	680	100		
Met 19/20a.4	1.70	870	0.77	27.4	0.12	1	670	82		
Met 19/20a.5	1.67	870	0.83	28.5	0.12	1	650	95		
Met 19/20a.6	1.81	860	0.85	25.6	0.12	1	620	110		
Met 19/20a.7	1.61	900	0.96	26.6	0.12	1	630	110		
Met 19/20a.8	1.71	827	0.91	26.1	0.12	2	560	107		
Met 19/20b.1	1.52	800	0.95	29.6	0.11	1	640	110		
Met 19/20b.2	1.57	840	0.91	30.3	0.12	2	610	95		
Met 19/20b.3	1.61	860	0.85	30.8	0.12	1	600	95		
Met 19/20b.4	1.59	840	0.83	29.6	0.12	1	650	122		
Met 19/20b.5	1.60	860	0.98	29.4	0.11	2	620	110		
Met 19/20b.6	1.47	800	0.85	29.9	0.11	1	650	107		
Met 19/20b.7	1.49	800	0.9	30	0.11	1	650	120		
Met 19/20b.8	1.47	850	0.93	32.8	0.12	2	580	110		
Met 19/20b.9	1.55	900	0.84	29.1	0.11	1	570	103		
Met 19/22.1	1.53	857	0.86	28	0.12	1	600	93		
Met 19/22.2	1.57	855	0.87	31.2	0.12	1	620	88		
Met 19/22.3	1.58	826	0.93	27.9	0.12	1	600	86		
Met 19/22.4	1.52	834	0.9	27.5	0.13	1	600	88		
Met 19/22.5	1.55	828	0.96	28	0.12	2	590	102		
MET 21A/1.1	2.67	310		12.3	0.08	2	720	60	<10	10
MET 21A/1.2	1.52	320		12.6	0.08	3	680	40	<10	10
MET 21A/1.3	1.69	330		12.3	0.08	2	620	40	<10	20
MET 21A/1.4	1.52	330		12.6	0.08	1	680	60	<10	20
MET 21A/6.1	1.82	315	0.59	10.8	0.09	2		57	5	16
MET 21A/6.2	1.70	297	0.67	12.8	0.08	2		60	6	14
MET 21A/6.3	2.13	342	0.63	12.8	0.09	2		60	<5	16
MET 21A/6.4	1.87	296	0.57	12.5	0.08	2		58	<5	16
MET 21A/6.5	2.23	301	0.58	9.23	0.08	2		39	<5	17
MET 21A/5.1	1.90	310	0.6	12.4	0.08	2	nalyses	30	<5	20
MET 21A/5.2	1.79	320	0.6	11.9	0.08	2	nalyses	50	<5	19
MET 21A/5.3	1.79	310	0.62	10.8	0.10	2	nalyses	50	<5	19
MET 21A/5.4	1.92	320	0.63	11.7	0.07	2	nalyses	50	<5	20
MET 21A/5.5	1.86	320	0.63	12.6	0.09	2	nalyses	70	10	18
MET 21A/5.6	1.72	330	0.65	12.5	0.06	2	nalyses	50	9	16
MET 21A/5.7	1.83	330	0.7	12.4	0.07	3	nalyses	50	7	16
MET 21A/8.1	1.67	350	0.6	12.8	0.08	2	720	60		
MET 21A/8.2	1.78	350	0.56	12.8	0.09	2	880	70		
MET 21A/8.3	1.47	300	0.69	12.7	0.08	1	560	70		
MET 21A/8.4	1.64	300	0.64	13.3	0.10	1	840	60		
MET 21A/8.5	1.74	370	0.55	15.7	0.12	2	800	60		
MET 21A/8.6	1.54	290	0.67	13.8	0.11	1	760	50		
MET 21A/8.7	1.94	370	0.6	15.3	0.11	2	680	70		
MET 21A/8.8	1.74	320	0.58	14.1	0.11	2	800	60		
MET 21A/8.9	1.85	310	0.56	14.4	0.09	4	920	50		
MET 21A/8CK	1.87	310		12.5	0.08	4	na	60	5	16
MET 21A/10.1	1.59	290	0.6	12.2	0.08	1		53	<5	16
MET 21A/10.2	1.98	296	0.67	12.5	0.08	2		48	<5	16
MET 21A/11.1	1.99	296	0.59	11.4	0.09	2	550	46		

Routine Met Std Assays(A)

Replicate #	Cu %	Co	Au	Fe %	Mn %	Ag	As	Ni	Pb	Zn
MET 21A/11.2	2.53	360	0.6	12.8	0.10	2	570	48		
MET 21A/11.3	2.54	285	0.6	15.4	0.10	2	620	43		
MET 21A/11.4	1.89	286	0.63	15.2	0.09	2	540	53		
MET 21A/11.5	2.20	318	0.6	16.2	0.07	2	590	66		
MET 21A/11.6	1.71	295	0.6	15.7	0.08	2	530	45		
MET 21A/11.7	1.92	330	0.7	19.2	0.08	2	490	67		
MET 21A/11.8	1.89	331	0.59	18	0.10	2	510	48		
MET 21A/11.9	2.26	300	0.64	15.5	0.09	2	540	42		
MET 21A/11.10	2.08	305	0.68	16.5	0.09	1	620	48		
Met 21/12.1	1.95	310	0.69	13.7	0.08	2	590	60		
Met 21/12.2	1.40	307	0.63	12.6	0.06	2	600	50		
Met 21/12.3	1.92	300	0.62	11.7	0.07	2	500	40		
Met 21/12.4	1.63	265	0.59	12.5	0.07	2	500	60		
Met 21/12.5	1.75	255	0.59	12.4	0.07	2	510	40		
Met 21/12.6	1.83	302	0.57	13.5	0.07	2	440	50		
Met 21/12.7	1.76	324	0.56	11.8	0.09	2	470	50		
Met 21/12.8	1.77	248	0.69	12.1	0.08	2	470	62		
Met 21/12.9	1.89	328	0.63	13.7	0.09	2	510	86		
Met 21/12.10	1.70	294	0.62	11.9	0.09	5	440	70		
Met 21/12.11	2.16	326	0.58	12.3	0.09	2	440	62		
Met 21/12.12	1.93	347	0.61	13.6	0.10	3	430	61		
Met 21/12.13	1.65	365	0.64	11.9	0.07	2	430	62		
Met 21/12.14	1.59	310	0.65	12.1	0.08	2	420	56		
MET 21/13a.1	1.79	290	0.56	12.5	0.09	2	590	60		
MET 21/13a.2	1.46	270	0.62	12.6	0.09	4	670	80		
MET 21/13a.3	1.82	287	0.56	12.7	0.08	2	580	80		
MET 21/13a.4	1.82	280	0.59	12.1	0.09	2	660	50		
MET 21/13a.5	1.97	300	0.58	12.1	0.09	2	650	40		
MET 21/13b.1	1.87	290	0.61	13.1	0.08	2	460	30		
MET 21/13b.2	1.59	293	0.62	12.7	0.08	2	570	40		
MET 21/13b.3	1.63	295	0.61	13.5	0.08	2	560	50		
MET 21/13b.4	1.62	300	0.55	12.8	0.09	2	580	40		
MET 21/13b.5	1.64	296	0.51	12.1	0.08	1	610	30		
MET 21/13b.6	1.40	296	0.52	12.1	0.08	1	590	20		
MET 21/13b.7	1.84	269	0.52	15.1	0.09	2	450	70		
MET 21/13b.8	1.88	281	0.55	13	0.09	2	550	40		
MET 21/13b.9	1.80	283	0.51	12.3	0.09	2	520	110		
MET 21/13b.10	1.75	296	0.53	12.1	0.08	2	600	40		
MET 21/13c.1	1.72	286	0.56	14.6	0.09	3	690	50		
MET 21/13c.2	1.77	284	0.57	13.8	0.09	1	600	60		
MET 21/13c.3	1.82	299	0.55	14.2	0.09	2	620	60		
Met 21/18.1	1.58	285	0.61	13.1	0.09	2	590	41		
Met 21/18.2	1.80	321	0.6	12.7	0.09	2	640	65		
Met 21/18.3	1.97	296	0.6	12.9	0.09	2	670	62		
Met 21/18.4	1.74	298	0.6	14.3	0.10	2	560	53		
Met 21/18.5	1.77	352	0.59	12.9	0.09	2	660	50		
Met 21/18.6	1.66	307	0.67	12.9	0.09	2	610	56		
Met 21/18.7	2.11	290	0.7	12.5	0.08	2	630	70		
Met 21/18.8	1.62	298	0.63	12.7	0.08	2	590	50		
Met 21/18.9	1.70	303	0.7	14	0.08	4	590	70		
Met 21/18.10	1.84	286	0.57	12.9	0.08	2	650	70		

Routine Met Std Assays(A)

Replicate #	Cu %	Co	Au	Fe %	Mn %	Ag	As	Ni	Pb	Zn
Met 21/18.11	1.60	315	0.67	12.4	0.08	2	590	70		
Met 21/18.12	1.62	317	0.6	12.5	0.08	2	630	60		
Met 21/18.13	1.93	307	0.6	12.7	0.08	1	480	50		
Met 21/20a.1	1.80	312	0.67	12.1	0.08	2	600	52		
Met 21/20a.2	1.90	309	0.49	12.7	0.08	2	680	47		
Met 21/20a.3	1.83	295	0.5	12.2	0.09	3	650	38		
Met 21/20a.4	1.75	286	0.63	12.6	0.09	2	710	40		
Met 21/20a.5	2.10	278	0.56	13.8	0.09	2	700	45		
Met 21/20a.6	1.60	288	0.69	12.8	0.08	2	680	59		
Met 21/20a.7	1.89	291	0.6	13.5	0.07	2	570	37		
Met 21/20a.8	1.73	334	0.6	13.4	0.09	2	580	53		
Met 21/20b.1	1.71	290	0.59	12.5	0.08	2	620	49		
Met 21/20b.2	1.58	274	0.67	11.9	0.08	2	580	46		
Met 21/20b.3	1.53	294	0.63	12.3	0.09	2	600	47		
Met 21/20b.4	2.18	285	0.59	12.8	0.08	2	590	44		
Met 21/20b.5	1.79	281	0.55	12.6	0.08	2	560	39		
Met 21/20b.6	1.72	296	0.59	12	0.08	2	660	53		
Met 21/20b.7	1.77	315	0.6	12.9	0.09	2	670	60		
Met 21/20b.8	1.76	280	0.65	14.7	0.09	2	610	52		
Met 21/22.1	1.80	272	0.64	14.8	0.09	2	610	44		
Met 21/22.2	1.60	289	0.63	14.5	0.09	2	670	44		
Met 21/22.3	1.50	304	0.67	14.2	0.09	2	570	55		
Met 21/22.4	1.67	304	0.63	14.6	0.10	2	610	49		

APPENDIX IIIa MAJOR ELEMENT ANALYSES (wt.%), Cu and Au (ppm) and MODAL MINERALOGY (from XRD analysis)

DH102

sample	SiO2	TiO2	Al2O3	CaO	Fe	MnO	MgO	P2O5	Na2O	K2O	CO2
EA10242	39.6	0.66	6.35	2.98	19.9	0.37	2.06	1.45	0.13	3.48	13
EA10243	32.9	0.56	5.45	4.14	25.6	0.21	1.25	2.4	0.12	2.96	10.7
EA10244	46.1	1.39	13.9	0.84	12.3	0.09	1.4	0.37	0.23	9.65	2.15
EA10245	47.7	1.45	14.4	0.87	12.8	0.09	1.45	0.4	0.24	10.1	2.65
EA10246	42.1	1.37	13.2	0.82	17.6	0.06	1.06	0.32	0.19	7.7	7.5
EA10247	39.3	0.32	2.9	3.56	28.1	0.1	1.03	2.08	0.06	0.53	4.98
EA10248	46.7	1.03	9.25	2.46	17	0.13	2.2	0.5	0.13	5.8	2.15
EA10249	46.3	1.26	13.3	1.44	14.4	0.09	2.1	0.09	0.19	8.65	3.3
EA10250	44	1	10.2	2.86	15.7	0.14	3.38	0.97	0.12	5.4	5.3
EA10251	52.2	0.27	2.56	5.55	18.9	0.2	1.58	3.64	0.05	0.77	4.1
EA10252	40.6	0.26	2.4	4.98	26.4	0.13	1	3.38	0.05	0.54	7.75
EA10253	48.4	1.26	14.6	0.85	13.1	0.07	1.22	0.46	0.23	9.65	1.45
EA10254	46.8	1.18	13.9	1.24	15	0.07	0.64	0.88	0.24	9.15	1.2
EA10255	41.8	1.02	12	1.01	20.9	0.07	0.71	0.79	0.19	6.55	0.8
EA10256	44.4	1.07	12.3	0.76	19.8	0.08	0.58	0.57	0.17	5.95	1.05
EA10257	47.3	1.14	13.7	0.84	16.3	0.1	0.83	0.58	0.21	8.1	0.35
EA10258	49.5	1.07	12.8	1.11	15.6	0.11	0.81	0.61	0.23	8.2	0.8
EA10259	49.7	1.34	16.1	0.6	12	0.13	1.2	0.28	0.31	10.3	0.6
EA10260	48.9	0.97	11.6	1.48	14.7	0.5	0.56	0.48	0.25	8.6	4
EA10261	47.1	1.23	14.5	0.8	13.8	0.47	0.72	0.43	0.28	9	1.95
EA10262	48.7	1.18	14.4	0.75	14	0.22	0.79	0.34	0.28	9.75	1.3
EA10263	45.4	1.13	13.4	0.7	17.3	0.4	0.86	0.41	0.22	8.05	1.6
EA10264	45.1	1.18	13.5	1.9	15.6	0.18	0.52	1	0.3	9.55	1.75
EA10265	42	0.85	9.95	2.58	20.4	0.14	0.37	1.81	0.27	6.5	1.05
EA10266	31.7	0.49	5.15	2.74	30.7	0.25	0.54	1.74	0.13	2.22	5.45
EA10267	45.2	0.68	9.65	2.04	19.5	0.12	0.44	1.41	0.18	4.92	0.8
EA10268	40.4	0.62	7.9	1.46	23.3	0.16	0.4	0.91	0.18	4.78	1.45
EA10269	40.9	0.75	8.8	0.75	23.3	0.15	0.27	0.47	0.23	5.75	1.7
EA10270	46.5	0.81	10	1.23	18.4	0.1	0.45	0.83	0.29	6	1.2
EA10271	36.7	0.63	7.55	0.85	23	0.12	0.44	0.6	0.21	4.4	1.6
EA10272	21.9	0.28	3.4	0.65	35.7	0.05	0.27	0.67	0.07	2.06	1.45
EA10273	39.4	0.57	6.95	0.86	23.6	0.11	0.48	0.26	0.16	4.9	6.8
EA10274	25.4	0.48	5.6	1.47	31.3	0.14	0.83	0.6	0.14	3.5	9.35
EA10275	39.6	0.8	9.5	0.95	21.6	0.17	0.86	0.27	0.28	5.65	4.8
EA10276	43.2	0.83	10.1	0.44	20.1	0.2	1.17	0.15	0.26	5.6	3.55
EA10277	48	0.76	9	0.86	19.3	0.22	0.8	0.24	0.33	5.45	3.5
EA10278	65.3	0.56	13.8	0.57	6.5	0.19	0.98	0.21	3.76	4.42	1.04
EA10279	61.2	0.59	14.3	0.59	8.6	0.07	1.4	0.18	2.4	4.34	0.35
EA10280	46.4	0.62	9.35	0.59	21.4	0.16	2.12	0.22	0.32	4.58	0.65
EA10281	37.3	0.57	6.5	0.39	28.4	0.27	3.14	0.23	0.1	2.28	0.85
EA10282	42.3	0.77	10.1	0.48	19.1	0.16	2.06	0.14	0.23	5.45	2.4
EA10283	34.5	0.65	7.95	1.09	23.2	0.24	1.63	0.09	0.19	3.8	6.65
EA10284	32.1	0.72	8.65	0.84	23.9	0.16	1.17	0.05	0.2	3.9	8.05
EA10285	37.8	0.87	10.8	0.76	23.4	0.13	1.27	0.09	0.2	3.9	5.5
EA10286	38.4	0.87	10.8	0.78	22	0.06	1.55	0.14	0.15	3.68	5.2
EA10287	34.6	0.74	9.35	1.12	26.3	0.09	2.28	0.43	0.1	2.44	4.6
EA10288	36.5	0.68	8.1	0.59	21.8	0.04	1.25	0.1	0.13	3.3	4.05
EA10289	32	0.66	7.75	1.04	17.5	0.01	0.44	0.1	0.13	4.68	1.95
EA10290	31	0.54	6.4	0.69	26.4	0.02	0.62	0.1	0.11	4.22	5.35
EA10291	50.2	0.85	12.1	0.32	10.4	-0.01	0.4	0.08	0.2	9.55	1.1
EA10292	43.4	1.03	11	0.21	14.9	0.01	0.79	0.11	0.17	7.55	0.62
EA10293	46.9	1.11	11.8	0.24	12.2	-0.01	0.73	0.19	0.18	8.8	0.15
EA10294	51.6	1.21	13.3	0.07	9.1	-0.01	0.69	0.12	0.22	10.3	0.2
EA10295	52.7	1.21	13.7	0.36	9.55	0.04	0.94	0.15	0.37	9.3	0.75
EA10296	58.2	1.31	15.1	0.35	5.9	0.04	0.49	0.15	0.34	11.9	1
EA10297	53.5	1.41	13.8	0.24	8.65	0.03	0.44	0.14	0.28	10.2	0.75
EA10298	40.1	1.26	10.8	0.25	17	0.03	0.32	0.17	0.28	7.75	0.1

DH102

sample	SiO2	TiO2	Al2O3	CaO	Fe	MnO	MgO	P2O5	Na2O	K2O	CO2
EA10299	52.3	1.46	13.1	0.18	10.4	0.04	0.21	0.09	0.25	10.2	0.35
EA10300	51.6	1.5	12.9	0.22	10.4	0.04	0.15	0.14	0.27	10.3	0.05
EA10301	42.5	1.14	9.85	0.31	15.9	0.05	0.46	0.18	0.28	6.15	0.1
EA10302	48.3	1.33	11.3	0.22	13.3	0.05	0.6	0.17	0.24	8.05	0.1
EA10303	53.2	1.66	14.4	0.13	6.15	0.05	0.69	0.13	0.25	11.2	0.3
EA10304	52.9	1.8	15.4	0.09	6.1	0.04	0.57	0.1	0.25	12.3	0.2
EA10305	52.8	1.57	13.7	0.5	6.85	0.09	0.46	0.3	0.29	10.3	0.95
EA10306	40.6	1.2	11.4	0.61	11.4	0.18	0.68	0.39	0.24	7.75	2.45
EA10307	50.6	1.23	13.1	0.25	11.3	0.07	0.38	0.1	0.28	9.75	0.5
EA10308	56	1.57	14.4	0.26	7.85	0.09	0.48	0.15	0.29	10.8	0.3
EA10309	50.9	1.53	13.4	0.41	11.5	0.11	0.66	0.22	0.29	9.65	0.35
EA10310	45.5	1.11	12.9	0.26	18.4	0.13	1.1	0.12	0.23	8.2	0.35
EA10311	45.3	1.06	12.7	0.24	17.2	0.13	1.11	0.07	0.24	7.9	1.15
EA10312	50.2	1.13	13	0.2	12.3	0.04	0.34	0.05	0.31	9.2	0.75
EA10313	48.6	1.17	12.8	0.19	12	0.04	0.4	0.1	0.29	8.45	0.5
EA10314	55.3	1.21	12.8	0.26	9.35	0.07	0.22	0.1	0.27	9.95	1.5
EA10315	55.7	1.26	13	0.32	8.8	0.06	0.23	0.15	0.24	9.8	1.25
EA10316	46.8	1.24	13.1	0.37	13.7	0.05	0.52	0.1	0.32	9.05	1.45
EA10317	43.1	1.21	12.6	0.84	14.2	0.07	0.79	0.45	0.33	7.8	3.3
EA10318	54.9	1.32	13.5	0.3	9.3	0.05	0.25	0.15	0.27	10.3	1.95
EA10319	53.7	1.77	14.9	0.23	9.95	0.07	0.14	0.13	0.28	11.7	1.45
EA10320	50.3	1.68	14.5	1.17	10.9	0.1	0.28	0.16	0.24	10.7	2.75
EA10321	46.2	1.74	13.7	0.9	12.3	0.13	0.4	0.24	0.2	9.15	3.25
EA10322	44.5	1.69	13.8	0.92	12.8	0.09	0.35	0.19	0.21	9.05	2.25
EA10323	54.9	1.98	16.5	0.32	7.55	0.06	0.23	0.13	0.24	11.9	0.75
EA10324	53.2	1.55	14.9	0.54	10.1	0.08	0.61	0.27	0.33	8.55	1.25
EA10325	57.2	1.34	13.1	0.3	9.75	0.06	0.75	0.13	0.34	7.35	0.5
EA10326	52.6	1.17	12.9	0.43	9.75	0.13	0.55	0.19	0.38	7.85	1.15
EA10327	51.3	1.52	15	0.85	11	0.11	0.55	0.42	0.34	8.65	2.35
EA10328	55.2	1.48	15.4	0.35	8.8	0.08	0.86	0.19	0.25	10.1	0.3
EA10329	56.3	1.67	15.9	0.29	8	0.12	1.35	0.06	0.23	9.75	0.2
EA10330	54.9	1.67	15.9	0.11	8.95	0.09	1.2	0.05	0.24	10	-0.05
EA10331	58.8	1.59	15.5	0.59	6.55	0.13	0.9	0.13	0.24	9.75	0.6
EA10332	59.5	1.6	15.3	0.4	6.4	0.09	0.59	0.13	0.25	9.9	0.4
EA10333	53.2	1.61	16.7	0.5	7.7	0.12	1.11	0.2	0.3	9.95	0.25

Appendix IIIa chemistry, mineralogy...continued

DH102

sample	LOI	Gangue Zone	sulphide zone	Cu	Au	S	chalco-cite	chalco-pyrite	Pyrite	Siderite
EA10242	13.2	ch		2104	-0.01	-0.05	0	0	0	31
EA10243	11.7	hm		1156	-0.01	0.06	0	0	0	25
EA10244	3.62	ch		651	-0.01	-0.05	0	0	0	5
EA10245	5.45	si	py	385	-0.01	-0.05	0	0	0	6
EA10246	9	si		1690	-0.01	0.07	0	0	0	19
EA10247	4.94	si	cc	9230	-0.01	0.62	1	0	1	10
EA10248	2.92	si	cc	9940	-0.01	0.63	1	0	1	2
EA10249	5.85	si	cc-py	12200	0.05	2.35	2	0	4	6
EA10250	5.3	si	py-cc	607	-0.01	0.43	0	0	1	10
EA10251	6.35	si		404	-0.01	-0.05	0	0	0	7
EA10252	8.95	hm		368	-0.01	-0.05	0	0	0	17
EA10253	3.28	si		859	-0.01	-0.05	0	0	0	3
EA10254	3.62	si		485	0.02	-0.05	0	0	0	2
EA10255	4.64	hm	cc	724	-0.01	-0.05	0	0	0	2
EA10256	4.8	hm	cu-cc	8069	0.02	-0.05	1	0	0	2
EA10257	2.68	hm	py-cc	1430	0.02	-0.05	0	0	0	0
EA10258	2.54	frox		743	-0.01	-0.05	0	0	0	1
EA10259	2.3	frox	cu-py	781	0.11	-0.05	0	0	0	1
EA10260	4.42	frox	cu	5560	0.09	-0.05	0	2	0	8
EA10261	4.6	frox	cu-cc	4110	-0.01	-0.05	0	1	0	4
EA10262	2.94	frox	cu-py	3670	0.03	-0.05	0	1	0	3
EA10263	3.78	frox	cu-py	4340	0.02	-0.05	0	1	0	4
EA10264	3.8	frox	cp	5050	0.11	-0.05	0	1	0	3
EA10265	3.98	hm		1440	0.55	-0.05	0	0	0	1
EA10266	9.5	hm	cp	16000	2.06	0.8	2	0	1	12
EA10267	5.65	hm	cu	7130	0.8	0.15	1	0	0	0
EA10268	5.85	hm	cu	16500	0.9	0.95	2	0	1	3
EA10269	4.84	hm		6550	0.85	0.45	1	0	1	4
EA10270	4.46	hm	cu	6780	0.97	0.1	1	0	0	2
EA10271	6.25	hm	cu-cc	40200	0.81	1.1	5	0	0	4
EA10272	13.4	hm	py	37600	1.08	16.3	5	0	29	4
EA10273	7.8	hm	py	31900	0.69	3.5	4	0	5	17
EA10274	10.3	si	py	24400	1.14	5.35	3	0	9	23
EA10275	6.65	si		13500	0.64	3	2	0	5	11
EA10276	4.54	si		22500	0.58	2.55	3	0	4	9
EA10277	2.58	si		14000	0.89	0.6	2	0	0	8
EA10278	1.09	si	cu-py	2700	-0.01	0.25	0	1	0	2
EA10279	2.74	frox	cu-cc	3100	-0.01	0.15	0	1	0	0
EA10280	3.28	frox	py	12200	0.63	3.2	0	4	4	1
EA10281	4.92	hm	py-cp	18600	0.88	5.7	0	5	7	2
EA10282	5.4	hm	cp-py	28140	0.66	4.65	0	8	3	6
EA10283	8.35	hm	cp-py	43720	0.75	4.3	0	13	0	15
EA10284	9.2	hm		57500	0.79	2.6	0	17	0	20
EA10285	8.2	hm		1470	0.92	0.55	0	0	1	13
EA10286	8.05	ch		8300	1.14	0.9	1	0	1	12
EA10287	8.1	ch		15360	1.29	0.55	2	0	0	11
EA10288	7.25	ch	cc	58600	1.71	4.8	7	0	6	10
EA10289	8.45	hm	py-cc	131900	6.62	15.2	17	0	22	3
EA10290	9.85	hm	py-cc	60700	0.91	9.55	8	0	15	13
EA10291	6.9	si	py-cu	38440	0.22	9	5	0	15	2
EA10292	8.85	si	py-cu	50660	0.19	12.2	6	0	20	1
EA10293	8.05	si	py	40470	0.44	11.8	5	0	20	0
EA10294	6.2	si	py-cp	32150	0.43	9.05	4	0	15	1
EA10295	5.9	si	py	13940	0.19	7.1	0	4	11	2
EA10296	3.7	si	py	13430	0.08	2.9	0	4	3	2
EA10297	5.8	si	py	9810	0.2	7.5	0	3	12	2
EA10298	12.3	frox	py	9620	0.43	17.6	0	3	31	0

DH102 sample	LOI	Gangue Zone	sulphide zone	Cu	Au	S	chalco-cite	chalco-pyrite	Pyrite	Siderite
EA10299	6.75	frox	py	6590	0.22	8.25	0	2	14	1
EA10300	7.2	frox	py	7690	0.57	9.35	0	2	16	0
EA10301	10.6	frox	py	20410	0.12	14.7	0	6	24	0
EA10302	8.8	frox	py	19240	0.05	12.9	0	6	20	0
EA10303	3.82	frox	py	24660	0.03	4.45	0	7	4	1
EA10304	4.02	frox	py	31650	0.01	4.85	0	9	3	1
EA10305	3.2	frox	py	27350	0.01	4.9	0	8	4	2
EA10306	7.65	frox	cc-py	92600	0.04	8.1	0	27	0	6
EA10307	6.65	frox	py	14230	0.02	8.1	0	4	12	1
EA10308	3.62	frox	py	25380	0.01	3.75	0	7	2	1
EA10309	3.94	frox	py	4670	0.1	3.2	0	1	5	1
EA10310	3.08	frox	py	8410	0.35	2.5	1	0	4	1
EA10311	4.52	frox	py	9020	0.57	3	1	0	5	3
EA10312	7	frox	py	6740	0.09	8.15	0	2	14	2
EA10313	7.9	frox	py	11550	0.13	6.3	0	3	10	1
EA10314	5.3	frox	py	2910	0.23	5.45	0	1	10	4
EA10315	4.68	frox	py	3780	0.11	4.55	0	1	8	3
EA10316	7.05	frox	py-cc	8980	0.11	7.55	0	3	12	3
EA10317	7.45	frox	py	34080	0.13	6.9	0	10	6	8
EA10318	3.96	frox	py-cc	5740	0.06	2.45	0	2	3	5
EA10319	2.74	frox	py	5720	0.34	1.2	0	2	1	4
EA10320	5.55	frox	py-cp	3900	0.11	0.25	0	1	0	5
EA10321	8	si		12100	0.19	4.5	2	0	8	7
EA10322	7.8	si	cp	15560	0.23	6.1	2	0	11	4
EA10323	2.74	si	cc	371	0.07	-0.05	0	0	0	2
EA10324	4.3	si	py-cp	7720	0.13	1.2	1	0	2	3
EA10325	3.6	si		6870	0.2	1.15	1	0	2	1
EA10326	4.7	si		5730	0.17	4.35	1	0	8	3
EA10327	4.94	ch	py	2140	0.05	0.05	0	0	0	5
EA10328	2.52	frox	cu	5920	0.03	0.25	0	2	0	0
EA10329	2.7	frox		1860	0.06	-0.05	0	1	0	0
EA10330	2.38	frox		3240	0.01	-0.05	0	1	0	0
EA10331	3.18	frox	cu-cc	4060	0.02	0.2	0	1	0	1
EA10332	2.42	frox	py	2210	0.03	0.2	0	1	0	1
EA10333	3.06	frox	py-cc	5250	-0.01	0.6	0	2	0	0

DDH 102 chemistry, mineralogy...continued

DDH102 sample	Calcite	haema-tite	K'spar	Quartz	berth-ierine	Chlorite	musco-vite	Biotite	plagio-clase	Apatite	Total
EA10242	3	0	8	25	6	0	0	20	0	3	98
EA10243	3	14	9	21	9	0	0	12	0	6	97
EA10244	1	10	55	4	4	0	0	14	0	1	94
EA10245	1	8	55	5	8	0	0	14	0	1	98
EA10246	1	4	43	7	15	0	0	9	0	1	99
EA10247	3	29	0	35	6	0	0	8	0	5	97
EA10248	3	19	34	20	0	5	0	12	0	1	98
EA10249	2	6	42	10	8	0	0	21	0	0	100
EA10250	3	8	17	20	2	0	0	34	0	2	97
EA10251	3	21	5	47	0	8	0	0	0	9	99
EA10252	3	21	0	37	9	0	0	5	0	8	99
EA10253	1	11	57	6	8	0	0	12	0	1	98
EA10254	1	14	56	6	11	0	0	5	0	2	97
EA10255	0	19	36	12	21	0	0	5	0	2	96
EA10256	0	15	33	16	25	0	0	3	0	1	98
EA10257	0	15	48	10	15	0	0	7	0	1	97
EA10258	1	21	53	12	0	4	4	0	0	1	98
EA10259	1	15	67	3	0	6	5	0	0	1	98
EA10260	2	14	59	10	0	3	0	0	0	1	99
EA10261	1	15	55	7	0	4	8	0	0	1	96
EA10262	1	17	65	4	0	4	2	0	0	1	98
EA10263	0	21	49	9	0	4	8	0	0	1	97
EA10264	2	19	65	2	0	3	1	0	0	2	98
EA10265	1	28	45	13	0	0	0	0	0	4	93
EA10266	2	35	15	22	0	0	0	0	0	4	93
EA10267	1	22	34	23	12	2	0	0	0	3	98
EA10268	1	28	33	19	5	2	0	0	0	2	95
EA10269	0	30	39	15	0	0	0	0	0	1	92
EA10270	1	25	41	20	0	0	0	0	0	2	91
EA10271	0	30	30	17	0	0	0	0	0	1	88
EA10272	0	29	14	13	0	0	0	0	0	2	95
EA10273	1	18	34	17	0	2	0	0	0	1	99
EA10274	2	22	24	9	0	4	0	0	0	1	97
EA10275	1	13	30	15	12	0	0	8	0	1	97
EA10276	1	14	30	17	11	0	0	11	0	0	98
EA10277	1	19	37	23	4	4	0	0	0	1	99
EA10278	1	7	27	21	0	5	0	0	38	0	100
EA10279	1	10	22	25	0	7	10	0	24	0	100
EA10280	1	24	31	23	0	11	0	0	0	1	98
EA10281	0	29	16	23	0	16	0	0	0	1	99
EA10282	1	16	37	15	0	10	0	0	0	0	97
EA10283	2	16	26	15	0	8	0	0	0	0	95
EA10284	1	13	27	13	0	6	0	0	0	0	96
EA10285	1	22	27	19	0	6	0	0	0	0	90
EA10286	1	8	13	19	27	0	0	12	0	0	94
EA10287	1	15	6	19	25	0	0	17	0	1	97
EA10288	1	9	16	19	20	0	0	11	0	0	99
EA10289	2	6	32	11	5	2	0	0	0	0	99
EA10290	1	18	29	11	1	3	0	0	0	0	99
EA10291	0	3	65	8	0	0	0	0	0	0	99
EA10292	0	6	52	9	0	4	0	0	0	0	99
EA10293	0	4	60	8	0	0	0	0	0	0	98
EA10294	0	2	71	6	0	0	0	0	0	0	99
EA10295	0	3	64	10	0	5	0	0	0	0	98
EA10296	0	3	82	5	0	0	0	0	0	0	100
EA10297	0	1	69	8	0	2	1	0	0	0	98
EA10298	0	2	53	5	0	2	0	0	0	0	96

DH102 sample	Calcite	haema-tite	K'spar	Quartz	berth-ierine	Chlorite	musco-vite	Biotite	plagio-clase	Apatite	Total
EA10299	0	4	70	7	0	1	0	0	0	0	99
EA10300	0	3	71	6	0	1	0	0	0	0	99
EA10301	0	4	42	15	0	2	0	0	0	0	93
EA10302	0	2	55	12	0	3	0	0	0	0	99
EA10303	0	2	77	2	0	3	0	0	0	0	97
EA10304	0	2	73	5	0	3	0	0	0	0	95
EA10305	0	2	71	6	0	2	0	0	0	1	96
EA10306	0	0	53	5	0	3	0	0	0	1	96
EA10307	0	5	67	7	0	2	0	0	0	0	99
EA10308	0	6	74	7	0	2	0	0	0	0	100
EA10309	0	11	66	7	0	3	0	0	0	1	96
EA10310	0	16	46	10	12	0	0	10	0	0	99
EA10311	0	11	43	11	14	0	0	10	0	0	98
EA10312	0	6	63	9	0	0	0	0	0	0	97
EA10313	0	8	58	10	0	2	0	0	0	0	93
EA10314	0	4	68	11	0	0	0	0	0	0	98
EA10315	0	5	67	12	0	0	0	0	0	0	97
EA10316	0	7	62	6	0	3	0	0	0	0	97
EA10317	1	6	53	7	0	4	0	0	0	1	96
EA10318	0	7	71	9	0	0	0	0	0	0	97
EA10319	0	10	80	2	0	0	0	0	0	0	99
EA10320	2	11	73	2	0	1	0	0	0	0	97
EA10321	1	5	63	4	5	2	0	0	0	1	96
EA10322	1	5	62	2	6	1	0	0	0	0	96
EA10323	0	9	82	2	2	1	0	0	0	0	97
EA10324	0	5	59	11	13	2	0	0	0	1	97
EA10325	0	6	50	21	11	3	0	0	0	0	97
EA10326	0	3	54	15	8	2	0	0	0	0	94
EA10327	1	6	59	9	13	2	0	0	0	1	97
EA10328	0	11	69	9	0	4	0	0	0	0	96
EA10329	0	10	61	12	0	7	7	0	0	0	97
EA10330	0	11	64	9	0	6	6	0	0	0	97
EA10331	1	8	61	15	0	5	7	0	0	0	98
EA10332	0	8	63	15	0	3	7	0	0	0	97
EA10333	1	9	60	8	0	6	10	0	0	0	96

App IIIa MAJOR ELEMENT ANALYSES (wt.%), Cu and Au (ppm) and MODAL MINERALOGY (from XRD analysis)

EH109

Sample	SiO2	TiO2	Al2O3	CaO	Fe	MnO	MgO	P2O5	Na2O	K2O	CO2
EA10643	33.2	0.44	9.5	4.84	21.9	0.65	1.18	1.04	0.04	0.08	16
EA10644	31.9	1.5	1.78	3.14	27.9	0.62	1.43	0.54	0.04	-0.01	20.3
EA10645	25.2	1.17	1.95	2.14	31.1	0.44	1.21	0.55	0.04	-0.01	20.1
EA10646	29.3	0.49	4.06	1.25	24.6	0.06	0.31	0.13	0.03	0.15	3.85
EA10647	34.4	0.9	8.3	0.73	20.6	0.02	0.47	0.15	0.05	0.64	1.15
EA10648	28.7	0.56	6.1	0.45	25	0.04	0.51	0.11	0.03	0.02	3.8
EA10649	19.9	0.84	4.7	1.12	26.7	0.03	0.4	0.18	0.03	-0.01	3.4
EA10650	24.8	1.12	6.5	0.9	25.3	0.04	0.54	0.28	0.06	-0.01	5.85
EA10651	38.3	0.75	13.4	0.75	20.3	0.02	0.52	0.19	0.05	-0.01	2.15
EA10652	35.2	0.69	14	0.37	20.7	0.01	0.47	0.19	0.04	-0.01	2.15
EA10653	34.1	0.67	12.1	0.39	25.2	0.01	0.52	0.26	0.04	-0.01	1.8
EA10654	32.3	0.85	11.9	0.38	33.3	0.03	0.68	0.17	0.04	-0.01	2.35
EA10655	37	0.76	16.3	0.29	26.4	-0.01	0.7	0.23	0.05	-0.01	0.85
EA10656	39.3	0.61	22.8	0.36	20	-0.01	0.65	0.15	0.06	0.12	0.1
EA10657	37.7	0.96	16.2	0.46	23.3	0.02	0.76	0.42	0.08	0.04	2.1
EA10658	38.7	0.97	14.7	0.53	25.3	0.02	0.7	0.2	0.06	0.01	2.15
EA10659	31.3	0.87	7.9	1.43	30.8	0.09	0.75	0.15	0.04	-0.01	12.5
EA10660	40.3	1.27	11.8	0.71	24.4	0.05	0.59	0.16	0.06	0.93	5.3
EA10661	42.6	1.07	15.4	0.36	20.9	0.03	0.58	0.12	0.09	1.85	2.35
EA10662	42.3	1.17	15.4	0.28	23	0.01	0.57	0.08	0.06	0.71	0.7
EA10663	39.5	1	13.7	0.29	28.6	-0.01	0.59	0.03	0.06	0.1	0.05
EA10664	36.2	1.22	14.1	0.32	29.3	-0.01	0.57	0.11	0.06	-0.01	0.1
EA10665	28.9	0.99	11.6	0.43	36	0.05	0.55	0.15	0.06	-0.01	2.5
EA10666	25.3	0.89	9.25	0.29	42.5	0.07	0.47	0.09	0.04	-0.01	2.2
EA10667	31.1	1.18	10.9	0.72	33.7	0.08	0.68	0.32	0.06	-0.01	3.9
EA10668	29.2	0.93	14.7	0.31	33.6	0.03	0.7	0.12	0.05	0.25	0.9
EA10669	32.9	1.32	18.9	0.51	23.9	-0.01	0.67	0.23	0.06	0.56	0.2
EA10670	38.8	1.06	15	0.7	24.3	0.02	0.59	0.2	0.06	0.7	0.1
EA10671	31.9	0.86	13.2	0.44	23	-0.01	0.24	0.22	0.09	2.44	1.3
EA10672	43.9	0.81	13.2	0.16	14.1	-0.01	0.05	0.08	0.18	7.45	0.05
EA10673	51.7	1.02	13.6	0.22	11.1	-0.01	-0.01	0.18	0.25	10.5	0.5
EA10674	44.8	0.18	2.76	0.23	17.9	0.02	-0.01	0.11	0.06	1.39	0.45
EA10675	65.4	0.69	9.75	0.1	6.45	-0.01	-0.01	0.07	0.21	7.6	0.6
EA10676	38.4	0.95	10.6	0.3	18.3	0.01	0.08	0.19	0.25	7.45	1.75
EA10677	40.7	0.93	11.6	0.36	20	0.04	0.2	0.27	0.26	6.55	2.15
EA10678	52.3	1.29	13.6	0.4	14.7	0.08	0.46	0.16	0.35	6.75	1.55
EA10679	53.2	1.52	15.9	0.48	10.1	0.03	0.52	0.22	0.45	8.95	2.05
EA10680	52	1.57	15.9	0.44	10.8	0.01	0.69	0.19	0.53	8.7	1
EA10681	53.5	1.39	14.8	0.59	11.2	0.02	0.58	0.25	0.48	8.4	1.05
EA10682	57.2	1.29	13.5	0.29	8.75	0.03	0.38	0.12	0.38	7.45	1.05
EA10683	58.5	1.44	15.3	0.38	7.25	0.01	0.44	0.18	0.46	9	0.5
EA10684	58.2	1.68	15.6	0.36	8	0.03	0.38	0.37	0.42	10.2	-0.05
EA10685	56.2	1.79	15	0.27	8.75	0.03	0.24	0.22	0.35	11.5	1.1
EA10686	55.5	1.76	14.4	0.1	8.1	0.05	0.32	0.17	0.27	10.2	1.21
EA10687	37.4	1.63	15	0.23	17.2	0.03	0.7	0.2	0.23	4.26	0.75
EA10688	50.3	2.1	14.7	0.39	13.2	0.07	0.56	0.24	0.26	7.05	2.75
EA10689	54.3	1.82	11.7	0.52	15	0.07	0.65	0.21	0.19	3.68	2.6
EA10690	55.4	1.88	15.6	0.33	8.75	0.1	0.65	0.17	0.28	10.7	1.4
EA10691	49.6	1.31	9.55	0.42	16.3	0.1	0.86	0.17	0.24	1.29	2.05
EA10692	46.3	1.46	11.8	0.38	15.3	0.09	0.64	0.23	0.27	6.15	2.45
EA10693	52.5	1.07	8.8	0.42	12.7	0.08	1.16	0.09	0.48	1.55	0.75
EA10694	45.2	1.15	13.4	0.26	18.8	0.15	1.82	0.18	0.17	7.6	1.15
EA10695	53.3	1.52	13.7	0.46	11.8	0.13	0.41	0.28	0.21	10.6	1.7
EA10696	58.4	1.69	15.5	0.34	6.95	0.08	0.24	0.25	0.25	12.8	0.6
EA10697	56.4	1.68	14.8	1.01	7.9	0.07	0.28	0.6	0.27	11.6	2
EA10698	68.7	1.11	11.5	0.72	5.55	0.04	0.22	0.48	0.2	8.45	0.75
EA10699	59.4	1.18	12.1	0.64	9.65	0.07	0.34	0.29	0.2	9.05	2.65

EH109											
Sample	SiO2	TiO2	Al2O3	CaO	Fe	MnO	MgO	P2O5	Na2O	K2O	CO2
EA10700	61	1.38	14.2	0.51	5.95	0.07	0.39	0.32	0.25	11.4	1.55
EA10701	56.8	1.75	16.3	0.35	6.05	0.09	0.41	0.2	0.25	13.6	1.3
EA10702	31	1.32	10.2	1.1	20.1	0.27	0.93	0.32	0.18	6.15	6.05
EA10703	49.5	1.85	13.9	0.39	8.3	0.15	0.36	0.07	0.24	11.9	3.35
EA10704	44.4	1.55	14.7	0.31	13.6	0.05	0.81	0.12	0.23	8.2	0.9
EA10705	74.5	0.64	9.25	0.27	5.15	0.07	0.24	0.13	0.19	6.7	1
EA10706	52.9	0.83	10.4	3.76	13.3	0.17	1.29	0.24	0.22	6.25	4
EA10707	46.4	0.76	9.05	7.25	13.8	0.19	0.52	0.23	0.2	6.25	6.3
EA10708	43.4	0.63	6.9	5	22.3	0.23	1.04	0.14	0.13	4.4	4.5
EA10709	37.7	0.58	6.45	4.12	25.2	0.19	1.17	0.5	0.12	3.88	4.1
EA10710	37.8	0.6	6.95	0.77	30.5	0.11	1.19	0.26	0.13	4.36	1.4
EA10711	32.4	0.48	5.75	3.54	29.2	0.19	1.24	0.13	0.09	3.3	7.25
EA10712	32.9	0.57	6.8	0.52	33.9	0.17	1.13	0.07	0.13	3.82	2
EA10713	37.6	0.62	7.4	0.63	29.9	0.18	1.14	0.16	0.16	4.28	1.85
EA10714	38.1	0.68	7.95	0.67	29.3	0.16	1.3	0.4	0.15	4.38	0.5
EA10715	36.8	0.74	8.7	0.94	28.6	0.15	1.24	0.35	0.21	4.9	0.65
EA10716	31.8	0.59	7.25	0.39	35.8	0.12	0.87	0.25	0.2	4.36	-0.05
EA10717	45	0.8	9.9	1.14	22.1	0.15	0.91	0.23	0.22	6.1	1.7
EA10718	63.3	0.57	13.6	1.1	9.25	0.19	0.84	0.18	3.68	3.22	1.85
EA10719	64.1	0.57	13.7	3.44	6.05	0.23	0.8	0.14	5.65	1.67	2.25
EA10720	58.8	0.67	13.2	3.5	9.8	0.19	0.81	0.2	5.05	1.7	2.15
EA10721	27.5	0.56	7.2	11.6	26.2	0.45	0.59	0.21	1.72	0.62	8.25
EA10722	62.3	0.65	14	4.02	7.4	0.17	0.56	0.14	6.05	1.29	2.4
EA10723	63.9	0.62	14.1	3.82	6.6	0.21	0.41	0.15	6.65	1.01	2.2
EA10724	64.5	0.57	13.8	2.92	5.65	0.14	1.22	0.14	4.5	3.12	2.05
EA10725	61.6	0.57	13	3.06	7.05	0.18	1.88	0.17	2.84	4.7	2.7

Appendix IIIa chemistry, mineralogy...continued

EH109 Sample	LOI	Gangue Zone	sulphide zone	Cu	Au	S	Cu sulfide	Pyrite	Siderite	Calcite
EA10643	17.9	ch		6180	1.71	0.6	1	1	34	7
EA10644	19.7	ch		5580	2.67	0.6	1	1	48	5
EA10645	22.6	ch	py-cc	23600	2.39	4.4	3	7	50	3
EA10646	16	ch	cc-py	114000	2.2	21.7	14	35	8	2
EA10647	13.3	ch	py-cc	112000	1.33	13.8	14	21	2	1
EA10648	13.7	ch	py-cc	112000	2.81	16.6	14	26	9	1
EA10649	16.6	ch	py-cc	149000	3.95	21.9	19	34	7	2
EA10650	14.1	ch	py-cc	127000	2.69	13.2	16	19	14	1
EA10651	11.6	ch	py-cc	58000	0.95	6.55	7	10	5	1
EA10652	12.1	ch	py-cc	68000	1.06	7.35	9	11	5	0
EA10653	11.3	ch	py-cc	51000	0.82	6.9	6	10	4	0
EA10654	8.75	ch	py	2300	0.8	2.35	0	4	6	0
EA10655	9.05	ch		1360	0.62	0.25	0	0	2	0
EA10656	11	ch		970	0.05	0.1	0	0	0	0
EA10657	11.5	ch		1120	1.02	0.8	0	1	5	0
EA10658	10.5	ch		1218	1.32	0.25	0	0	5	1
EA10659	15.6	ch		740	1.2	0.5	0	1	30	2
EA10660	11.3	ch		1070	0.87	0.65	0	1	13	1
EA10661	9.85	ch		950	0.68	0.5	0	1	6	0
EA10662	8.55	ch		760	0.72	0.1	0	0	1	0
EA10663	7.1	ch		743	1.2	0.2	0	0	0	0
EA10664	7.6	ch		900	1.66	0.45	0	1	0	0
EA10665	7.85	ch		830	1.48	0.35	0	1	6	0
EA10666	5.05	ch		640	1.71	0.1	0	0	5	0
EA10667	9.8	ch		590	1.29	0.4	0	1	9	1
EA10668	8.45	ch		1690	0.5	0.25	0	0	0	0
EA10669	11.1	ch	py-cp	13400	0.6	2.05	2	3	0	0
EA10670	10.4	ch	py-cc	6350	0.99	1.05	1	2	0	1
EA10671	12.1	ch	py-cc	101000	0.59	10.9	13	16	3	0
EA10672	8.25	si	py-cc	60000	0.37	8.9	8	14	0	0
EA10673	5	si	py-cc	29100	0.67	6.2	4	10	1	0
EA10674	15.6	si	py-cc	81000	2.3	19.3	10	32	1	0
EA10675	4.96	si	py-cc	31900	0.87	5.3	4	8	2	0
EA10676	11.5	si	py-cc	28200	1.82	13.5	4	24	4	0
EA10677	8.25	hm		19200	0.43	7.4	2	13	5	0
EA10678	4.08	hm		630	0.21	-0.05	0	0	4	0
EA10679	4.52	hm		518	0.49	0.05	0	0	5	0
EA10680	3.94	hm	py-cc	2410	0.09	1.35	0	2	2	0
EA10681	1.75	hm		900	0.06	0.15	0	0	2	1
EA10682	5.05	hm	py	14500	0.07	3.75	2	6	2	0
EA10683	3.72	hm	py-cc	2260	0.21	1.8	0	3	1	0
EA10684	3.06	hm		1460	0.007	0.75	0	1	0	0
EA10685	3.68	si	py	6580	0.08	3.4	1	6	3	0
EA10686	5.4	si	py-cc	7720	0.09	6.05	1	11	3	0
EA10687	13.1	hm	py	20200	0.12	13.3	3	24	2	0
EA10688	6.9	ch		2990	0.09	1.5	0	3	7	0
EA10689	7	ch		670	0.08	0.1	0	0	6	1
EA10690	3.68	hm	cc	1101	0.03	0.1	0	0	3	0
EA10691	9.75	hm	py-cc	25500	0.08	6.95	3	12	5	0
EA10692	8.9	hm	py-cc	20500	0.11	8.55	3	15	6	0
EA10693	7.25	hm	py-cc	5700	0.07	10.4	1	19	1	1
EA10694	3.76	hm	cp-cc	4690	0.47	0.3	1	0	3	0
EA10695	3.08	hm		1671	0.15	0.05	0	0	4	0
EA10696	1.94	hm		800	0.09	-0.05	0	0	1	0
EA10697	3.56	hm		311	0.41	-0.05	0	0	4	1
EA10698	2.3	hm	cc	580	0.65	-0.05	0	0	2	0
EA10699	3.98	hm		527	0.13	-0.05	0	0	6	1

EH109		Gangue	sulphide				Cu			
Sample	LOI	Zone	zone	Cu	Au	S	sulfide	Pyrite	Siderite	Calcite
EA10700	3.04	hm	cc	3098	0.22	0.05	0	0	4	0
EA10701	2.76	hm	cc	4980	0.09	0.1	1	0	0	0
EA10702	11.9	hm	cc-py	62000	0.36	6.95	8	10	14	1
EA10703	5.05	hm	cc-py	44800	0.18	3.05	6	4	8	1
EA10704	6.5	hm		33600	0.23	2.9	4	4	2	0
EA10705	2.24	si		2090	0.96	0.05	0	0	3	0
EA10706	5.7	hm		6970	0.88	0.1	1	0	3	6
EA10707	7	hm	cu	26800	0.82	0.25	3	0	2	13
EA10708	5.05	hm	cu	21100	0.62	0.1	3	0	2	9
EA10709	5.7	hm	cu-cc	35700	0.66	0.1	4	0	3	6
EA10710	3.5	hm	cu-cc	10200	0.28	0.4	1	0	3	1
EA10711	7.45	hm	cu	24500	0.96	0.8	3	0	12	6
EA10712	2.84	hm		24100	1.04	1.85	3	2	4	1
EA10713	2.64	hm		20900	0.95	1.75	3	2	4	1
EA10714	2.34	si	cp-py	10600	0.48	2.9	1	5	1	0
EA10715	2.36	si	cp-py	11600	0.54	2.8	1	5	1	1
EA10716	1.24	si	cp-py	14500	0.97	3	2	5	0	0
EA10717	3.46	si	py-cc	10600	0.53	1.25	0	2	3	2
EA10718	2.36	fr		624	0.05	0.15	0	0	3	2
EA10719	2.9	fr		315	0.04	0.1	2	0	0	5
EA10720	3.32	fr	py-cp	1870	-0.01	0.75	0	1	0	5
EA10721	8.25	fr	py-cp	10700	0.15	6.55	1	12	0	19
EA10722	3.08	fr	py-cp	1130	0.01	0.15	0	0	0	5
EA10723	2.36	fr	py	290	0.02	0.1	0	0	0	5
EA10724	2.82	fr	py	358	-0.01	0.05	0	0	0	5
EA10725	4.12	fr		330	-0.01	0.05	0	0	1	6

	DDH 109 chemistry, mineralogy...continued										
EH109 Sample	hema-tite	K'spar	Quartz	berth-ierine	Chlorite	musc-ovite	kaol-inite	plagio-clase	tourm-aline	Apatite	Total
EA10643	1	1	23	15	0	0	15	0	0	2	99
EA10644	5	0	30	3	0	0	3	0	0	1	96
EA10645	4	0	23	3	0	0	3	0	0	1	97
EA10646	3	0	25	6	0	0	6	0	0	0	101
EA10647	9	4	23	12	0	0	12	0	0	0	98
EA10648	8	0	22	10	0	0	10	0	0	0	99
EA10649	7	0	15	7	0	0	7	0	0	0	99
EA10650	9	0	18	10	0	0	10	0	0	1	98
EA10651	10	0	24	21	0	0	21	0	0	0	99
EA10652	9	0	20	22	0	0	22	0	0	0	99
EA10653	17	0	21	19	0	0	19	0	0	1	99
EA10654	32	0	19	19	0	0	19	0	0	0	100
EA10655	25	0	19	26	0	0	26	0	0	1	99
EA10656	13	0	14	36	0	0	36	0	0	0	100
EA10657	17	0	20	26	0	0	26	0	0	1	97
EA10658	22	0	23	23	0	0	23	0	0	0	98
EA10659	17	0	23	13	0	0	13	0	0	0	99
EA10660	18	6	25	17	0	0	17	0	0	0	98
EA10661	16	13	20	20	0	0	20	0	0	0	98
EA10662	22	5	23	23	0	0	23	0	0	0	98
EA10663	31	0	25	22	0	0	22	0	0	0	100
EA10664	32	0	21	22	0	0	22	0	0	0	99
EA10665	39	0	16	18	0	0	18	0	0	0	99
EA10666	39	0	16	38	0	0	0	0	0	0	100
EA10667	34	0	19	17	0	0	17	0	0	1	99
EA10668	35	0	13	30	0	0	20	0	0	0	99
EA10669	16	4	11	36	0	0	24	0	0	1	97
EA10670	21	5	20	28	0	0	19	0	0	0	97
EA10671	12	17	10	20	0	0	13	0	0	1	104
EA10672	5	51	7	14	0	0	0	0	0	0	99
EA10673	7	66	8	3	0	0	0	0	0	0	100
EA10674	2	10	38	4	0	0	0	0	0	0	97
EA10675	3	52	32	0	0	0	0	0	0	0	100
EA10676	6	51	5	3	0	0	0	0	0	0	97
EA10677	14	45	9	5	0	0	5	0	0	1	98
EA10678	16	46	17	5	0	0	5	0	4	0	99
EA10679	9	61	9	4	0	0	4	0	4	1	98
EA10680	11	60	9	4	0	0	4	0	5	0	98
EA10681	13	58	12	3	0	0	3	0	5	1	98
EA10682	5	51	20	4	0	0	4	0	3	0	98
EA10683	6	62	15	3	0	0	3	0	3	0	98
EA10684	11	66	12	0	0	5	0	0	3	1	99
EA10685	7	77	5	0	0	1	0	0	0	1	100
EA10686	1	70	9	1	0	0	1	0	0	0	99
EA10687	2	29	8	12	0	0	12	0	6	0	98
EA10688	10	48	13	6	0	0	6	0	4	1	99
EA10689	14	25	30	8	0	0	8	0	5	0	98
EA10690	9	73	6	2	0	0	2	0	0	0	97
EA10691	8	9	35	9	0	0	9	0	7	0	98
EA10692	6	42	15	3	0	0	3	0	5	1	99
EA10693	3	11	38	4	0	0	7	0	9	0	94
EA10694	23	52	9	0	9	0	0	0	0	0	97
EA10695	13	64	11	2	0	0	2	0	0	1	97
EA10696	9	77	8	1	0	0	1	0	0	1	97
EA10697	7	70	10	2	0	0	2	0	0	1	97
EA10698	6	51	34	2	0	0	2	0	0	1	99
EA10699	9	62	19	0	0	0	0	0	0	1	98

EH109 Sample	hema-tite	K'spar	Quartz	berth-ierine	Chlorite	musc-ovite	kaol-inite	plagio-clase	tourm-aline	Apatite	Total
EA10700	6	69	16	0	0	0	0	0	0	1	96
EA10701	9	82	4	0	0	0	0	0	0	0	96
EA10702	10	37	4	5	0	0	5	0	0	1	95
EA10703	4	72	3	0	0	0	0	0	0	0	97
EA10704	12	49	7	8	0	0	8	0	0	0	95
EA10705	5	40	47	2	0	0	2	0	0	0	99
EA10706	15	31	27	0	6	9	0	0	0	1	100
EA10707	18	43	18	0	3	0	0	0	0	1	100
EA10708	30	30	23	0	5	0	0	0	0	0	100
EA10709	33	27	19	2	0	0	2	0	0	1	98
EA10710	40	30	17	0	6	0	0	0	0	1	99
EA10711	32	23	16	0	6	0	0	0	0	0	99
EA10712	43	26	14	0	6	0	0	0	0	0	100
EA10713	37	29	17	0	6	0	0	0	0	0	100
EA10714	37	30	17	0	7	0	0	0	0	1	99
EA10715	36	34	13	0	6	0	0	0	0	1	98
EA10716	47	30	11	0	4	0	0	0	0	1	100
EA10717	27	42	17	0	5	0	0	0	0	1	97
EA10718	10	16	25	0	4	8	0	33	0	0	102
EA10719	8	11	20	0	4	2	0	51	0	0	103
EA10720	12	8	19	0	4	4	0	46	0	0	100
EA10721	29	0	13	0	3	6	0	16	0	0	99
EA10722	10	7	18	0	3	3	0	55	0	0	101
EA10723	9	6	17	0	2	1	0	61	0	0	101
EA10724	7	21	21	0	6	1	0	41	0	0	101
EA10725	7	26	23	0	9	3	0	26	0	0	102

Appendix IIIb – Statistics data for DDH 102 and 109

DDH 102

THE FOLLOWING RESULTS ARE FOR:
gangue zone = ch (chlorite)

TOTAL OBSERVATIONS: 6

	SIO2	TIO2	AL2O3	CAO	FE
N OF CASES	6	6	6	6	6
MINIMUM	34.600	0.660	6.350	0.590	11.000
MAXIMUM	51.300	1.520	15.000	2.980	26.300
MEAN	41.083	0.977	10.583	1.193	18.883
VARIANCE	40.398	0.144	11.233	0.795	35.950
STANDARD DEV	6.356	0.380	3.352	0.892	5.996
MEDIAN	39.000	0.805	10.075	0.845	20.850

	MNO	MGO	P2O5	NA2O	K2O
N OF CASES	6	6	6	6	6
MINIMUM	0.040	0.550	0.100	0.100	2.440
MAXIMUM	0.370	2.280	1.450	0.340	9.650
MEAN	0.127	1.515	0.485	0.180	5.200
VARIANCE	0.015	0.380	0.244	0.008	9.640
STANDARD DEV	0.122	0.616	0.494	0.090	3.105
MEDIAN	0.090	1.475	0.395	0.140	3.580

	CO2	LOI	CU	AU	S
N OF CASES	6	6	6	6	6
MINIMUM	2.150	3.620	651.000	-0.010	-0.050
MAXIMUM	13.000	13.200	58600.000	1.710	4.800
MEAN	5.225	7.527	14525.833	0.695	1.033
VARIANCE	15.989	10.964	.496442E+09	0.598	3.551
STANDARD DEV	3.999	3.311	22280.982	0.774	1.884
MEDIAN	4.325	7.650	5220.000	0.595	0.300

	CUSULFID	CPY	PYRITE	SIDERITE	CALCITE
N OF CASES	6	6	6	6	6
MINIMUM	0.000	0.000	0.000	5.000	1.000
MAXIMUM	7.000	0.000	6.000	31.000	3.000
MEAN	1.667	0.000	1.167	12.333	1.333
VARIANCE	7.467	0.000	5.767	92.667	0.667
STANDARD DEV	2.733	0.000	2.401	9.626	0.816
MEDIAN	0.500	0.000	0.000	10.500	1.000

	HEMATITE	KSPAR	QUARTZ	BERTHIER	CHLORITE
N OF CASES	6	6	6	6	6

MINIMUM	0.000	6.000	4.000	4.000	0.000
MAXIMUM	15.000	59.000	25.000	27.000	2.000
MEAN	8.000	26.167	15.833	15.833	0.333
VARIANCE	24.400	584.567	60.167	94.167	0.667
STANDARD DEV	4.940	24.178	7.757	9.704	0.816
MEDIAN	8.500	14.500	19.000	16.500	0.000

	MUSCOVIT	BIOTITE	PLAGIOCL	APATITE	TOTAL
N OF CASES	6	6	6	6	6
MINIMUM	0.000	0.000	0.000	0.000	94.000
MAXIMUM	0.000	20.000	0.000	3.000	99.000
MEAN	0.000	12.333	0.000	1.000	96.500
VARIANCE	0.000	47.467	0.000	1.200	4.300
STANDARD DEV	0.000	6.890	0.000	1.095	2.074
MEDIAN	0.000	13.000	0.000	1.000	97.000

DDH 102

THE FOLLOWING RESULTS ARE FOR:

gangue zone = (fr) fresh metavolcanics

TOTAL OBSERVATIONS: 38

	SIO2	TIO2	AL2O3	CAO	FE
N OF CASES	38	38	38	38	38
MINIMUM	40.100	0.590	9.350	0.090	6.100
MAXIMUM	61.200	1.800	16.700	1.900	21.400
MEAN	50.555	1.325	13.532	0.489	11.675
VARIANCE	26.210	0.080	2.847	0.152	14.763
STANDARD DEV	5.120	0.283	1.687	0.390	3.842
MEDIAN	50.450	1.260	13.400	0.335	11.350

	MNO	MGO	P2O5	NA2O	K2O
N OF CASES	38	38	38	38	38
MINIMUM	0.030	0.140	0.050	0.220	4.340
MAXIMUM	0.500	2.120	1.000	2.400	12.300
MEAN	0.119	0.685	0.222	0.324	9.186
VARIANCE	0.012	0.175	0.035	0.120	2.790
STANDARD DEV	0.110	0.418	0.186	0.347	1.670
MEDIAN	0.090	0.595	0.155	0.270	9.750

	CO2	LOI	CU	AU	S
N OF CASES	38	38	38	38	38
MINIMUM	-0.050	2.300	743.000	-0.010	-0.050
MAXIMUM	4.000	12.300	92600.000	0.630	17.600
MEAN	0.970	4.854	11763.526	0.130	4.016
VARIANCE	0.914	5.916	.258493E+09	0.029	20.337

	1	2	3	4
SIO2	-0.808	0.014	-0.384	-0.199
TIO2	-0.768	-0.330	0.348	0.243
AL2O3	-0.893	0.219	-0.135	0.148
CAO	0.225	0.835	0.351	-0.031
FE	0.889	0.187	-0.045	0.294
MGO	0.152	0.419	-0.679	0.114
P2O5	0.294	0.723	0.434	-0.070
NA2O	0.028	0.240	-0.592	-0.620
K2O	-0.767	-0.191	0.454	0.332
CO2	0.231	0.558	0.526	0.034
CU	0.214	-0.129	0.387	-0.258
AU	0.539	-0.312	-0.237	0.483
S	0.491	-0.774	0.236	-0.278
CUSULFID	0.294	-0.044	-0.367	0.662
PYRITE	0.479	-0.774	0.111	-0.192

VARIANCE EXPLAINED BY COMPONENTS

1	2	3	4
4.525	3.308	2.303	1.575

PERCENT OF TOTAL VARIANCE EXPLAINED

1	2	3	4
30.165	22.055	15.354	10.499

DDH 102

THE FOLLOWING RESULTS ARE FOR:

gangue zone = hm (hematite/limonite)

LATENT ROOTS (EIGENVALUES)

1	2	3	4	5
6.258	4.249	1.632	1.041	0.726
6	7	8	9	10
0.400	0.252	0.233	0.094	0.060
11	12	13	14	15
0.034	0.013	0.004	0.003	0.001

COMPONENT LOADINGS

	1	2	3	4
SIO2	-0.877	-0.086	0.185	0.036
TIO2	-0.861	0.356	-0.038	0.064
AL2O3	-0.872	0.412	-0.062	0.039
CAO	0.175	-0.777	0.543	0.151
FE	0.735	-0.383	-0.346	-0.360
MGO	0.031	-0.170	-0.722	0.480
P2O5	0.090	-0.793	0.531	-0.094
NA2O	-0.801	0.263	0.056	0.049
K2O	-0.797	0.499	0.152	-0.111
CO2	0.385	-0.519	-0.021	0.555
CU	0.566	0.692	0.134	0.364
AU	0.460	0.638	0.387	0.291
S	0.755	0.579	-0.110	-0.102
CUSULFID	0.563	0.677	0.410	0.082
PYRITE	0.749	0.519	-0.025	-0.293

VARIANCE EXPLAINED BY COMPONENTS

1	2	3	4
6.258	4.249	1.632	1.041

PERCENT OF TOTAL VARIANCE EXPLAINED

1	2	3	4
41.718	28.326	10.880	6.941

DDH 102

THE FOLLOWING RESULTS ARE FOR:

gangue zone = si (silica, pitted)

LATENT ROOTS (EIGENVALUES)

1	2	3	4	5
5.886	4.331	1.671	1.287	0.782
6	7	8	9	10
0.364	0.265	0.147	0.118	0.084
11	12	13	14	15
0.032	0.022	0.006	0.003	0.000

COMPONENT LOADINGS

	1	2	3	4
SIO2	0.512	0.605	0.544	-0.047
TIO2	0.718	0.316	-0.486	0.254
AL2O3	0.872	0.384	-0.229	-0.053
CAO	-0.871	0.164	0.217	0.360
FE	-0.822	-0.441	-0.281	-0.111
MGO	-0.537	0.222	-0.003	0.260
P2O5	-0.784	0.142	0.336	0.351
NA2O	0.125	0.324	0.539	-0.687
K2O	0.885	0.154	-0.314	0.195
CO2	-0.755	-0.186	-0.458	-0.203
CU	0.319	-0.888	0.225	0.078
AU	-0.093	-0.699	-0.264	-0.489
S	0.495	-0.772	0.234	0.198
CUSULFID	0.230	-0.889	0.157	0.050
PYRITE	0.483	-0.774	0.221	0.217

VARIANCE EXPLAINED BY COMPONENTS

1	2	3	4
5.886	4.331	1.671	1.287

PERCENT OF TOTAL VARIANCE EXPLAINED

1	2	3	4
39.242	28.872	11.140	8.583

Appendix IV

TEM Profiles

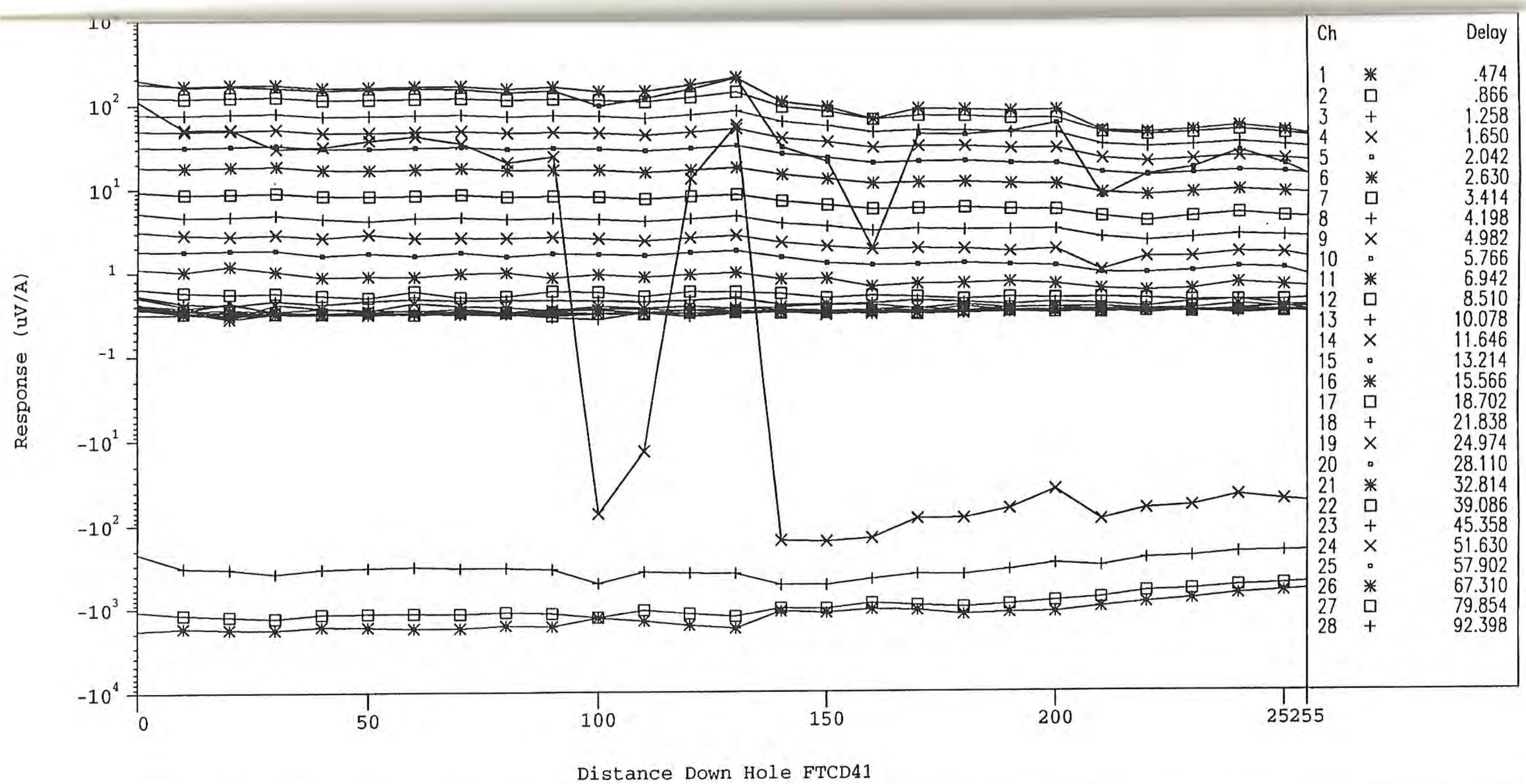

MIM Exploration Pty. Ltd.	MIM EM
Configuration : Down Hole Instrument : SiroTem Mk3 Channels : Standard Times Loop # 1 : 69480,39400 AMG GRID : 69760,39680	Horizontal Scale : Default Vertical Scale : Default Time Delay In : Milliseconds Date : 15/03/94 Figure : 2.1.16

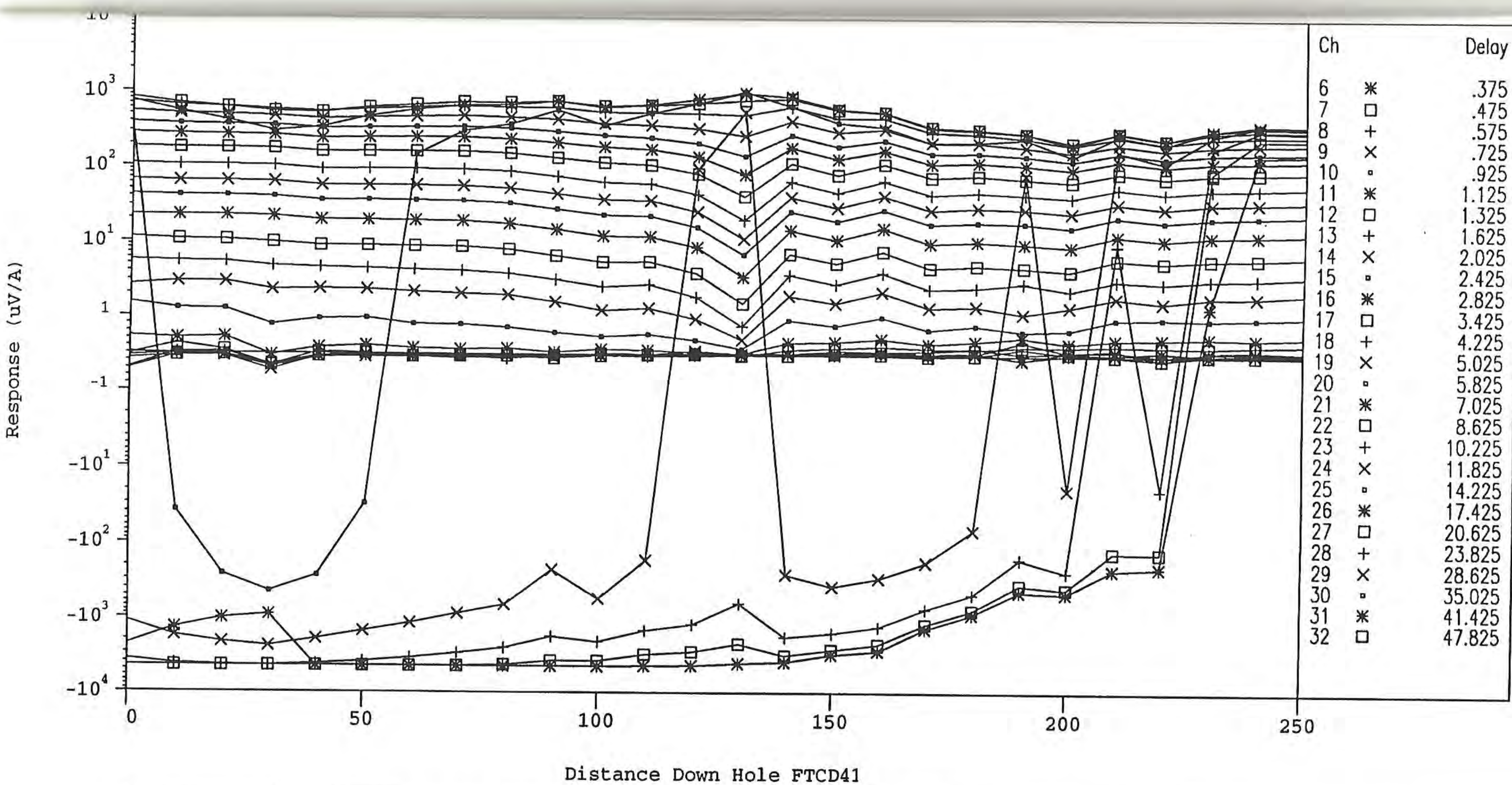

MIM Exploration Pty. Ltd.	MIM EM
Configuration : Down Hole Instrument : SiroTem Mk3 Channels : Composite Times Loop # 2 : 69200,39040 AMG GRID : 69480,39320	Horizontal Scale : Default Vertical Scale : Default Time Delay In : Milliseconds Date : 15/03/94 Figure : 2.2.1

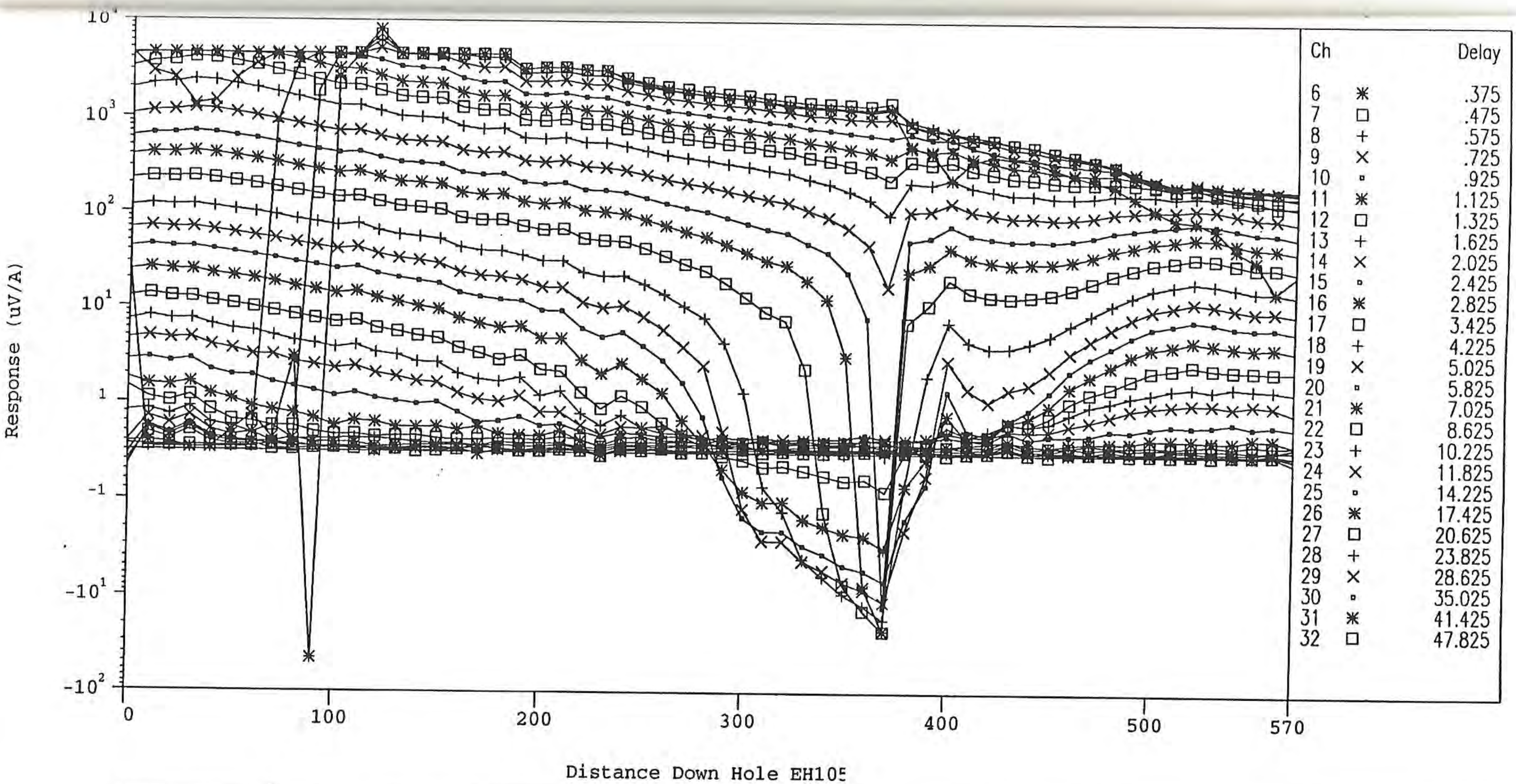

MIM Exploration Pty. Ltd.	MIM EM
Configuration : Down Hole Instrument : SiroTem Mk3 Channels : Composite Times Loop # 2 : 69200,39040 AMG GRID : 69480,39320	Horizontal Scale : Default Vertical Scale : Default Time Delay In : Milliseconds
	Date : 15/03/94 Figure : 2.2.5